Committee III.2: Fatigue and Fracture

Garbatov, Y.; Ås, S.K.; Branner, Kim; Choi, B.K.; den Besten, Henk; Dong, P.; Lillemäe, I.; Lindstrom, P.; Lourenço de Souz, M.; Parmentier, G.

DOI
10.3233/978-1-61499-862-4-441

Publication date
2018

Document Version
Final published version

Published in
Proceedings of the 20th International Ship and Offshore Structures Congress (ISSC 2018)

Proceedings of the 20th International Ship and Offshore Structures Congress (ISSC 2018) Volume I – M.L. Kaminski and P. Rigo (Eds.)

doi:10.3233/978-1-61499-862-4-441

COMMITTEE III.2

FATIGUE AND FRACTURE

COMMITTEE MANDATE

Concern for crack initiation and growth under cyclic loading as well as unstable crack propagation and tearing in the ship and offshore structures. Due attention shall be paid to the suitability and uncertainty of physical models and testing. Consideration is to be given to practical application, statistical description and fracture control methods in design, fabrication and service.

COMMITTEE MEMBERS

Chairman: Y. Garbatov, *Portugal*
S.K. Ås, *Norway*
K. Branner, *Denmark*
B.K. Choi, *South Korea*
J. H. Den Besten, *The Netherlands*
P. Dong, *USA*
I. Lillemäe, *Finland*
P. Lindstrom, *Sweden*
M. Lourenço de Souza, *Brazil*
G. Parmentier, *France*
Y. Quéméner, *China* (*Taiwan*)
C.M. Rizzo, *Italy*
J. Rörup, *Germany*
S. Vhanmane, *India*
R. Villavicencio, *UK*
F. Wang, *China*
J. Yue, *China*

EXTERNAL CONTRIBUTORS

Andoniu, A., *France*, Chen, K-C., *China* (*Taiwan*), Dong, Y., *Portugal*, Eggert, L., *Germany,* Negi, A., *India*, Parihar, Y., *India,* Parsoya, V., *UK*, Uzunoglu, E., *Portugal,* Qin, Y., *The Netherlands*

KEYWORDS

Fatigue, fracture, steel, aluminium, polymer composites, damage accumulation, crack growth, fabrication, inspection, maintenance, reliability, design, verification, fitness for service, rules, standards.

CONTENTS

1. FATIGUE AND FRACTURE LOADING

Fatigue loading may act either sequentially or simultaneously at different periods of the ship and offshore structures lifetime. The Chapter focus is on environmental loading, e.g. associated with waves, wind, current and temperature as well as operational loadings like the successive loading and unloading of the cargo and motion-induced contributions. For offshore structures, it also includes loading encountered during transit/transportation (e.g. from the yard to the operating location), as well as during installation (e.g. piling of fixed foundation).

Fracture is related to unstable crack propagation, depending on strain rate and temperature effects.

1.1 Fatigue loading

The time-varying fatigue loadings are typically environment and operations induced.

1.1.1 Metocean description

The metocean description aims to determine the environmental conditions in which a ship or offshore structure may experience during its service life based on past observations. Data may be obtained from meteorological records combined with hind-casting for locations where data is not available or insufficient. In the last decades, satellite data has been used as a source for defining the sea states. Such data is obtained as a sequence of historical sea states, wind, current, temperatures, etc. The basic assumption is that climate change may be neglected in view of the time scale of typical design lives, and thus that the statistical distribution of the environmental parameters (sea states, wind, current and temperature) are assumed to stay unchanged. Then, the information is organized according to the need of the designer to estimate the fatigue damage. A common procedure consists of defining a table of long-term distributions of sea states, referred to as a Scatter Diagram. Scatter Diagrams provide information regarding statistical distributions of sea states without consideration regarding the sequence of those sea states, e.g. evolution of sea states before and after a storm event. When the linear Palmgren-Miner rule for damage assessment is employed the Scatter Diagrams are sufficient to provide a reasonably accurate lifetime estimate. On the contrary, when the damage accumulation is nonlinear as for the crack growth model that involves the threshold effect, the sequence of sea state occurrences may significantly influence the fatigue damage and crack growth estimates. Therefore, the statistical description of sea states can be improved using a storm model. For ships, the environmental conditions experienced by the structure depend not only on the metocean description of each region along the shipping route but also on the time spent in each area, which implies its forward speed. The forward speed also significantly influences the ship motions and thus the load amplitudes, as well as the number of waves encountered during the design life and thus the number of load cycles. Finally, when needed by the designer, the Scatter Diagram can be reorganized per seasons, wave directions, and, especially for offshore units, according to current and wind speeds and directions. As such, all relevant environmental parameters, with respect to fatigue, can be statistically correlated.

For ships, the design metocean description depends on the trading pattern of the ship. Ships designed for deep sea operations are supposed to be able to navigate worldwide. It is generally admitted that the worst navigating condition corresponds to the North Atlantic environment and that a Scatter Diagram is accordingly provided by IACS (2001) in association with an assumed averaged ship speed set to ¾ of the ship service speed for any relative wave headings. Although this approach may be considered too conservative given the negligible part of the world fleet of bulk carriers and oil tankers continuously operating in North Atlantic environment, IACS (2014b) justifies this assumption by the appropriate margin it provides for the rules fatigue assessment methodology that omits the dynamic response contribution, e.g. springing and whipping, to the total fatigue damage. Therefore, for ships not verified accordingly to the CSR, the utilization of a milder environment for the fatigue assessment of ships should be conditional

on the assessment of the fatigue considering the quasi-static and dynamic wave loads. An alternative metocean description, the so-called "Worldwide Environment", results in a significant wave height 20% smaller than the one produced by the IACS North Atlantic scatter diagram. So far, no standard metocean description has been commonly accepted by Classification Societies for ships with restricted navigation conditions. Upon Class agreement, a specific metocean description may be employed for ships operating in a dedicated area.

For offshore structures, an accurate metocean description for the dedicated site can be carried out from meteorological data when long-term measurements are available. Contrary to ships fatigue assessment that only considers waves, the good statistical reproduction of the correlation between all involved environmental parameters, e.g. wave, winds and current, can have a significant effect on the accuracy of the fatigue assessment. Additionally, in contrast to ships, an offshore structure cannot avoid the worst meteorological conditions by changing their route. Those extreme events may have a significant impact on the fatigue life of the unit, especially when considering the underload and overload effects on the fatigue retardation. The metocean description of waves is generally available far from the shore. To determine the fatigue load history, a first step in the analysis involves rebuilding the local metocean description at the actual location of the offshore structure, commonly in shallow water. Different approaches have been proposed to transfer spectrum energy from deep sea to nearshore (Wang et al., 2016a), but simplified approaches are not easily validated and fully nonlinear approaches such as the Enhanced Spectral Boundary Integral (ESBI) remain more reliable despite the calculation cost. This local metocean description is generally checked by in situ measurements, but the measurements duration is generally not sufficient to provide an exhaustive description of the local metocean description.

1.1.2 Waves

Amongst all the loads and environmental effects considered in this Chapter, the wave-induced loads are generally the most influential. Especially for ships, fatigue analysis is usually based on wave-induced loads only. The wave-induced loads are estimated based on the ships patterns in navigation or operation, i.e. the metocean description, and the response of ship and offshore structures in terms of motions. For the metocean description, the Scatter Diagram is a simplified way to provide a statistical representation of the sea state for each area. The drawback of such wave scatter diagrams is that information regarding the evolution of the sea states at a specific event, such as before and after a storm, is lost. The storm model aims to organize sets of sea states to simulate the sequence of sea states during a depression. The current sources of sea states for design such as those in (Hogben et al., 1986) are not suitable for identifying the correlation among the sea-states. A model based on a Fourier series expansion is proposed in (Minoura, 2016) involving both seasonal and non-seasonal parameters. The parameters involved in the model are the significant wave height, wave period, wind velocity, and their correlations. This approach allows the consideration of retardation of crack propagation as a result of overloads observed in the previous storm, as presented in (Yan et al., Hodapp et al., 2015), that may lead to more optimistic predictions compared to assessments employing the usual assumption of linear fatigue damage accumulation.

Actual ship routes are driven by trade request, time of delivery and fuel consumption, but they can also occasionally be modified due to meteorological considerations. At the design stage, for ships with unrestricted notation, the most conservative environment is generally considered, and it supposes continuous operations in the North Atlantic Ocean. This conservative assumption can be mitigated by the fact that the crew may modify the route according to the meteorological forecast condition.

Additionally, forward speed is a function of sea conditions. In the head sea, cargo ships experience involuntary speed reduction due to added hydrodynamic resistance and power limitation of the propulsion engine. Besides, the crew may voluntarily reduce the speed or slightly change

the heading to reduce motion which will modify the load distribution in terms of intensity and period.

Ships navigating in coastal conditions may avoid the worst sea conditions due to the proximity to a harbour. Their mission profile involves the area of operation that implies the maximum distance between a port and the operational limitations including the speed. This speed limitation is, so far, only dependent on sea state conditions in terms of wave height as observed by organizations appointed by national authorities, although wave steepness and relative heading are equally important for determining the severity of wave loads.

In addition to the Class Notation, an unrestricted and other navigation notation may be assigned to ships such as summer zone, the tropical zone of the coastal area or sheltered area. The actual area of navigation of a merchant ship has not been exhaustively analysed. Some analyses are available on the actual routes versus the seasons. Data obtained using an Automatic Identification System, AIS, completed with the Geo-maritime-economy for a deep-sea navigation between the Gibraltar and North America coast is provided in (Vettor & Guedes Soares, 2015). On another hand, decreasing fatigue loads in a coastal navigation are the results of not only a lower level of wave heights but also the proximity to a port or safe sheltered anchorage which allows access before a storm.

Ships may be subjected to operational limitations. High-Speed Crafts are not allowed to navigate beyond a certain wave height and their ship-master/crew must observe the speed limitations that depend on the sea states. Some operations for offshore structures are not allowed beyond certain sea conditions, considered as not permissible.

Sea States Wave Spectra

Generally speaking, sea-state description involves significant wave height, wave period (e.g. mean zero up-crossing period), and wave direction. In addition, parameters related to the bandwidth and the corresponding wave spread (Li et al., 2015c) lead to lower fatigue load predictions.

Some more sophisticated models involve multi-directional spectra with different height and period according to direction. These multi-directional spectra may be important for moored offshore structures where heading in addition to wave direction depends on wind and the current. With multi-directional spectra, wave spectrum can be combined with wind spectrum inducing transverse responses that cannot be reproduced by unidirectional load considerations.

In near-shore conditions, the metocean description is generally not known a priori and designers use a dedicated methodology to obtain near-shore sea states from the known deep-water metocean description (Jaouën et al., 2016). It involves translating deep water sea states to shallow water sea states with combined effects of wind and current, with respect to the bathymetry and the boundary conditions. This involves a large number of combined sea states, winds and currents, in the order of thousands. These methodologies should be more detailed by Committee I.1.

Slamming, Whipping, and Springing

With the increasing size of the ship and offshore structures, e.g. container ships, floating airports or large fixed platforms, wave effects can induce resonant responses to natural frequencies of the hull girder. The resulting vibration due to the resonance phenomenon, namely springing, may increase the fatigue damage even in moderate sea states. For large ships in moderate sea states, the forward speed may favour the springing phenomenon, especially in head seas where the forward speed increases the wave encounter frequency to the level of the hull girder Eigenfrequency. For more severe sea states, the slamming of the ship's fore end and, occasionally, of the aft end can induce transient hull girder vibrations, also named whipping, with higher amplitude than those occurring during springing events (Liao et al., 2015). However, it can be anticipated that the crew will appropriately modify the course and speed of the ship to mitigate

the slamming load's intensity and consequently will reduce the whipping contribution to total fatigue.

Very large floating structures, e.g. offshore structures, are sensitive to springing, and its contribution to total fatigue damage is thus significant. Therefore, the evaluation of springing contribution to fatigue life is essential for the demonstration of the feasibility of a project. So far, there is no common approach to calculate the springing response of large container ships and its effect on the fatigue life of the ship structural details. The critical wave frequencies method is used in (Lee et al., 2014) to predict the springing response and fatigue life of a 10,000 TEU container ship, where fluid-structure interaction models were used to investigate the springing response and effects on design bending moments. A boundary element method and a finite element method were employed for coupling the fluid and structure domain problems, while the ship vibration modes and natural frequencies were calculated by idealizing the ship structure with the Timoshenko beam. The numerical analyses were validated by comparison with small-scale and full-scale measurements. The case of the study showed that the fatigue life of a large container ship can be reduced by 20% when considering the springing effect. Following the study in (Lee et al., 2014), the springing contribution to the total fatigue of a 20,000 TEU container ship at hotspot locations dominated by wave-induced vertical bending and torsional moments was investigated in (Im et al., 2015). A hydro-elastic numerical approach was employed that took into account the springing effect in the frequency-domain, for which the ship motions and associated bending and torsion moments were evaluated using a hydrodynamic software. Such load responses were compared between rigid and flexible bodies to investigate the effect of springing response on fatigue damage.

Furthermore, slamming may induce a high level of resonant response and, when repeated, the resulting damage can significantly contribute to the total fatigue damage. Tests on plating subjected to slamming loads show that the pressure history was not significantly affected by structural distortions due to repeated impacts as investigated in (Shin et al., 2016). Additionally, FE analyses were carried out, which produced progressive damage results for comparisons with those observed on test specimens. Alternatively, a computational fluid dynamic (CFD) method based on RANS formulation were used in (Zhu et al., 2016) to evaluate slamming pressure history on the wet deck of a SWATH. The numerical model's prediction compared well with the model tests' measurements. In order to extrapolate those test results to ships, the authors proposed a pressure coefficient to relate the slamming pressure to the velocity of water entry. A complete procedure to assess the whipping loads and their effect on fatigue is provided in (BV, 2015) that involves slamming load evaluation based on CFD formulations or Boundary Element Methods, seakeeping analysis and hydro-structure computations in the time-domain. Full-scale measurements have been carried out on container ships and are presented in (Kahl et al., 2015, Storhaug & Kahl, 2015) to evaluate the effect of whipping on the fatigue damage. Those large ships are prone to respond to slamming either with vertical or torsional modes of vibration. For the analysed ship in (Storhaug & Kahl, 2015), the observed damping corresponding to the torsional mode of vibrations is higher than that of the vertical mode when whipping occurs. Consequently, the torsional whipping contributes less to the total fatigue compared to the vertical bending mode from which the contribution was found to be significant. The combination of the quasi-static and whipping response is addressed in (Kahl et al., 2015), and a simplified approach is proposed that considers only the quasi-static wave induced loads magnified by the whipping effect, while the remaining whipping load cycles are disregarded, being deemed as having a negligible effect on fatigue.

1.1.3 Current

Current induces both constant and variable loads. Generally, current effects are disregarded for ships as being negligible compared to the forward speed effect. For bottom-fixed offshore structures, the current effect can significantly contribute to the total load and is considered as a constant load with slow variations, e.g. a few cycles per day for tidal current, a few cycles per week

or even per year for wind-induced currents. For moored floating offshore units, the current can induce indirect quasi-statically varying loads by changing mooring conditions. For pipes and risers, current may produce vortices with relatively high frequencies that generate the Vortex Induced Vibration (VIV) phenomena, whereas, for offshore moored floating units (e.g. Spars, semi-submersibles, TLPs and buoys) the current can generate vortices with a low frequency that can induce Vortex Induced Motions (VIM) phenomena.

For pipes and risers, VIV occurs when the vortex frequency that mainly relates to the structure diameter and current velocity is close to an eigenfrequency of the structure. For the case of a Steel Catenary Riser (SRC), numerical simulations were conducted in (Yin et al., 2015), which show that the predicted VIV-induced fatigue damage is very sensitive to the Reynolds number and the surface roughness according to flow regime (e.g. subcritical, critical or supercritical). Especially, higher fatigue damage is produced in a supercritical condition.

The boundary conditions of pipes and risers lying on the seabed are difficult to reproduce as they relate to soil behaviour, contact conditions, etc... As a result, fatigue assessment in the frequency-domain that assumes the linearity of the loads may become inaccurate with the variation of the stiffness and damping induced by the contact with the soil. Time-domain simulations were conducted in (Kahl et al., 2015) using Thorsen's hydrodynamic forces where the vortex shedding frequency corresponds to the pipe Eigen-frequency and which the lock-in is modelled through an empirical relationship. For a given current velocity, the results show a high sensitivity of the structure response to the various boundary condition settings in terms of stiffness and damping.

The VIM phenomena, encountered by moored floating offshore units subjected to current can degrade fatigue lives of the mooring lines' connections and risers. VIM occurs when the current-induced vortex shedding frequency meets the natural period of the floating unit, and it is usually predicted based on model tests or CFD simulations (Ye et al., 2016), although, especially for design purpose, simplified approaches are available.

With respect to fatigue assessment, the difference between VIM leading to large efforts i.e. large fluctuating forces and moment, generally leading to large displacements, with a low number of cycles and VIV leading to lower efforts, but often exciting vibration modes, with a higher number of cycles, is not critical in the sense that only the result in terms of effort and number of cycles is important. However, for the analysis of the phenomena, the existence of a resonant response is always challenging to simulate numerically, especially regarding the setting of the damping at the design stage to which the resonant response is highly sensitive.

1.1.4 Wind

For ships, wind loads are considered negligible compared to wave loads and are omitted in the fatigue assessment.

For bottom-fixed offshore wind turbines, the loads due to wind fluctuations in terms of speed and direction are important to fatigue damage evaluation. A methodology that consists of reproducing the stress range distribution using a rain flow method and organizing the resulting signals in a set of "events" corresponding to typical patterns, and reducing each event in a set of equivalent constant amplitudes was proposed in (Dragt et al., 2016).

1.1.5 Temperature and ice

Temperature loads may contribute to the total fatigue damage following environmental and operational conditions in terms of low cycle fatigue. Temperature loads are considered for gas carriers and particularly LNG carriers due to temperature variations during loading/unloading operations as indicated in the International Code for the Construction and Equipment of Ships Carrying Liquefied Gases in Bulk (IGC code). But other sources of temperature loads exist, such as the daily variation of air temperature combined with the solar radiation on the steel

plates combined with sea temperature or ballast temperature. Based on information available to date, the contribution of temperature loads to total fatigue damage seems limited and is generally disregarded except for gas carriers during loading/unloading operations. The main reason is that the accurate evaluation of the thermal expansion of structural components requires a fine description of the temperature field in the structure, and those data are generally missing. Besides, for the LNG tanks of gas carriers, the thermal expansion is included in the scope of the design scenarios for fatigue assessment, particularly during loading and unloading operations. As the stress range due to thermal loads during loading and unloading is, for some details, considerably higher than the stress range due to waves, the resulting fatigue damage can be significant not only due to the thermal stress range itself but also due to its interaction with wave-induced stress ranges. The thermal load cycle is combined with loads due to loading and unloading and with loads at sea to form the largest cycle of a given voyage within the Rain flow cycles counting process.

Ice loads are difficult to assess for fatigue damage using a standard approach as there is no consensus on loading scenarios. For this reason, loads recorded from voyages are essential to deduce design loads from actual load sequences experienced by ships. An estimation of the fatigue damage of a Korean Icebreaker based on two recording sequences of 55 days and 99 days was conducted in (Hwang et al., 2016). The fatigue assessment was based on strain measurements conducted in the bow thruster room on the side-shell. Further research is needed in that domain as it seems difficult to extrapolate from such a low set of voyages to define patterns of ice fatigue loads. Additionally, it may be expected that the ice fatigue loads would strongly depend on the ice environment, and on the shape and the power of the ship. Moreover, it can be anticipated that ships designed for regularly navigating in ice conditions are significantly reinforced and that the wave loads contribution to the fatigue should decrease accordingly.

1.1.6 Earthquakes and soil interaction

Soil interaction effects are to be considered. Frequent earthquakes may contribute to the fatigue of bottom-fixed offshore units. But so far, few events have been experienced and no publication is available. However, soil reactions to loads applied on the foundation of a fixed offshore unit are largely considered during design. The soil stiffness depends on the level of loads applied and the soil response is not linear (Dubois et al., 2016). This implies that dynamic response calculation should involve a determination of the stiffness of the foundations.

1.1.7 Operations

Operational loads, such as the cargo loading conditions for ships, are considered as constant during each phase of its service life. However, these constant loads have an effect on the structural fatigue behaviours since the resulting mean stresses act in combination with residual stresses from fabrication processes as well as from previous load histories, as presented in Chapters 3 and 4. Additionally, the interactions between constant and time-varying loads should be considered consistently with meteorological conditions. For example, heavy ballast conditions occur in the case of a storm, while normal ballast conditions are encountered in mild sea states. Therefore, the combination of constant and time-varying loads need to be carefully addressed at the design stage.

For ships, Classification Societies provide a set of typical loading conditions, associated with a constant load and a fraction of life. The light ballast is disregarded as being exceptional. A partial loading is not accounted for in tankers since navigations in partial loading are highly dependent on the oil market. For bulk carriers, four loading conditions are typically considered for the fatigue assessment: homogenous, alternate, heavy, and normal ballast. For LNG carriers in navigation, the tanks are either full or empty. For container ships, barges and passengers-ships, a single representative loading condition may be considered. For dredgers, LNG carriers, and FPSOs, frequent loading and offloading may imply the possibility of low cycle fatigue damage which should be combined with wave-induced fatigue damage.

For submersibles and submarines, compressive loading due to deep diving may be a source of fatigue because local yielding at hot spot areas under maximum compression may change residual stress states, resulting in a local tensile residual stress field which may cause crack growths. For those units, the contribution of such low cycle fatigue damage induced by repeated deep diving can be significant comparing with wave-induced fatigue damage. Although this phenomenon is frequently observed on naval submarines, it is not often reported in the literature for the sake of confidentiality.

Loading/unloading caused damage is generally negligible for deep-sea ships. Nevertheless, for ships navigating in protected areas with short trips, loading/unloading-induced fatigue damage can become significant due to the large stress range resulting from loading/unloading allowed by rules, e.g. for large dredgers. Therefore, loading/unloading should be combined with the other loads. The same can be said for offshore structures, e.g. FPSOs, FSO tanks during operation. Moreover, for all types of cargo ships, loading and unloading caused fatigue damage cannot be ignored.

1.1.8 Loading interaction

As mentioned above, ship and offshore structures are subjected to different types of loads and the fatigue damage accumulation resulting from the superposition of different environmental loads e.g. wind, wave, current, is not a simple sum of the damages produced for each load calculated separately. However, it is extremely time-consuming to simulate numerically the integrated loads related to the considered unit in its design environment, as well as the associated structural response, especially for a long duration such as design life. Therefore, most of the researchers tend to address that question by proposing simplified approaches, defining a kind of equivalent cycles allowing calculating stress cycles giving the damage experienced by the structure. For example, a study presented in (Ormberg & Bachynski, 2015) simulated the contribution of waves to the fatigue of a spar wind tower and then super-imposed the wind contribution. Various simulations have been carried out to consider the individual effect of wind and associated turbulence with an increasing level of complexity of the wind models, and then by combining the different wind models with the wave loads. This work discusses the validity of the long-term data needed for the fatigue assessment that is often limited to the sea states distribution, whereas the good correlation between the distribution of wind spectra and waves can have a significant effect on the fatigue assessment.

1.2 Fatigue loading calculation

1.2.1 Rules, standards, codes and guideline-based assessment

For ships, Classification Societies mostly stipulate a simplified approach for the fatigue load determination by providing a set of simplified load cases defined in the “Rules” which provides expressions related to the principal and the subdivision arrangement of the ship navigating in various loading conditions for a given design wave environment. To define the set of simplified rules on loads, Classification Societies mostly adopted the Equivalent Design Wave method (EDW), which is based on the principle that a few design waves maximizing the load components will maximize the stress range response at given structural hot spots for a target probability level. The long-term stress range distribution is then usually represented by a two-parameter Weibull distribution scaled on that reference probability load response. More details are provided in Chapter 7 that compares four Class rules' fatigue assessment methodologies. The study presented in (Hauteclocque et al., 2016) employed the EDW method to define the rules loads to be applied for the fatigue assessment of container ships. IACS (2014a) described also the technical background of the determination of the CSR fatigue rules loads using the EDW methods.

For offshore units, Classification Societies mostly provide direct approaches for the fatigue loads determination. The fatigue loads assessment by direct approaches implies, firstly, an improved knowledge of environmental conditions which are usually applicable for offshore units that are designed for a given location, and then the direct evaluation of the loads through computational fluid dynamic (CFD) methods. The hydrodynamic loads exerted on slender structural members are usually evaluated using the Morison equation, while seakeeping analyses are often conducted through boundary element methods (BEM) using either a wave Green's function or Rankine source in frequency or time-domain to assess the loads and motions of floating units, as well as the associated mooring system's internal loads. Direct approaches are thus employed for ship-shaped offshore units such as FPSOs for which a set of simplified fatigue load cases are provided by the Class as for ships, but correction factors are applied to account for the specific wave environment. For offshore units made of slender structural members (e.g. jacket) or floating units with atypical floater design (e.g. semi-submersible) the loads directly evaluated using CFD methods for the design metocean description are to be applied on the structural model because the diversity of their arrangement makes the formulation of a set of simplified loads impractical. It is worth noting that, alternatively, the fatigue load assessment by direct approaches can be used for ships by the Classification Societies granted that the calculation method provides at least the same level of safety than that implicitly taken in the rules.

In general, although direct approaches may lead to more realistic long-term load predictions compared with the rule-based simplified approach, the design requirements of the Classification Societies include more or less explicit margins to ensure a safety level of the fatigue predictions, so that the fatigue life evaluations cannot be directly compared to that corresponding to actual structural conditions once in operation. Eventually, for the structural design, the level of safety of the fatigue predictions produced by direct approaches must be at least as high as the one implicitly taken by the rules' simplified approach.

1.2.2 Direct assessment

Ship and offshore structures are subjected to numerous environmental parameters, e.g. wind, wave current, which can induce various responses in terms of internal loads and also motions in the case of floating structures. Existing software packages used for ship and offshore structural design are generally able to calculate directly the stresses from environmental information and structural descriptions. Nevertheless, applied forces remain the criteria allowing for validating the calculations and helping for design improvement. This has been summarized in (Strach-Sonsalla & Muskulus, 2016) for Floating Offshore Wind Turbines considering the type of floating platform in terms of floating stability, accounting for wave effects, wind fluctuations effects, current combined with motion effects, inertial efforts and mooring effects.

The calculation methods employed to evaluate the applied forces can involve various levels of complexity. The most advanced methods involve time-domain calculations that give accurate results but are very time-consuming. Time-domain calculations (Lee et al., 2014) may be particularly relevant when the employed strength model considers the overload or underload effects on fatigue retardation. As at the design stage, an exact sequence of loads experienced by the structure is not known, methods are thus developed to create an equivalent load signal, that is consistent with the statistical characteristics of a design environment, enabling the reproduction of the sequence effect on fatigue. However, mostly, the fatigue assessment methodologies ignore such effects and assume the linearity of the fatigue process over the life of the unit, e.g. Palmgren-Miner's Sum. Indeed, the high computational cost required to reproduce accurately in the time-domain the design metocean description and to evaluate its effect on the entire design life of the unit motivates the researcher to propose methodologies that represent a good trade-off between accuracy and time-efficiency of the computations. Those methodologies lie thus on numerous assumptions that simplify the problem and which the validity with respect to the accuracy of the fatigue assessment is confirmed by comparison with time-domain simulations.

A wide-spread direct approach for the fatigue assessment of ships or offshore structures, is the spectral fatigue analysis that consists in deriving the load spectrum response to a wave spectrum by the determination of the Response Amplitude Operators (RAO) of the considered loads to a unit wave amplitude in a condition of period bandwidth (Li et al., 2015c). For ships, the loads exerted on the hull by the waves and the associated motions and motion-induced loads are generally assumed linear, while the wind and current effects are neglected. Therefore, the RAO of the loads can be evaluated in the frequency domain. When the applied efforts are not too dependent on wave frequency, fatigue calculation can be carried out on the base of a simplified distribution of loads which reduces the number of regular wave conditions to be analysed compare to long-term time-domain simulations, and the long-term fatigue assessment can be conducted through a spectral analysis. However, the assumption of the linearity of the loads may become questionable for broadband phenomena, e.g. slamming loads and slamming-induced whipping response, for which time-domain simulations are recommended for a more accurate consideration of their contribution to the fatigue. Besides, adjustments are also studied to overcome the linearity limitation of the spectral analysis. Although the intermittent wetting loading of ships' side shell is a non-linear phenomenon, a study (Bigot et al., 2016) analysed the fatigue of side longitudinal stiffeners using spectral analysis with a specific processing on the area of intermittent wetting responding to a fixed arbitrary probability of relative wave elevation set to 10^{-4}, called "footprint". The accuracy of the footprint method with irregular waves was validated, especially for stiffeners located above the mean free surface, by comparison with time-domain analyses. For bottom-fixed offshore units, the obvious non-linearity of the internal loads to the environmental parameters (e.g. wave, wind and current) makes the spectral approach not directly applicable. However, a possible approach for the fatigue assessment consists in mixing time-domain calculations and spectral approach. To limit the number of time-domain analyses, (Peng et al., 2015) carried out a condensation of sea states having the same zero-crossing period. An "equivalent" significant wave height was assumed to generate the same damage with all the sea states involved. Obviously, the structural internal loads were assumed proportional to the significant wave height, which is questionable in case of important non-linearity.

Yet, for some applications, the spectral analysis approach is deemed too time-consuming as it implies the load evaluations for numerous wavelengths and headings. The equivalent design wave (EDW) and equivalent design sea state (EDS) methods are thus developed to limit the amount of ship response calculations to regular waves and irregular waves, respectively. The sea states may thus be summarized by a single equivalent design wave which the frequency corresponds generally to the maximum response. A coefficient that considers the variation of the response according to the frequency is then applied to the equivalent wave's response. This equivalent sea state approach is not always accurate enough as the shape of the waves varies with the frequency. A multi equivalent wave that enables, in principle, a better distribution in space of the efforts was proposed in (Brandão et al., 2015). The Equivalent Design Waves approach depends on the assumed metocean description and the target return period. A generalization of design wave depending on the metocean description and the probability of the sea state selected for the design condition was proposed in (Hauteclocque et al., 2016). An example is provided with a probability of 10^{-2} accordingly to the CSR reference loads for fatigue assessment.

Finally, for some load cases, the conventional CFD methods, e.g. Morison equation, BEM, may not be accurate enough to provide reliable fatigue load assessment. Advanced CFD methods including viscous effect based on the RANS formulation can improve the precision of the load evaluation granted that the models are calibrated on measurements. In situ observations are too complex to be employed as reference data, whereas model testing in a basin with controlled conditions are more adapted to verify the accuracy of the considered numerical models. Such advanced CFD methods can be employed to assess the containerships' slamming loads that contribute to the fatigue, (BV, 2015) as well as to evaluate VIM-induced loads on risers or

semi-sub (DNV, 2010a, Hyunchul et al., 2017) for the floating offshore units. CFD VIM or VIV results are validated versus experimental tests (Maximiano et al., 2017) that do not always predict accurately in situ observations (Koop et al., 2016). For risers, the VIV phenomena are mostly determined based on the empirical model (Ulveseter & Sævik, 2017, Voie et al., 2017, Wu et al., 2017, Yin et al., 2017) using the Morison equation, but the hydrodynamic parameters are directly calibrated based on tests measurements in a basin (Yin et al., 2015). The results from testing on regular waves with the results of a simulation of a Multi-Body System representing a floating wind turbine, loaded using Computational Fluid Dynamic software were compared in (Beyer et al., 2015).

1.3 Fracture loading

Fracture is related to unstable crack propagation in one of three modes, i.e. opening Mode-I, sliding mode-II or tearing mode-III. Especially in the material toughness transition area, the fracture strength is highly dependent on the temperature and on the strain rate. Regarding the temperature, the concern goes for operations in low-temperature regions where higher steel grades are required to ensure a sufficient toughness of the material. Besides, the level of strain rate that influences the fracture is associated with the considered extreme load scenario that is commonly assumed to occur once in the life of the unit. On one hand, the static and quasi-static loads will induce a negligible strain rate at the crack tip and are described in the ultimate limit state (see Technical Committee III.1) which includes typically the maximum wave-induced bending moment for ships and overturning moment for bottom-fixed offshore units. On the other hand, the dynamic loads may generate significant strain rate response at the crack tip and are described in the accidental limit state (see Specialist Committee V.1) which typically includes the dropped object scenario, but also ice or slamming impact and earthquake for the case of bottom-fixed units. For example, the drop on a Sandwich Plate System of an object of 3 tons was considered in (Kennedy et al., 2016) to investigate the shock-absorption capacity of a ductile material. The settings of this accidental condition could also be considered to evaluate the fracture strength of a brittle material when associated with a pre-existing crack and low-temperature environment.

Temperature degrades material resistance to brittle fracture in the context of fracture mechanics. Service temperature can be inferred from meteorological records of minimum temperature established for air. Material requirements in terms of transition temperature are established according to the area where ships or offshore structure are operating.

Finally, despite the critical importance for the safety of the identification and the quantification of events that can lead to a sudden rupture related to fracture mechanics, it is worth noting that, observed fractures almost never occur for marine structure in as-built condition. When such events occur, they are generally analysed as the result of an abnormal extensive fatigue crack propagation that already strongly degrades the fracture strength.

2. MATERIAL PROPERTIES AND TESTING

2.1 Material properties

Current research on material properties is important for fatigue design of the ship and offshore structures. However, cyclic data is typically expensive to obtain, explaining why correlations to cheaper monotonic material properties are also the subject of studies (Zonfrillo, 2017).

2.1.1 Monotonic material behaviour

The current research is focused on failure strain and its dependency on stress triaxiality, strain path and strain rate. The traditional way of obtaining failure strain from tensile tests is questionable as upon necking both the stress state and strain path are changing. To obtain failure strain under various stress triaxiality conditions, e.g. pure shear, uniaxial tension, equi-biaxial tension and plane strain tension, different specimen geometries have been proposed (Choung et

al., 2014, Roth & Mohr, 2016, Erice et al., 2017, Gruben et al., 2017). Common failure criteria for uniaxial- (Calle et al., 2017), as well as proportional and non-proportional multiaxial loading conditions, have been investigated using dedicated tensile test specimen geometries for different strain rates. To improve the performance of phenomenological failure criteria, the strain hardening exponent has been involved as an independent parameter for better approximations of the fracture locus and envelope (Šebek et al., 2016).

Simulation of fracture behaviour in large stiffened panel type of structures often involves shell finite element models for computational efficiency reasons. The failure strain for shell elements is a mesh-size dependent and is usually calibrated using data from tensile tests involving a uniaxial stress state. However, a full-scale punch test of a clamped stiffened panel revealed a stress state dependency as well, varying between equi-biaxial and plane strain tension (Kõrgesaar et al., 2017).

2.1.2 Cyclic material behaviour

During cyclic loading, the material can exhibit cyclic strain hardening or softening. To model the elastic-plastic behaviour correctly, cyclic hardening or softening behaviour needs to be accounted for because of residual stress relaxation and is one of the consequences of cyclic material behaviour. High-Frequency Mechanical Impact (HFMI) of weld toe notches provides acyclic behaviour that needs to be sufficiently understood.

Fatigue strength improvement due to HFMI-treatment is attributed to beneficial compressive residual stress state and introducing strain hardening of the material if cyclic loading is applied. Investigation of a high-strength base material, heat affected zone and the HFMI-treated material shows continuous cyclic softening for all material zones (Mikkola et al., 2016). Using numerical simulations, including cooling-rate dependent phase transformations, and experimental results, an analytical relaxation model has been utilized to show that a reasonable residual stress state estimate for applications in the high-cycle fatigue region can be obtained. In particular, for carbon steels, the volume change due to austenitic-martensitic phase transformation is essential (Leitner et al., 2017). In addition to temperature dependent quasi-static material properties such as Young's modulus, ultimate strength, Poisson's ratio and density, the cooling-rate dependent phase transformation has also been considered in the simulation. It is highlighted that especially for carbon steels, volume change due to austenitic-martensitic phase transformation is essential in order to compute the local residual stress states properly. During HFMI-process the cyclic hardening needs to be considered.

2.1.3 Fracture properties

Fracture toughness is a general term referring to the resistance of a material to unstable crack growth and propagation. In case a small-scale yielding criterion is satisfied, i.e. the crack tip plastic zone is relatively small in comparison to the crack length, it can be characterized by means of the elastic crack-tip stress intensity factor, K or equivalently the elastic energy release rate, G. When a small-scale yielding criterion is not met, the non-linear elastic J-integral, crack-tip opening displacement, CTOD, crack-tip opening angle, CTOA or plasticity-corrected stress intensity factor should be used. While the fracture toughness of brittle material can be expressed as a single-valued property, fracture toughness is a general term referring to a material's resistance to crack extension, which may be more properly expressed as a function of temperature and crack tip constraint.

A thorough overview of fracture toughness testing including recent advances and ASTM standardization is available (Zhu & Joyce, 2012). Attention has been paid to guidelines on how to choose and measure the appropriate fracture parameter. Effects of loading rate, temperature, crack tip constraint as well as fracture instability have been reviewed as well.

The crack tip constraint significantly influences the measured fracture toughness and focus is typically on high constraint (plane strain) values. In case the crack tip constraint is low, dedicated specimens and procedures exist; subject of a comprehensive review (Zhu, 2015, 2016, Ruggieri, 2017). Comparative studies of available test methods using single edge notch tension specimens together with crack tip opening displacement- and J-integral values have been presented (Park et al., 2017, Zhu, 2017, Zhu et al., 2017).

For ultra-high-strength steel, the temperature dependent fracture properties have been investigated with respect to the transition between brittle and ductile fracture. An improved transition criterion has been proposed Wallin et al. (2015).

A new cohesive zone model has been introduced in order to provide a uniform description of both stable crack growth and elastoplastic fracture. Damage accumulation includes both monotonic as well as cyclic contributions. Computational results have been found in agreement with mixed-mode fracture and fatigue test data for austenitic stainless steel (Li et al., 2015a).

2.1.4 Fatigue properties

In order to obtain a better statistical description of material fatigue properties, probabilistic S-N curves have been proposed for constant and variable amplitude loading involving the spectral loading shape (Baptista et al., 2017, D'Angelo & Nussbaumer, 2017).

A Brinell hardness based definition of S-N curves has been proposed, covering fatigue resistance from the first cycle up to the giga-cycle region in a single function. Test results obtained using specimens of various steel grades are in agreement with lifetime estimates (Bandara et al., 2016).

The fatigue strength of welded structures hardly depends on static strength. High-frequency impact treatment can be used for improvement. Tests have been conducted to quantify the influence of HFMI-treatment induced compressive residual stress and modified strain hardening behaviour on the fatigue strength. HFMI-treated materials show increased fatigue strength at smaller strain amplitudes and decreased fatigue strength at larger strain amplitudes in comparison to the base material (Mikkola et al., 2016).

2.1.5 Materials

Very high cycle fatigue tests for three kinds of high strength low-alloy steels have been investigated (Li et al., 2015b). The steels included two high-carbon-chromium bearing steel and a chromium-nickel-tungsten gear steel subjected to axial loading and rotating bending. The subsurface inclusion-induced crack nucleation and propagation process could be divided into four stages: (i) crack nucleation around the inclusion within the Fine Granular Area (FGA); (ii) micro crack growth within the FGA; (iii) stable macro crack growth outside the FGA and within the fisheye; (iv) unstable macro crack growth outside the fisheye. A crack nucleation life prediction method for the stage (i) and a crack growth life prediction method for stages (ii) and (iii) were modelled respectively. The crack growth lives observed in tests by stage (ii) and (iii) occupied a tiny fraction of the whole fatigue life, while the predicted crack nucleation life was nearly equal to the total fatigue life.

High-cycle fatigue tests to determine the influence of mean stress on the initiation mechanism in a 2.5%Cr-1%Mo steel used in riser tube connectors for offshore oil drilling was conducted in (Gaur et al., 2016). Tests were run at 7 different R ratios: -1, -0.5, 0, 0.25, 0.5 (runout at $3 \cdot 10^6$ cycles), and 0.6 and 0.7 (runout at 10^7 cycles). Surfaces were polished (R_a<0.4μm), and fracture surfaces were investigated in Scanning Electron Microscopy (SEM), X-ray Powder Diffraction (XRD) and Energy Dispersive X-Ray Spectroscopy (EDS). For R=-1, -0.5 and 0, surface initiation was observed without any defect present. For R=0.25, cracks initiated predominately from internal flaws, which evolved to “fish-eye” patterns for a relatively low number of cycles. No crack growth was observed for R≥0.6 for N<10^7 cycles. The slope of specimen S-N curves

tended to decrease for higher mean stress, and the endurance limits were found to follow the Gerber parabola.

Uniaxial creep tensile tests using Cr-Mo-V steel round bar specimens with diameter 10 mm at different stress levels at 566℃ was carried out in (Zhang et al., 2015). The measurements showed that the creep behaviour of the steel complied with Norton's law and exhibited different Norton model parameters in low and high-stress regimes, which could be written as the stress-regime dependent creep model (2RN model). The transition stress was approximately 250 MPa.

High cycle dwell fatigue (HCD) tests on blunt compact tension specimens to understand and quantify the effect of creep-induced tensile residual stresses on crack growth was performed in (Chen et al., 2016). The creep/relaxation occurred in compression. The tests at 250ºC indicated that in two-minute HCD cycles tests the total life reduced fourfold relative to a baseline 0.5 Hz cycle, and that crack growth rate increased locally by a mean factor of 6 in the notch. In the baseline specimen, the creep-induced tensile residual stress was found to accelerate the local crack growth rate 4 times compared to not considering creep correction.

2.1.6 Arc-welded and laser welded joints

Welded steel structures are widely used in ship and offshore industries, where operational loading is typically stochastic, and the sequence may lead to either acceleration or retardation of the crack growth rate. Fatigue tests on welded thick-walled C-Mn steel specimens in as-welded and stress relieved conditions were conducted (Maljaars et al., 2015). Some of the specimens were subjected to constant amplitude (CA) loading, with and without overload (OL), while others were subjected to two types of variable amplitude (VA) loading, namely, random loads and wave loads. It has been observed that crack growth retardation in the as-welded and stress relieved specimens was similar in CA loading with OLs. The loading & response ratio ($R \geq 0.3$) showed little influence on the crack growth rate and random loading caused a crack growth rate of the same magnitude as that of the CA tests. Wave loading resulted in a crack growth rate that was substantially lower than for CA. The stress ranges were nearly equal for the two types of VA loads.

Welded X65 offshore pipes with an outer diameter of 32" and 1" wall thickness were cut into fatigue coupons and tested in four-point bending (Pang et al., 2017). Tensile stresses occur at pipe outer surface of the weld cap. The objective of the study was to observe the coalescence and shape evolution of multiple cracks in welded structures. During the tests, 12 to 22 cracks were observed by identifying the ratchet marks, and the locations of each crack initiation site are recorded to support the development of a new proposed model. The predicted crack propagation lifetime for the crack distributions observed using the BS 7910 (BS7910, 2005) design curve is about 10% of the experimental life, suggesting that the predicted life is overly conservative.

2.1.7 Friction stir welded joints

Friction stir welding (FSW) provides a lower cost alternative for steel pipelines construction, replacing the conventional arc welding processes (Sowards et al., 2015). FSW was not yet used in pipelines, but advances in the research suggest that this technique should become feasible soon. FSW does not involve melting of metal and does not require consumables or shielding gas. A solid-state weld is fabricated by inserting a non-consumable welding tool into the steel at the mating surfaces and mechanically mixing the metal to form a permanent joint. The heat input is lower than in conventional consumable welding, which prevents solidification cracking, reduces the size of the heat affected zone, and reduces the magnitude of the residual stresses (Aydin & Nelson, 2013).

The influence of FSW in the fatigue crack propagation of API X80 pipeline steel was analysed in (Sowards et al., 2015). Compact tension specimens were machined from two orientations in the base metal and the weld metal. Fatigue crack propagation in the stir zone and across the

welds was observed to be dependent on residual stresses interacting with the propagating cracks. Residual stresses reduce the rate of fatigue crack growth at all levels of applied stress intensity amplitude, but as the crack grows, the residual stresses are relieved, gradually reducing its effect. The fatigue crack growth rate in FSW welds of X52 pipeline steel was analysed in (Ronevich et al., 2017). Tests were performed for the base metal (BM), the centre of the weld and 15mm away from the weld. High-pressure hydrogen gas (21 MPa) was used to assess the effects of hydrogen accelerated fatigue crack growth. Results pointed out that accelerated fatigue crack growth of the FSW was marginally greater than in the base metal and off-centre regions. Also, similar hydrogen accelerated fatigue crack growth was observed for FSW and conventional arc welds from similar grade pipes.

An extensive experimental study on the fatigue performance of friction stir welded 6-mm thick DH35 marine grade steel was presented in (Polezhayeva et al., 2015b). The study included fatigue and tensile tests, geometry and hardness measurements, microstructure and fracture surface examinations. The effect of process speed was also investigated. The results showed higher fatigue strength compared to International Institute of Welding, IIW (Hobbacher, 2013, Jonson et al., 2016b) design curve for conventional welds and a newly developed S-N curve for friction stir welded joints was proposed.

2.1.8 Corrosive environment

Steel jackets are widely utilized in the offshore oil industry. The jackets are designed for a service life ranging from 15 to 20 years, however, it is estimated that over two-thirds of the world's jackets will be used for 5-10 years beyond their intended design life. Life extension is possible by managing the overall safety and uncertainties in terms of structural degradation and repair decisions (Tan et al., 2016). Fatigue and corrosion play major roles in structural degradation; thus much attention has been paid to assess the residual strength of ageing jackets, and to an extent, the jackets' life. An experimental study on the collapse of ageing steel jackets due to corrosion or fatigue cracks was conducted in (Ji et al., 2016). They prepared three jacket models (1:40-scale); one cracked, one corroded, and one intact as a reference. The damage and the corrosion degradation were imposed on the corresponding models according to the Paris' relation and unique corrosion (with different thickness-corrosion rates in submerged areas and atmospheric ones) to model 15-year ageing. Both the crack-damaged and corroded jacket models failed by local tearing, likely due to elevated localized stresses in the joints of the legs and braces. The intact model failed by global failure.

Experiments have shown that the fatigue life in a corrosive environment is remarkably decreased compared to air. The effect of general corrosion and pitting can be assessed by testing corroded and non-corroded specimens in the air (Garbatov et al., 2014a), whereas corrosion fatigue tests to assess the complex interacting effects of mechanical and environmental factors on fatigue are complex, especially when considering the time-dependent nature of corrosion. Engineering methods accounting for corrosion have been introduced in some design guidelines, defining levels of corrosion damage to reduce the ship structural strength.

The coupling effect of stress and the time-dependent corrosion deterioration in Q235 steel was studied in (Yang et al., 2016). The relation between mechanics and corrosion during elastic deformation was investigated by performing uniaxial tensile tests in 3.5 wt.% NaCl solution and 5 to 7 ppm dissolved oxygen. Time-dependent corrosion acceleration due to stress was analysed using FEA. They found that (i) the corrosion of welded joints was accelerated because of the combined effect of corrosion and stress concentration, (ii) the fatigue coupled with non-uniform corrosion was more detrimental than fatigue coupled with uniform corrosion.

Offshore wind farm monopile structures experience dominant cyclic frequencies in the range of 0.3-0.4Hz. To evaluate the fatigue crack propagation behaviour fatigue tests on six compact tension specimens made of S355J2+N steel in the air and in laboratory simulated seawater under free corrosion was carried out in (Adedipe et al., 2015). In the air tests, R=0.1 loading at 2

Hz was applied, and fatigue crack lengths were monitored by Alternating Current Potential Difference, direct current potential difference, and back face strain. For the tests in simulated seawater, a load ratio of R=0.1 was used with loading frequencies 0.3, 0.35 and 0.4 Hz, and BFS was adopted to monitor the crack growth. The tests showed that (i) similar crack growth rates were observed using the three test frequencies. (ii) The fatigue growth behaviour of S355J2+N steel both in the air and in seawater was consistent with BS7910 (2005).

2.1.9 Similarity

To translate test results into fatigue design, the link between the small-scale specimens and the actual structure needs to be understood. Similarity and transferability of small-scale fatigue test results have recently been studied using full-scale fatigue testing of structures. Fatigue tests of full-scale 4-mm thick laser-hybrid welded passenger ship deck panels and the small-scale specimens cut from the same structures were performed in (Lillemae et al., 2017). The results were in good agreement given that the initial distortion shape and geometrical nonlinearity are considered in the analysis. The fatigue strength of full-scale railway axels was compared to one of the scaled specimens in (Yamamoto et al., 2017) and the difference was found to be within the error margin. The fatigue strength of full-scale U-rib bridge steel deck specimens under the vehicle loads was investigated in (Kainuma et al., 2016). The fatigue crack propagation in bulb stiffeners was studied using numerical analysis and full-scale experiments in (Yue et al., 2017).

Full-scale structure testing and in-service measurements are also carried out to validate calculation models. Full-scale fatigue tests of ship propellers in order to validate the proposed fatigue model was carried out in (Ezanno et al., 2015). The results of a spectral fatigue analysis were compared to the strain gauge measurements carried out on the board of a naval vessel during the sea trial in (Thompson, 2016).

2.2 Polymer composites testing

This section focuses on how polymer composite materials and structures are tested with wind turbine blades as the application in focus. In the design process of wind turbine blades, tests at several scales can be performed to estimate the material properties and to verify the computational design models used to estimate the load-bearing capacity, illustrated in Figure 1. Currently, only coupon and full-scale tests are required to certify wind turbine blades according to the IEC 61400 standard for wind turbines.

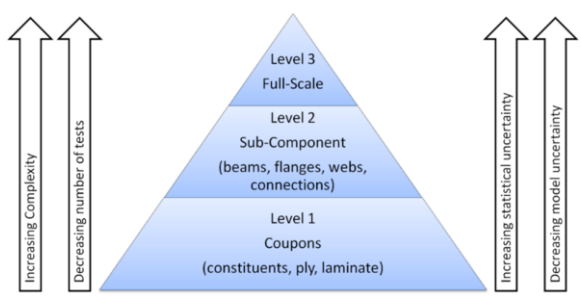

Figure 1: Level of tests assessing of load bearing capacity of wind turbine blades.

At the coupon level, small test specimens with the basic material are tested to determine the material properties and their statistical characteristics in both ultimate and fatigue limit states. The test specimens at the coupon level are normally relatively inexpensive to produce and several different tests with many repetitions can be performed.

At the subcomponent level, parts of a wind turbine blade are tested to determine the load-bearing capacity of selected parts and to verify computational models for potential critical details.

Subcomponents are in general more expensive and complicated to test than coupons, which lead to fewer tests for each subcomponent.

At the full-scale level, prototypes of the blade are tested both in static and dynamic conditions following the requirements of the IEC 61400-23 (IEC-61400-23, 2014) standard for full-scale testing. Full-scale blade tests are typically performed on one or two blades to verify that the blade type has the load carrying capability and service life provided for in the design. Since the cost of a blade itself is high and the time needed for the dynamic test can be several months for large blades, then also the cost due to the waiting time for market introduction is significant.

2.2.1 Sub-components

Initial work on how to plan and apply subcomponent tests; i.e. a simplified component test, in the design process of wind turbine blades was done in the project: "Experimental Blade Research – Phase 2 (EBR2)" (Sørensen et al., 2013, Eder et al., 2015). Parts of this work were then used for making the new DNV GL rotor blade standard (DNV-GL, 2015), which for the first time makes it possible to use subcomponent testing as part of the wind turbine blade certification (Pansart, 2015). A subcomponent test method designed to check the compressive strength of the trailing edge region in wind turbine blades under simplified loading was first proposed in (Eder et al., 2015, Branner et al., 2016) and then later further developed under the EU-funded project IRPWind in cooperation with Knowledge Centre WMC (Lahuerta et al., 2017) and Fraunhofer IWES Rosemeier (Rosemeier et al., 2017). Finite element simulations showing that the proposed static subcomponent test method is promising in obtaining the compressive strength of the trailing edge region under simplified loading were performed in (Branner et al., 2016). It was found that the failure load and the failure mode are very similar to that found in full-blade tests for the analysed test specimen.

2.2.2 Full-scale components

Currently the IEC61400-23 and DNVGL-ST-0376 standards require that blade fatigue testing is carried out by testing blades in two directions – flap wise and edgewise – one direction at a time. During their lifetime, wind turbine rotor blades are exposed to high dynamic loads, resulting from cyclic changes in gravity direction, centrifugal forces, and changing wind conditions such as average wind speed, turbulence intensity, rapidly changing wind direction, wind shear, extreme wind gusts and site-specific loads such as wake effects from neighbouring wind turbines. The broad and complex load spectrum results in the accumulation of a significant amount of fatigue damage over the turbine lifetime. Fatigue is, therefore, a major failure mechanism in wind turbine blades. The currently required fatigue testing methods are not representing the real service loads very well and there are therefore attempts to develop more realistic test methods. One method is dual-axis fatigue testing where the flap-wise and the edgewise directions are tested simultaneously (Hughes et al., 1999). This approach is shown to be more representative of the loading in service and can thus contribute to a potentially more realistic testing of wind turbine blades (Greaves et al., 2011).

A biaxial fatigue test performed in (Snowberg et al., 2014) is demonstrating how resonant fatigue test methods can be used to simultaneously apply flap-wise and lead-lag loads to a full-scale wind turbine blade. This biaxial resonant fatigue testing method will complete the test faster than single-axial testing because of this simultaneous application.

Several potential biaxial fatigue test scenarios for a fictional 60 m blade are examined in (Post, 2014). Three alternative approaches for configuring a biaxial fatigue test were considered: (i) a quantum biaxial fatigue test where the flap and lead-lag directions are excited at separate resonance frequencies resulting in a variable and nominally random phase angle between the two test directions; (ii) a phase-locked test with frequency ratio of 1:1 where the lead-lag frequency is reduced to the flapping frequency by adding virtual mass at multiple stations; and finally (iii) a phase-locked test with a frequency ratio of 1:2 where the flapping frequency is reduced

slightly using virtual masses to run at exactly one-half of the lead-lag frequency. It was found that the ability to achieve moment distributions relatively close to the target with relatively small virtual masses gives the 1:2 phase-locked test approach a good chance of success in a commercial test program including a possible reduction in test time.

A method for calibrating strain gauges was developed in (Greaves et al., 2016). It accounts for the misalignment of the applied loads by including the effects of winch cable angle during calibration pulls, which are only partially accounted for with the crosstalk method. This has shown to be a significant cause of errors with the current best practice technique proposed in the standards. The method also has the advantage that it allows strain readings from an arbitrary number of gauges to be included in any given blade section, which would reduce errors arising due to noise.

For wind turbine blade testing, there are two research needs – more realistic loading and faster testing. The standard certification tests used today are not representing the real world very well. Blades are exposed to torsion and bending in different directions at the same time. There is consequently a need for fatigue test methods that better match the loads to which the blades are exposed to in real operational conditions. As blades become larger the time needed to perform the necessary certification tests become longer as blades are tested at resonance. This is a challenge for the industry as 100 m blades are expected to take more than a year to test. There is, therefore, a need to shorten the test time. Multi-axis test methods seem to answer to both these needs.

2.3 Testing methods and measurement techniques

For material model calibration and simulation verification purposes, material testing is virtually indispensable, although often costly and time-consuming. Research efforts have been put into the characterization of the very high cycle fatigue resistance (lifetimes exceeding 10^7 cycles) using different techniques. In contrast to high cycle fatigue showing crack development predominantly at the surface, very high cycle fatigue cracks typically start to develop subsurface at fine granular regions introducing fisheyes at the fracture surface (Stanzl-Tschegg, 2014).

Ultrasonic testing permits frequencies up to 20-30 kHz. It is energy efficient and makes a low noise, but the specimen design is limited. Other challenges include strain rate- and thermal effects. The frequency effects on quenched and tempered steel and aluminium alloy were recently investigated in (Schneider et al., 2016), showing that fatigue resistance of aluminium is more dependent on the environment (laboratory air versus vacuum) and steel on the strain rate.

Ultrasonic fatigue testing under multiaxial and variable amplitude loading conditions has recently also received an increasing research attention. Biaxial ultrasonic fatigue tests with axial and torsional load components were carried out and compared to the strain gauge data obtained with the equivalent specimen tested in the biaxial servo-hydraulic machine with the frequency of 0.5 Hz in (Vieira et al., 2016). The results showed good agreement. A new ultrasonic testing device for biaxial testing of flat smooth disc specimens was presented in (Brugger et al., 2017). Ultrasonic variable amplitude fatigue tests on aluminium alloy with stress ratios R=-1.0, 0.1 and 0.5 was performed in (Mayer et al., 2014). The results were compared to ultrasonic constant amplitude tests as well as to results obtained from a servo-hydraulic testing machine in (Fitzka & Mayer, 2016). Similar tests for high strength steel were performed in (Sander et al., 2016).

One alternative testing methodology of servo-hydraulic and ultrasonic testing includes electrodynamic shakers, with testing frequencies up to approximately 1 kHz. Their advantage is the response amplification in the resonant area, which means that the excitation can be small. As for ultrasonic testing, the method is limited by specimen design. Example of research carried out using such equipment is given by e.g. (Khalij et al., 2015).

The use of digital image correlation (DIC) in fatigue and fracture testing as an alternative measuring technique has increased in recent years. Examples can be found in (Lopez-Crespo et al.,

2015a, Hos et al., 2016, O'Connor et al., 2016, Vasco-Olmo & Diaz, 2016, Gonzales et al., 2017, Hosdez et al., 2017, Jandejsek et al., 2017, Mokhtarishirazabad et al., 2017). Also, the calibration of the potential drop technique to determine the crack size has recently been presented by e.g. (Doremus et al., 2015, Tumanov et al., 2015, Berg et al., 2017). DIC and thermographic measurements to define the fatigue strength from static tests and validation with the fatigue tests was presented in (Corigliano et al., 2017).

Fatigue crack sizing method in a larger structure using ultrasonic guided waves was presented in (Pahlavan & Blacquiere, 2016). A thermographic method to detect the exact crack initiation location and the crack growth time is presented in (Krewerth et al., 2015).

The fatigue cracks growth in stainless steel by comparing simultaneously measured acoustic emissions and infrared thermography data was studied in (Barile et al., 2016). An experimental technique to assess the fatigue damage accumulation rate by evaluating the heat energy around the crack tip with an infrared camera was presented in (Meneghetti & Ricotta, 2016). Crack length measurements under non-continuous thermal conditions are carried out and discussed in (Ewest et al., 2016).

3. FATIGUE DAMAGE ACCUMULATION APPROACHES

Fatigue involves physics across several interactive resistance dimensions, distinct contributions in different stages of the (accumulative) damage process and a range of scales. Joints connecting ship and offshore structural members are typically fatigue sensitive and require particular attention in this respect. For arc-welded joints in metallic structures, assessment concepts developed over time are classified with respect to the type of information, geometry, parameter and process zone, including plane and life regime annotations, providing an overview (Section 3.1). Recent advances are highlighted (Section 3.2).

Continuum and discrete damage mechanics models can be adopted as well to estimate crack initiation and growth lifetime using respectively damage evolution functions which describe the deterioration of the material mechanical properties and cohesive zone or damage mechanism formulations (Section 3.3).

The fatigue damage criterion defines the fatigue strength and lifetime estimate accuracy from a modelling perspective and controls the reliability level that can be achieved, while confidence is a matter of sufficient test data. Developments aim to improve the still incomplete similarity (equal strength value should provide the same lifetime) and trends can be observed towards complete strength, total life and multi-scale modelling. Fatigue damage criteria tend to become more generalized formulations and the number of corresponding fatigue resistance curves reduce accordingly, satisfying small-scale specimen, large-scale specimen and full-scale structure welded joint fatigue resistance similarity at the same time.

Incorporating all four interacting fatigue resistance dimensions explicitly in the model description eliminates influence factors (e.g. for multiaxiality, residual stress, variable amplitude loading & response and corrosion) and provides a complete fatigue damage criterion (Section 3.4). Correlation of medium and high cycle fatigue; involving respectively a crack growth and initiation governing lifetime, requires matching of crack damaged and intact geometry parameters to provide a total life fatigue damage criterion (Section 3.5). Additional macro, meso and micro fatigue damage mechanism information – physics at a smaller scale – can be used to enhance an engineering based model, providing a multi-scale fatigue damage criterion (Section 3.6).

Because the fatigue damage sources in materials are randomly distributed, the critical (i.e. largest) one defines the fatigue resistance. The probability of fatigue induced failure can conceptually be estimated using a series system description: a geometry (i.e. structural member assembly) is as weak as its weakest material link, introducing the statistics of extremes to the fatigue damage criteria formulations (Section 3.7).

3.1 Overview

Fatigue involves physics across four interacting dimensions: material, geometry, loading & response and environment. Material and geometry typically define the reference resistance; loading & response and environment are involved as influence factors.

Different assessment concepts; fatigue damage criteria and corresponding resistance curves, accounting for endurance and mechanism contributions, have been developed over time and reviewed, including recent contributions (Fricke, 2003, Radaj et al., 2006, Hobbacher, 2009, Radaj et al., 2009a, Radaj et al., 2009b, Rizzo, 2011, Fricke, 2015, Radaj, 2015, Vormwald, 2015, Hobbacher, 2016, Lotsberg, 2016), proposed to be classified (Den Besten, 2019) according to (Figure 2):

- global or local information criteria,
- intact or crack damaged geometry criteria,
- stress (intensity), strain (intensity) or energy (density) parameter criteria,
- point, line or area/volume- and defect size or crack increment process zone criteria
- with annotations:
- critical, integral or invariant plane criteria,
- infinite or finite life region criteria.

The scale relative to the hotspot defines if the fatigue damage criterion is a global one at structural detail level or a local one taking (weld) notch information into account.

Fatigue damage criteria involving the structural response of the intact geometry type: stress, strain or energy, depending on work hardening, elastoplasticity and multiaxiality considerations, are related to the stress or strain concentration factor as governing crack initiation parameter. Crack damaged geometry criteria: crack tip stress intensity, strain intensity or energy density, are linked to the growth controlling stress or strain intensity factor. Alternatively, continuum and discrete damage mechanics models can be adapted to estimate the initiation and growth lifetime contribution using respectively damage evolution functions which describe the deterioration of the material mechanical properties and cohesive zone or damage mechanism formulations.

Following the critical distance theory (Taylor, 2007) the considered process zone relates the response mode-I, -II and -III specific, plane geometry characteristic and (elastoplastic) microstructural material properties for a particular environment at the different stages of the fatigue damage process to the weld notch geometry effective fatigue damage criterion: a fatigue limit- or threshold parameter in the infinite life region and initiation- or growth resistance criterion in the finite life region. For intact geometry parameters the process zone can be defined in terms of distance, length, area or volume; for crack damaged ones in terms of defect size or crack increment. The process zone values are either constant in the infinite life region or response level dependent on the finite life region since the relative initiation and growth contributions to the total fatigue lifetime are response level dependent.

Fatigue damage criteria are typically developed for a certain plane and lifetime region as reflected in the annotations. Shifting application from one plane or region to another, however, has modelling consequences, particularly important for multiaxial loading & response conditions.

3.2 Damage criterion advances

Following the fatigue assessment concept overview, damage criteria advances and highlights will be discussed and evaluated regarding modelling capabilities and assessment results.

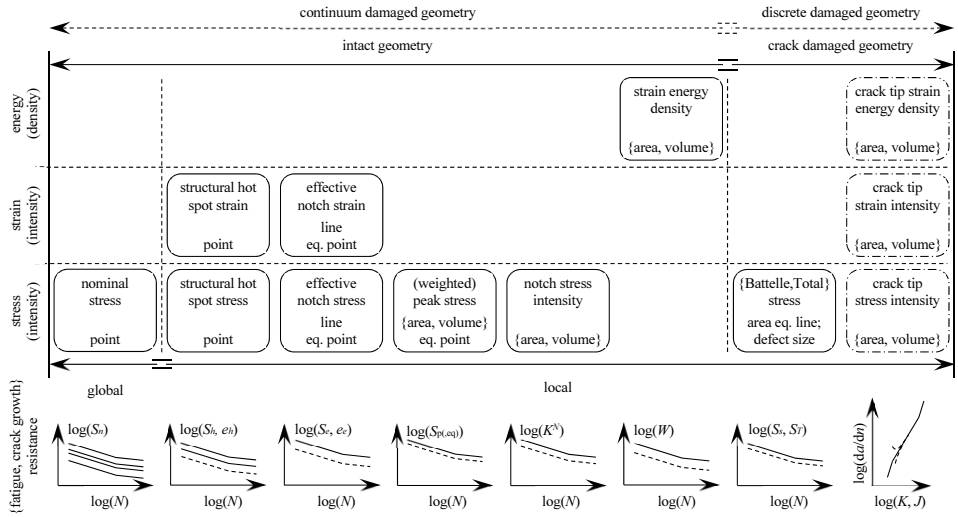

Figure 2: Fatigue assessment concept overview (Den Besten, 2019).

3.2.1 Hotspot structural stress

Based on a 3D solid finite element formulation, a less mesh-sensitive calculation procedure has been proposed and verified satisfying the original definition. The traction based structural stress has been calculated using either a force- or work equivalent approach involving the internal nodal forces on the imaginary cut planes (Lotsberg, 2016), in a similar manner as has been proposed before (Dong, 2005, Taylor, 2007, Kim et al., 2015).

Following the '1 [mm]' and 'equivalent zero' stress location proposals in through-thickness direction, the weld toe hotspot location value itself has been adopted in order to obtain a structural hot spot stress estimate eliminating thickness (i.e. stress gradient) effects (Dong, 2010).

Fatigue test results for arc-, laser- and hybrid welded steel thin plate specimens have been analysed using the structural hot spot stress concept. Angular misalignment induced secondary bending requires (non-linear) plate straightening to be explicitly incorporated because of significant structural response effects (Fricke et al., 2015, Remes et al., 2015). A resistance curve slope value of 5 shows a better fit in comparison to the commonly adopted value of 3.

For box-stiffened panels in watertight (hot spot type C) and non-watertight (hot spot type A) configuration fatigue resistance information has been obtained and compared to data available in the literature using the structural hot spot stress concept. Particular attention has been paid to the local weld geometry induced structural stiffness for shell finite element models (Yokozeki & Miki, 2016).

A comparison of tubular joint structural hot spot stress concentration factors obtained using DNV·GL guidelines and FE analyses showed that for simple uni-planar joints the guideline-based values provide realistic estimates. However, the influence of local (weld) geometry can be significant (Maheswaran & Siriwardane, 2016).

3.2.2 Effective notch stress

An effective notch stress estimate can be obtained by averaging the notch stress distribution over a microstructural material characteristic length (Neuber) or by adopting a value at a critical distance from the notch (Peterson). Average characteristic length values have been proposed analysing fatigue resistance data of steel welded joints: 0.40 [mm] and 0.10 [mm] respectively (Baumgartner et al., 2015), although principally response level dependent ones are required in

the finite lifetime region because the initiation and growth contributions are response level dependent. An averaged stress or a critical distance value can be adopted to prevent for structural strengthening or weakening in case of thin plate joint applications like typically introduced for the IIW based fixed reference radius of 1 [mm] using the peak stress as effective notch stress estimate.

Examining the fatigue lifetime consequences of small notches, the classical results of Neuber and Peterson can be interpreted as average/critical stress or strain over a small volume that depends on the solution of a continuum mechanics elasticity problem. Using examples, this interpretation permits generalization of results to cases outside the range of parameters considered in conventional design (Szabo et al., 2016).

Using notched bar specimen fatigue test results, the microstructural material characteristic length has been shown to be loading & response level dependent indeed. A linear relationship has been proposed (Krzyzak et al., 2015).

The fatigue strength data scatter observed for laser-hybrid welded 3 [mm] steel plate butt joints have been related to the actual weld profile using high-resolution measurements (Liinalampi et al., 2016). Adopting the effective notch stress as damage criterion, captured using stress averaging rather than a fictitious notch radius, shows that the most likely – material characteristic – stress averaging length is significantly smaller than the commonly assumed value of 0.4 [mm] for joints with larger plate thickness – a geometry parameter.

The fatigue strength of Invar (Fe-Ni) alloy welded joints, typically used in LNG containment systems, has been established using raised edge- and overlap joint specimens adopting the effective notch stress concept. The IIW prescribed reference radius of 0.05 [mm], a blunt crack tip value, has been applied because the plate thickness is less than 1.5 [mm]. For a resistance curve slope of 5, the FAT class is established at 434 [MPa] for a principal stress based response; a value below 630 [MPa] corresponding to the IIW steel FAT class (Oh et al., 2014).

Using ordinary- and total least squares regression (the latter does not distinguish an independent- and a dependent parameter), fatigue resistance data of as-welded butt joints has been investigated using the effective notch stress concept. The strength value obtained using ordinary least squares and a fixed slope of 3, FAT198, is below the IIW defined value: FAT225. For a total least squares regression the fatigue strength value increases significantly. The local mean (residual) stress may explain some inconsistencies between data series as reported in the literature (Nykanen & Bjork, 2015).

Crack initiation locations in lap joints and cover plates for weld toe- and weld root notches have been identified by using Neuber´s stress averaging rather than the IIW procedure involving the peak stress related to a reference radius of 1 [mm]. The reference radius induced key-hole for weld root notches typically provides an overestimated effective notch stress. Results are in agreement with experimental observations (Dong & Guedes Soares, 2015b).

For mixed mode-I and -II response conditions at V-shaped notches with a root hole, the loading & response and geometry dependent support factor have been investigated analytically and numerically adopting a maximum tangential stress based crack angle in order to enable Neuber's stress averaging along the crack path (Berto, 2015b).

In case the weld notch stress concentration is relatively low, like for weld toe notches of butt joints containing a non-negligible real notch radius, the typically adopted IIW reference radius of 1 [mm] may require a modification. Depending on the response level the plane geometry reference resistance may become important since fatigue damage could develop in the base material rather than in the heat affected zone; the base material curve is governing in the medium cycle fatigue range (Rother & Rudolph, 2011).

3.2.3 Effective notch strain

The far-field structural response is typically elastic, whereas cyclic (notch) plasticity is a requirement to develop fatigue damage, illustrating the importance of elastoplasticity relations. Neuber's rule has been widely adopted.

Analytical elastoplastic stress and strain estimates at the root of V-shaped sharp and blunt notches have been obtained for a mode-III response condition, relating the elastic and plastic control volume averaged strain energy density contour lines. For blunt notches the point-wise relation is in agreement with Neuber's rule; for sharp notches, a strain hardening correction becomes involved (Zappalorto & Lazzarin, 2014, Zappalorto, 2015).

Introducing an advanced mean (residual) stress model, the effective notch strain formulation has been modified (Savaidis & Malikoutsakis, 2016). Fatigue test data of motor truck axle casings containing intermittent welds including the governing starts and stops, obtained for different types of loading at different load ratios, has been used for verification purposes and good agreement has been observed.

Paying particular attention to the fatigue assessment of weld ends (starts and stops) in thin-plated structures, effective notch strain concept improvements concerning mean (residual) stress effects including relaxation have been proposed and verified (Malikoutsakis & Savaidis, 2014).

An effective notch strain estimate has been obtained for a welded joint in a web-frame corner of a ship (Dong & Guedes Soares, 2015a). Uncertainties with respect to material and geometry properties have been taken into account (Dong & Guedes Soares).

Abnormal (freak) wave loading induced low cycle fatigue consequences have been investigated for an offshore wind turbine. Adopting Neuber's rule the linear elastic stress has been translated to a local strain criterion (Yeter et al., 2014b, 2015e, 2016a).

3.2.4 Notch stress intensity

A benchmark study regarding the numerical computation of the weld notch stress intensity shows that an extensive effort in terms of a very fine mesh or a high polynomial degree in case of *p* refinement is required in order to obtain accurate estimates (Fischer et al., 2016a).

The available resistance design curves for the notch stress intensity concept have been questioned with respect to misalignment effects, which should be included for local fatigue damage criteria (Fischer et al., 2016c).

3.2.5 Strain energy density (SED)

A state-of-the-art concept review (Radaj, 2015) shows the modelling developments for the fatigue strength assessment of sharp and blunt V-notches subjected to uniaxial loading, systematically extended to (mixed) multiaxial conditions. Applications to welded joints are provided and numerical computations using coarse finite element meshes are proven to be acceptable for accurate local strain energy density evaluations.

Taking advantage of coarse mesh finite element models sufficient to obtain the peak stress (Section 3.2.6) based notch stress intensity factor estimates, closed-form expressions for the strain energy density as a function of the notch stress intensity have been related to the peak stress and have been verified to be a rapid procedure to evaluate the strain energy density in a systematic comparison to direct (fine mesh) finite element results (Meneghetti, 2015, Meneghetti et al., 2015). Using nodal stresses, modelling of the control volume is even not required anymore, and still accurate averaged strain energy density values can be obtained. Extending the application for long cracks to short cracks (at notches) require that except the first order stress intensity higher order terms need to be considered as well, the second order

term; the T-stress. The first order term is obtained using the crack tip node, the second order term using selected nodes along the crack edge (Campagnolo et al., 2016).

Re-analysis of welded joint fatigue test data provided a slightly different strain energy density control volume radius; a material property. The notch stress intensity based fatigue strength values changed accordingly (Fischer et al., 2016c).

Fatigue tests have been conducted using specimens containing artificial notches with different notch radius, opening angle, material structure and material strength to validate the strain energy density fatigue design curve for different types of welded joints and failure locations. Differences in endurance (intercept logC) and mechanism (slope m) show that care should be taken when assessing welded joints with geometry and loading and response conditions different from the data used to establish the design curve (Fischer et al., 2016b).

A benchmark study regarding the numerical computation of the strain energy density shows that accurate estimates can be obtained, even for a relatively coarse mesh. However, if the involved control area increases more than the local stress concentration, the strain energy density can be underestimated, like that shown for a butt joint geometry (Fischer et al., 2016a). Using the weld notch stress intensity based strain energy density fatigue damage criterion, fatigue test data involving joints connecting bulb profiles has been re-analysed and shows in relation to the available design curve similar or even better accuracy if compared to other criteria (Fischer et al., 2015).

3.2.6 Peak stress

The (elastic) peak stress is a simplified finite element based fatigue damage criterion approximating the weld notch stress intensities and weld notch strain energy densities at V-shaped notches. A state-of-the-art review shows a link to the effective notch stress as well, allowing for knowledge transfer from one concept to the other (Radaj, 2015).

Using the weld notch stress intensity based peak stress fatigue damage criterion, fatigue test data involving joints connecting bulb profiles have been re-analysed and shows in relation to the available design curve similar or even better accuracy if compared to the nominal-, structural hot spot- and effective notch stress concept (Fischer et al., 2015).

The weld toe and weld root failure induced fatigue strength of butt joints has been investigated using the weld notch stress intensity based peak stress as damage criterion. Since the loading and local geometry effects like notch angle and plate thickness are considered, a single design curve has been established for steel and aluminium as typical construction materials. The peak stress calculation has been verified for specific element types in the commercial software Ansys library (ANSYS, 2009, Meneghetti, 2015, Meneghetti et al., 2015).

3.2.7 Battelle structural stress

Fatigue-induced failure of welded joints is either weld toe or weld root-induced. Following previous developments, an analytical effective stress formulation involving the normal and shear traction structural stress components has been established to determine the failure mode transition and can be used as well to obtain the minimum required weld dimensions to ensure weld toe induced failure. The closed form solution defines, for weld root-induced failures, the critical weld throat plane and provides a weld toe failure induced equivalent stress, meaning the master S-N curve formulation can be adopted to estimate fatigue lifetime (Xing & Dong, 2016). Low cycle fatigue applications have developed as well involving the structural strain (Dong et al., 2014, Xing et al., 2016, Xing et al., 2017).

3.2.8 Total stress

Aiming to improve similarity, another crack damaged geometry baseline (equivalent point) criterion has been proposed (Besten, 2015). The Mode-I far-field stress distribution in each cross-section along the weld seam has been related to semi-analytical through-thickness weld notch

stress distribution formulations along the expected crack path, involving a self-equilibrating weld geometry stress – consisting of a local V-shaped notch- and weld load carrying part – and equilibrium equivalent global structural field stress contribution; a refinement of a well-known definition. Exploiting (non-)symmetry conditions, a generalized formulation demonstrating stress field similarity has been observed and extends to the welding induced thermal residual stress distribution. A linear superposition of the two distributions provides the total one. Fatigue scaling requires the complete distribution to be considered and the stress intensity factor has been adopted to translate the intact geometry related notch stress distributions into a crack damaged equivalent, turning the stress field similarity into a stress intensity similarity. Cyclic mechanical- and quasi-constant thermal residual loading introduce a crack growth driving force and defects may develop into cracks. Modifying Paris' equation, a two-stage micro- and macro-crack growth relation is developed to include both the weld notch and far-field characteristic contributions. The crack growth model integration yields a medium cycle fatigue single slope resistance relation, a joint resistance curve correlating arc-welded joint lifetime and the (finite life) total stress criterion. A random fatigue limit formulation has been adopted to incorporate high cycle fatigue taking the transition in fatigue damage mechanism from growth dominant to initiation controlled into account. As-welded small-scale specimen complete and censored data has been used to establish one (family of damage tolerant engineering) joint fatigue resistance curve(s). Full-scale structure representative large-scale specimen data has been examined to verify a small-scale specimen data scatter band fit.

3.2.9 Crack tip stress or strain intensity

An improved crack growth rate model involving the crack tip stress intensity has been proposed and validated using titanium alloy test data to estimate and unify a wide range of (creep) crack growth rates, including loading & response ratio-, overload- and dwell time effects. A simplified model has been derived and can be easily used to obtain lifetime estimates based on two series of basic mechanical properties of material (Wang et al., 2014, Wang et al., 2015a, Wang et al., 2015b).

Taking advantage of a new normalized fatigue crack growth model, an extension has been proposed and validated by adopting the cyclic J-integral or crack tip strain intensity rather than the stress intensity in order to incorporate the generalized elastoplastic crack tip conditions (Correia et al., 2016).

A previously proposed crack growth rate model for prediction of the S-N characteristics of metallic components with large microstructural defects has been extended to materials that do not show large defects on the fracture surfaces (Zerbst & Madia, 2015). An approach based on a cyclic R-curve analysis is proposed to establish the initial defect size. The principle is explained and demonstrated by a first application to welded joints.

A theoretical model for the fatigue crack growth rate has been established based on the effective crack tip cyclic plastic zone involving an empirical crack closure expression and the low cycle fatigue properties. A good fit with experimental data has been obtained (Shi et al., 2016).

Recognizing the difference between the analysis tools needed for design and maintenance to estimate crack growth, modelling of small defects developing into cracks and ways to determine the short crack growth rate characteristics from long crack growth data have been discussed (Jones, 2014). It is shown how existing models can be used and how variations in crack growth histories can be accounted for.

Adopting the strategy to model crack growth as shape perturbation of a domain with existing cracks, a numerical approach has been proposed to simplify the crack growth computation and yet yield accurate results. Results prove the accuracy in comparison to numerical and experimental results available in the literature (Formica & Milicchio, 2016).

Williams' crack tip stress field power series expansion has been used to estimate the extent of the nonlinear zone, important for the fatigue assessment of non-brittle materials (Vesely et al., 2016). The characteristics could be potentially incorporated into methods to determine the fatigue behaviour descriptors of materials exhibiting nonlinear failure. The developed procedures simplify the analysis of the description of mechanical fields at a greater distance from the crack tip considerably.

A modification of the Gauss–Chebyshev method for stress intensity factor computation has been proposed, incorporating the Richardson extrapolation method (Dubey & Kumar, 2016). The more accurate solution has been obtained after a few numbers of iterations in comparison to the method in its original form.

A procedure for fatigue life assessment of welded joints based on a plasticity-corrected stress intensity factor range is developed using monotonic fracture mechanics techniques and has been modified for cyclic loading. A so-called cyclic resistance R-curve for short cracks has been introduced (Madia et al., 2017). The procedure has been validated with a large number of test results for different materials and welding methods. The stress intensity factor solutions of semi-elliptical cracks with high aspect ratios in plates and thick walled cylinders have been parametrically investigated under various stress distributions adopting a virtual crack closure-integral method (Okada et al., 2016). For the cracks in thick-walled cylinders, the stress intensity can be approximated using flat plate solutions.

Different (extended) finite element method based mode-I stress intensity factor calculation methods have been compared (Fischer & Fricke, 2015) for compact tension specimens. The J- and interaction-integral provide relatively accurate results. Although extended finite element methods show crack modelling advantages, oscillations in 3D have been observed due to extraction domains. The best results are obtained with domain integrals using the finite element method with a refined mesh.

Finite element- as well as analytical solutions are employed to obtain the stress intensity factor for similar and dissimilar welds in lap-shear joints underpinned and clamped boundary conditions (Sung & Pan, 2016). Solutions indicate that clamped boundary conditions reduce the stress intensity factor for a given geometry about 7% for similar welds and about 20% for dissimilar welds, providing a higher welded joint fatigue lifetime.

The limitations associated with implicit and explicit representations of cracks in the extended finite element method are investigated for non-planar 3D cracks in a numerical study and a novel hybrid approach has been developed. Effectiveness has been demonstrated using examples (Sadeghirad et al., 2016).

An overview of adaptive re-meshing techniques to evaluate the crack front shape evolution and fatigue life has been provided, including a systematic identification of the main numerical (and physical) variables affecting the accuracy (Branco et al., 2015). Several issues are still unsolved. Future challenges include the development of more efficient procedures to estimate (3D) crack paths and fatigue lives in complex geometries subjected to non-proportional mixed-mode loading. Computational algorithms being able to perform automatic transitions from the surface or corner cracks through cracks for both in-plane and out-of-plane propagation are required as well. Other challenges include non-symmetrical crack growth, propagation in non-isotropic materials, defect-crack interactions and crack interaction in case of mixed-mode loading.

To estimate the residual fatigue life once cracks are identified, a semi-analytical approach has been proposed involving analytical stress intensity factor formulations as well as finite element method solutions. Its potential is demonstrated by studying the crack propagation effects on the fatigue lifetime of typical joints (Lou et al., 2015).

Numerical crack propagation simulations have been performed for different welded joint geometries to investigate the influence of geometry complexity (Fischer et al., 2015, Fischer et

al., 2016c, Fischer et al., 2016b). The stress gradient over the plate thickness, the apparent plate thickness and the notch effect slows down the crack propagation rate if the same stress value being effective for fatigue appears at the weld toe. The weld load-carrying level, the weld flank angle and the geometrical configuration affect both the notch effect and the local stress concentration. Accordingly, the fatigue assessment using a single-point fatigue parameter might be problematic because the crack propagation phase is strongly affected by the stress distribution along the crack path.

An equivalent initial defect size has been determined to estimate the fatigue strength of welded joints. One experimental data point is involved, reflecting the stress concentration effect at the fatigue critical location which is assumed to be approximately equivalent to a crack in an unwelded plate. The fatigue lifetime is calculated using the Paris relation accordingly. Application using constant amplitude fatigue data shows good agreement between the calculated and experimental fatigue lifetimes (Mikkola et al., 2015).

3.2.10 Crack tip energy release rate

Linear elastic fracture mechanics have provided a basis to describe damage growth using stress intensity factors or strain energy release rates. Discussing the fatigue crack growth equations presented in the literature, it is demonstrated that the principles of similarity in current methodologies have not yet been well established. As a consequence, corrections for the loading & response ratio effect are misunderstood and an alternative principle of similitude using cyclic work and strain energy release is proposed (Alderliesten, 2016).

The complex-valued finite element method is proposed as a new virtual crack extension method to compute the energy release rate (Millwater et al., 2016). Using a complex Taylor series expansion, the energy release rate is obtained as a numerical derivative of the strain energy with respect to a crack extension. This method retains the conceptual simplicity of numerical differentiation but eliminates numerical issues regarding perturbation of the crack size. The obtained energy release rate shows the same accuracy as the J-integral based results.

3.3 Damage mechanics criterion advances

Continuum or discrete damage mechanics criteria can be adopted to estimate the initiation and growth lifetime contribution using respectively damage evolution functions to describe the deterioration of the material mechanical properties (e.g. based on effective stress or Young's modulus as intact geometry parameters) and crack cohesive zone or -damage mechanism formulations (Den Besten, 2019).

To address plasticity – particularly useful for notched geometries, a damage-coupled elasto-plastic constitutive model has been employed enhancing the typically linear elastic continuum damage mechanics criteria. Both uniaxial and multiaxial non-proportional loading & response conditions can be dealt with. Damage estimates are compared to experimental data and agree well (Shen et al., 2015).

3.4 Complete strength criteria

The fatigue damage criterion defines in terms of resistance the fatigue strength scatter; i.e. structural integrity, and can be improved towards complete strength (Den Besten, 2019) by taking the resistance dimensions: material, geometry, loading & response (e.g. multiaxiality, mean- and residual stress) and environment (e.g. corrosion) dimensions explicitly into account.

3.4.1 Multiaxiality and amplitude variability

Although the ship and offshore structural stiffness distribution is predominantly orthotropic (stiffened panels) or member orientation defined (trusses, frames), both loading and geometry induced multiaxial welded joint far field response locations can be observed, consisting of Mode-I and mode-III contributions in the typically thin-walled structural members; a 3rd fatigue

resistance dimension aspect. At the weld notch locations, the response is multiaxial by definition because of cross-sectional (stiffness) changes, introducing the (geometry induced) mode-II component. The considered plane, i.e. of the critical, integral or invariant type can principally be adopted for all fatigue damage criteria and is typically correlated to another loading & response component: (random) variable amplitude behaviour, paying attention to non-proportionality coming along with principal stress directional changes.

For critical plane based multiaxial fatigue damage criteria, plane selection is very important. In order to understand crack development, calculated stress-strain fields have been represented in polar diagrams to show the loci of maximum stresses or strains with respect to the plane orientation. Measured crack paths can be superimposed. Cracks in plane geometries were found to develop at both planes of maximum normal or shear strains and there might be equal chances for a crack to initiate and grow along different paths. Regions showing at which planes cracks could possibly initiate and grow have been obtained (Albinmousa, 2016).

The ratio of the Mode-I normal- and mode-III shear resistance is lifetime-dependent, meaning that in case the fatigue damage criterion is an equivalent stress the involved coefficients are principally lifetime dependent as well. For several critical planes based on equivalent stress fatigue damage criteria, the lifetime estimate consequences have been investigated using experimental data for several materials. In comparison to the conventional approach involving constant coefficients, improved results have been obtained (Karolczuk et al., 2016).

The accuracy of the Modified Manson Coffin Curve concept in estimating fatigue lifetime of metallic materials subjected to complex constant and variable amplitude multiaxial loading & response has been investigated (Wang & Susmel, 2016). The adopted critical plane is based on the maximum shear strain variance of the deviatoric strain time series. Resolving shear strain cycles using rain-flow counting and incorporating mean stress effects using the hydrostatic strain component, the sound agreement between lifetime estimates and experimental data has been obtained.

Taking damage contributions from the normal- and shear strain amplitude, the hydrostatic mean strain as well as path-dependency into account a critical plane approach has been proposed for plane geometry low cycle fatigue applications. Validation using experimental data for different materials demonstrates the effectiveness (Li et al., 2014a, Jiang et al., 2016, Tao et al., 2016). Elastoplastic response calculations are an important element of low cycle fatigue assessment. In case of non-proportional multiaxiality 6D, incremental plasticity calculations are required to correlate all stress and strain components. However, a large number of multiaxial fatigue problems involve tension/compression, bending and torsion loads, which are associated with only one normal and one shear stress component. A new 2D incremental elastoplasticity formulation has been introduced integrating non-linear kinematic hardening models and non-proportional hardening effects in a very efficient way. Tension-torsion calculations from more general 6D models are exactly reproduced, but with less than one-fifth of the computational cost. Validation provided good agreement (Wu et al., 2016).

A critical plane based model utilizing the theory of critical distances has been proposed for multiaxial high-cycle fatigue lifetime evaluation (Liu, 2015). The maximum shear stress range plane is defined as the critical one. The maximum effective shear stress amplitude and the maximum effective normal stress, obtained by averaging the stress in the hemisphere volume around the maximum stress point, are the involved damage parameters. Lifetime estimates are in good agreement with aluminium plane- and notched geometry test data.

An elastoplastic generalized strain parameter involving normal- and shear contributions, representing respectively growth and initiation contributions, has been proposed as fatigue damage criterion. The plane showing maximum damage is adopted as the critical one. Analysis results and notched geometry experimental data are in agreement (Ince & Glinkab, 2016).

The effective notch stress has been obtained for V-shaped notches with root hole subjected to mixed-mode I and II response conditions (Berto, 2015a). The involved fictitious notch radius is determined as a function of the real notch radius, the microstructural support length and the notch opening angle. Adopting Neuber's original procedure an analytical formulation has been established to provide the microstructural support factor as a function of the mixed-mode ratio and the notch opening angle. Values have been verified using finite element models.

Relating the structural hot spot stress fatigue damage criterion and a critical plane approach, the welded joint multiaxial fatigue resistance has been investigated for different loading & response conditions, showing its effectiveness through substantive test data (Li et al., 2014a, Jiang et al., 2016, Tao et al., 2016).

Although not much mixed-mode crack growth rate test data under non-proportional loading conditions are available in the literature, some presented data (Feng et al., 2006) continues to be a subject of intense investigations (Mei & Dong, 2016, 2017b, a). The 90 [deg] out-of-phase mixed-mode I and III loading & response case seems the most puzzling one and available models hardly offer a reasonable explanation of the data trends. Adopting the moment-load-path based fatigue damage criterion definition (Dong et al., 2010), coupled with a geometric mean based maximum effective stress intensity factor, a two-parameter non-proportional mixed-mode crack growth model seems to provide a rather satisfactory data correlation (Mei & Dong, 2017b). In addition to its ability to consistently capturing proportional and non-proportional loading & response fatigue damage effects, the path-dependent-maximum-range and moment-load-path based approach has been adapted for fatigue design and lifetime evaluation of welded structures (Dong, 2001) by developing an equivalent structural stress range parameter, which includes the mean stress- and far-field stress gradient induced size effects (Dong et al., 2010). A comparison of lifetime estimates for welded joint test data available in the literature to IIW (Hobbacher, 2013) as well as Eurocode 3 (CEN, 2005) results demonstrates its effectiveness.

Experimental studies show that a non-proportional multiaxial constant amplitude loading & response is more damaging than a proportional one and depends on the involved loading & response path as well as material. Under non-proportional multiaxial variable amplitude loading & response conditions, any fatigue assessment concept must also provide an effective method to establish the number of cycles, either by counting or a stochastic approach.

One important development towards developing an integrated definition of a multiaxial fatigue damage criterion and a multiaxial (half) cycle counting procedure is the path-dependent-maximum-range / moment-load-path based approach (Mei & Dong, 2016, 2017b, a). One deficiency in the original path-dependent-maximum-range approach (Dong et al., 2010, Wei & Dong, 2014) addressed is that non-proportionality induced fatigue damage is calculated based on path length traversed in either stress or strain space. Both simple and rather complex forms of non-proportional multiaxial loading & response paths were examined for demonstrating the method's effectiveness in test data correlation (including structural steel and aluminium welded joints) as well as its applications for fatigue design of welded structures (Wei & Dong, 2014). Based on Wang and Brown's reversal counting method, a new critical plane approach has been proposed for plane geometries based on a weight-averaged maximum shear strain range. For low- and medium cycle fatigue test data the approach shows satisfactory lifetime estimates (Li et al., 2014a, Jiang et al., 2016, Tao et al., 2016).

For random amplitude multiaxiality, a stochastic damage estimate can be obtained by adopting Laplace distributions (Karlsson et al., 2016). Explicit formulae for the expected value of the rain flow damage index as a function of excess kurtosis are provided for correlated loads. Measurement results have been used for illustration and demonstration purposes showing the accuracy of the damage estimate.

The effectiveness of common equivalent stress- and strain-based fatigue damage criteria have been evaluated and areas of improvement have been discussed. Mixed-mode hypotheses, sequence- and size effects are considered to be most important and require further investigation, as well as the development of simplified procedures in order to reduce computation time (Vormwald, 2015).

Bi-axial fatigue tests have been conducted using plane geometry specimens in order to validate critical plane based fatigue damage criteria with respect to crack orientation and lifetime estimate. Conservative, as well as non-conservative results, have been obtained (Lopez-Crespo et al., 2015b).

Common equivalent stress- and strain based multiaxial fatigue damage criteria have been evaluated using experimental data (Gates & Fatemi, 2016). Mean stress effects were considered as well using different models. Variable amplitude lifetime estimates are compared to constant amplitude values to highlight similarities and differences in lifetime trends. Overall, mixed results were obtained. Both constant and variable amplitude fatigue lifetimes are predicted well for notched geometries. The importance of stress gradient effects has been demonstrated as well. However, for plane geometries, a consistent trend of non-conservative lifetime estimates for variable amplitude loading conditions has been observed.

Observing fatigue test results for the plane- and notched geometries, cracks initiate at the maximum shear plane. Lifetime estimates obtained using different multiaxial fatigue damage criteria show mixed results, typically lacking consistency for different loading & response paths (Gates & Fatemi, 2014).

Laser-stake welding can be used to produce steel sandwich panels, joining plates of 10 [mm] thickness with web plates. Fatigue tests were performed applying axial, shear and in-phase multiaxial loading to the panels. A nominal- and effective notch stress fatigue damage assessment shows that Eurocode 3 and IIW interaction equations can provide safe designs (Fricke et al., 2016).

To evaluate the performance of different multiaxial fatigue damage criteria for welded joints, the probability of achieving a non-conservative fatigue lifetime estimate has been calculated using experimental data collected from the literature. A large variety in safety has been observed, especially for non-proportional loading & response (Pedersen, 2016).

For the assessment of multiaxial fatigue in welded joints, a wide variety of methods have been suggested. For comparison purposes, several load cases were defined. Considering codes as well as models available in the literature, it has been concluded that non-proportional variable amplitude loading has a significant negative impact on the fatigue lifetime estimates (Van Lieshout et al., 2016).

A preliminary study has shown up to what extent multi-axiality can affect fatigue damage for welded joints in a container ship (Bufalari et al., 2017).

The weld root-induced fatigue strength of inclined butt joints in a proportional multiaxial far field response condition has been investigated using the nominal- and effective notch stress as fatigue damage criterion (Khurshid et al., 2016). To account for multi-axiality, the former has been used in combination with the modified Gough–Pollard interaction equation, the Eurocode 3 guideline and the DNV standard; the latter criterion involved a principal stress- and Von Mises stress hypothesis as well as the modified Wöhler curve approach. Results are evaluated along with data published in the relevant literature. The modified Wöhler curve approach seems to be the most suitable tool for multiaxial fatigue evaluation in case of a far-field multiaxiality.

Adopting a single edge notch specimen subjected to eccentric non-symmetric four-point bending, crack growth has been investigated incorporating the mixed-mode I and II contributions. The crack growth direction is estimated using different criteria including the maximum tangential stress, the strain energy density and the crack tip displacement. Multi-parameter fracture

mechanics involving several terms of Williams' power series solution has been employed. Whereas for the tangential stress and strain energy density criteria the first order term is accurate enough, the crack tip displacement criterion requires higher order terms to be involved (Malikova et al., 2015, 2016).

To improve understanding of proportional and non-proportional mixed-mode I and III loading & response conditions the crack growth behaviour at notches have been investigated experimentally using digital image correlation, providing a crack path, crack growth lifetime, crack tip deformations and crack closure information (Hos et al., 2016).

Fatigue crack propagation in case of biaxial tensile loading has been investigated (Gotoh et al., 2015). Tests are performed by investigating phase effects. An advanced fracture mechanics approach has been developed based on the re-tensile plastic zone generating a stress criterion for crack propagation and simulation results are compared to measurement data.

Mixed-mode I, II and III propagation of a pressurized circular crack subjected to various loading conditions has been investigated numerically (Schwartzkopff et al., 2016). The proposed crack front propagation algorithm based on the maximum tangential stress criterion aligns well with published results. The algorithm consumes only a fraction of the time needed for a numerical simulation and could be useful for design.

3.4.2 Mean- and residual stress

A mechanical loading & response cycle is defined by two parameters, for example, amplitude or range and mean stress; another 3rd fatigue resistance dimension aspect. Both parameters contribute to fatigue damage up to some extent, depending on (base) material properties; either metals or polymer composites. For welded joints, the quasi-constant welding-induced residual stress acts as mean stress as well.

A phenomenological fatigue resistance relation for single crystal metals, including lower and upper bound asymptotic behaviour corresponding to respectively ultimate strength and endurance limit, has been established. The stress amplitude- and mechanical mean stress contribution have been superimposed. Validation using experimental data with mechanical loading & response ratios in a large range varying from negative up to high positive values provided good results. Application to polycrystalline metals is suggested (Chandran, 2016).

Low- and medium cycle displacement controlled fatigue resistance information for base metal has been obtained at different mean strain values. Mean strain has been found to be more important in the medium cycle fatigue range. In terms of modelling, different existing models have been validated and in particular, Morrow's model provides good results (Carrion et al., 2017).

More displacement controlled fatigue resistance information for base metal has been obtained at several mean strain values. In general, the fatigue life decreases with increasing loading & response ratio and becomes more important for decreasing amplitude. An empirical model has been modified in order to obtain more accurate lifetime estimates (Hao et al., 2015).

For a super elastic metal, the mean stress and -strain effects on low- and medium cycle fatigue resistance have been investigated. Adopting a stress or strain based fatigue damage criterion including respectively a mean stress or strain correction, no satisfactory results have been obtained. An energy-based fatigue damage criterion incorporating both stress and strain has been selected, involving the dissipated energy density as well as the tensile elastic energy density to incorporate tensile mean stress effects (assuming that compressive mean stress does not affect fatigue damage), in order to obtain accurate lifetime estimates (Mahtabi & Shamsaei, 2016).

Knowing that for increasing loading & response level, the material temperature increases as well, a two-parameter heat energy fatigue damage criterion has been proposed. The criterion includes the specific heat loss and thermos-elastic temperature corresponding to the maximum cycle level, respectively incorporating the stress range and mean stress contributions. The

model correlates base metal medium cycle fatigue test data for a wide range of loading & response ratios (Meneghetti et al., 2016).

In case of high-temperature applications, both mechanical and thermal loading & response cycles can be important, and creep-fatigue may become an important failure mode. A modified strain energy density exhaustion model has been proposed, including mean stress effects. Accurate lifetime estimates have been obtained in comparison to base metal test data at different temperatures and loading & response conditions (Wang et al., 2016b). Based on a strip-yield methodology a new creep-fatigue crack extension model has been presented. Comparison to experimental data for a range of materials, temperatures and stresses shows its capabilities and limitations (Andrews & Potirniche, 2015).

The quasi-constant welding-induced residual stress distribution close to the weld notch is typically tensile like the mechanical loading induced response. To quantify the residual stress effects on fatigue strength, the residual stress distribution in terms of the weld notch stress intensity has been translated into a strain energy density formulation. Numerical analysis has shown that for high far-field stress levels the residual stress is redistributed and even converted into a compressive distribution. The residual stress redistribution has been found to be negligible for lower far field response levels. A tensile residual stress reduces the fatigue strength (Ferro, 2014).

The fatigue crack growth behaviour of high strength steel welds has been investigated, paying attention to the influence of microstructure and welding-induced residual stress. An effective stress intensity factor range has been proposed as a crack growth driving force (Wang et al., 2017b).

Using thermo-mechanical finite element calculations, the welding-induced residual stress redistribution has been investigated for cyclic loading & response conditions. The first few cycles show a significant residual stress release. An analytical model validated using measurements, has been proposed to estimate the relaxation (Xie et al., 2017). Redistribution is cyclic loading & response magnitude and -ratio dependent (Wang et al., 2017a). Adopting non-linear continuum damage mechanics, the high-cycle fatigue consequences has been investigated for a welded T-joint. A comparison to test results demonstrates its effectiveness (Lee et al., 2016).

The influence of mean stress on the fatigue resistance of polymer composite materials has been investigated and a phenomenological model has been proposed; a sum of two power terms. Six calibration parameters are involved, reflecting from loading and response point of view the tension and compression contributions from the amplitude and mean; two parameters defining a cycle, as well as material dependency. Accurate lifetime estimates have been obtained for different materials and loading & response ratios using a one parameter set, even for material data not involved in the calibration process, meaning material dependency is limited and the loading & response and geometry effects are generally applicable (Flore & Wegener, 2016).

The modified Chaboche continuum damage model has been proposed introducing non-linear mean stress dependence for fatigue assessment of polymer composites based on orthotropic damage evolution. Haigh diagrams and fatigue resistance curves have been constructed to illustrate the model capabilities (Desmorat et al., 2015).

3.4.3 Time and frequency domain

The loading & response characteristics allow for analysis in the time and frequency domain; another 3rd fatigue resistance dimension aspect. Generally speaking, frequency (i.e. spectral) domain approaches are considered less reliable but more efficient, as concluded when addressing the recent developments in the multiaxial frequency domain (Benasciutti et al., 2016). Time domain approaches, on the other hand, are more accurate but computationally expensive.

A new frequency domain approach for fatigue damage calculation in case of random multiaxial loading has been developed adopting an equivalent critical plane criterion, combining the power

spectral density functions of the involved stress components. A comparison of lifetime estimates and test results shows satisfactory agreement (Carpinteri et al., 2016).

A frequency-domain fatigue life estimation algorithm based on statistical energy analysis for structures subjected to high-frequency loading has been proposed as well. It has been observed that when evaluated at 1/3-octave bands, the root mean square value of the power spectral density function was sufficiently refined to provide meaningful life estimates (Wang et al., 2016c).

To take mean stress corrections into account, a frequency domain approach has been presented based on a direct transformation of the zero-mean stress power spectral density, which is applicable for both narrow and broadband signals. Four different probability density functions have been adopted and the Derik's formula provides a good description in comparison to test results (Niesłony & Böhm, 2016).

Based on machine learning a frequency domain method has been developed for fatigue analysis in the case of random loading (Durodola et al., 2017). The network is trained on readily identifiable parameters, such as resistance curve parameters and spectral moments. Obtained lifetime estimates are similar to time domain simulation results and improve the classical frequency domain values.

For critical hot spots in offshore wind turbines, typically a time domain analysis is performed to account for the simultaneous wind and wave induced loading as well as structure-soil interaction. For the less critical ones, a frequency domain approach can be adopted. Lifetime estimates have been obtained for different long-term response distributions, including Rayleigh and Dirlik. Akaike's information criterion has been adopted to judge the results and Dirlik's formula provides results closest to time domain simulation results (Yeter et al., 2014b, 2015e, 2016a).

Frequency domain results can consistently provide lower fatigue lifetime estimates. Two sources have been identified: an overestimated response spectrum and the Rayleigh distribution assumption. Opting for time domain calculations, the damage surface in the scatter diagram has been approximated meaning only a few sea states have to be simulated. The computational efforts are significantly reduced while maintaining high accuracy (Mohammadi et al., 2016b).

To combine the advantages of time and frequency domain approaches, the structural response spectral density function is obtained in the frequency domain and consequently converted into a response time history by using an improved signal conversion approach. The fatigue damage can be assessed using rain flow counting – important for non-proportional multiaxiality as well – and a damage accumulation model, like the one from Palmgren-Miner. The advantage is that a Rayleigh distribution assumption associated with a narrow band random process is not required. Calculations show that the hybrid approach results are more accurate in comparison to the frequency domain results and takes less computation time in comparison to a time domain approach (Du et al., 2015).

3.4.4 Environment

Ship and offshore structures, including oil and gas transport systems, operate in an aqueous and often sulphide containing sour-brine environment, meaning corrosion may appear in the material (geometry) surface. Corrosion, a 4th resistance dimension element, accelerates the fatigue damage process by deteriorating the material and geometry defined reference resistance (Den Besten, 2019). A considerable interest in improving empirical models has been observed by accounting for some of the mechanisms involved in corrosion and corrosion fatigue. The aim is to reduce conservatism and improve assessment concepts to estimate remaining lifetimes. The latter is particularly relevant since improvements have resulted in structures being operational beyond their intended lifespan. Alternative energy sources point to hydrogen storage and transportation, meaning hydrogen assisted cracking investigations are needed as well.

Using 3D surface measurements, the pitting distribution and morphology of pre-corroded steel plates have been established. Deep-narrow and wide-shallow pits have been identified, as well as a superposition of the two. For different exposure times, fatigue tests provided resistance information. Sharp and interacting pits significantly reduce the fatigue lifetime. An FE model has been used to establish the critical pit dimensions, providing the defect size for fracture mechanics based calculations to estimate the fatigue lifetime. Measurements and calculation results provided comparable results (Xu & Wang, 2015).

Single pit corrosion fatigue strength information at 10^9 cycles for steel at three different mean stress levels has been used to validate a modified El Haddad crack growth threshold model. Safe estimates are generally obtained, in contrast to the Murakami's empirical model (Harkegard, 2015).

Murakami's empirical fatigue damage criterion is difficult to apply in case the local stress state is multiaxial, like for irregular corrosion induced pitting geometries. A non-local Crossland equivalent stress criterion has been proposed; an averaged circular volume based criterion involving a critical distance, i.e. diameter. Corrosion affected fatigue strength information obtained at 10^7 cycles has been used to estimate the most likely critical diameter. FE analysis shows that for identical defects there is no interaction if the distance exceeds three times the critical diameter (May et al., 2015).

The corrosion rate in the heat affected zone, at the weld toe location, is typically higher in comparison to base material values because of the welding-induced residual stress level close to yield and the mechanical loading and geometry induced stress concentration, introducing non-uniform corrosion. The probability of fatigue induced failure increases and taking the time-dependent response into account, mechanochemical fatigue damage estimates have been obtained adopting the structural hot spot stress concept (Yang et al., 2016).

To incorporate mean stress effects affecting crack growth in a corrosive environment, a modified linear elastic crack growth model has been proposed, considering the relative crack opening period; i.e. area rather than amplitude only, as a damaging portion of a cycle. Both the strength and mechanism parameters, intersect logC and slope m, are affected. Model estimates and sinusoidal constant amplitude experimental data correlate fairly well (Adepipe et al., 2016).

To model crack growth in gaseous hydrogen conditions, a corrosion-crack correlation model has been proposed, based on Foreman's modification of the Paris relation incorporating the mechanical loading & response ratio and fracture toughness. Adopting a hydrogen-enhanced de-cohesion theory, the crack tip plastic zone size has been used to include frequency effects as well. Experiments demonstrated the model effectiveness (Cheng & Chen, 2017b).

3.5 Total life criteria

Correlation of medium and high cycle fatigue; involving respectively a crack growth and initiation governing lifetime, requires matching of crack damaged and intact geometry parameters to provide a total life fatigue damage criterion (Den Besten, 2019).

During the time, the arc-welding induced defect size has become smaller because of technological and modelling developments (Lassen, 1990, Verreman & Nie, 1996, Darcis et al., 2006, Zhang & Maddox, 2009, Hobbacher, 2010, Chattopadhyay et al., 2011, Zerbst & Madia, 2015). Values decreased from 1.00 [mm] down to 0.05 [mm], meaning even for welded joints, although the lifetime is often assumed to be growth dominated, the crack initiation contribution to the total lifetime increases in the high-cycle fatigue region.

Correlation of the initiation and growth lifetime quantifies the individual contributions and requires matching crack damaged and intact geometry parameters (e.g. notch stress intensity factor and crack tip stress intensity factor) to provide a total life fatigue damage criterion improving the strength and lifetime estimates.

Several 2-stage 2-parameter models have been proposed involving an assumed transition crack size based on different arguments: theoretical (e.g. fracture mechanics modelling restrictions), practical (e.g. detectability) as well as phenomenological (e.g. critical distance), affecting the (initiation/growth) ratio up to a large extent. A slightly different 2-stage 2-parameter model is based on a transition rate: the intact geometry stress distribution rate is equal to the crack growth rate, meaning the transition is not defined a priori. The adopted initiation and growth contributions have been incorporated adopting respectively a critical plane criterion and the crack tip stress intensity factor. Lifetime estimates are in good agreement with experimental results (Socie et al., 1979, Chakherlou et al., 2012, Mohammadi et al., 2016b).

Question is whether a 2-parameter concept is the best solution to include 2-stage behaviour. Except for the transition size, the actual as-welded joint fatigue test data is only used for calibration purposes of some crack initiation model parameters or not involved at all, assuming a series of initiation and growth similarity conditions of (standard) specimen and as-welded joints rather than a one-to-one correspondence between model lifetime estimate and *S-N* test data; a welded joint fatigue resistance similarity. As an alternative to a 1-stage 1-parameter model (e.g. the stress intensity factor as crack damaged geometry parameter and the Paris relation using a defect size equal to the intact geometry material characteristic micro and meso structural length; (Mikheevskiy et al., 2015)) or a 2-stage 2-parameter model, a 2-stage 1-parameter model like the Battelle equivalent- or Total stress can be adopted. A natural transition from a growth governing to an initiation dominated lifetime is, for example, possible by introducing a loading & response level dependent elastoplasticity coefficient (Besten, 2015), changing the crack growth characteristic from non-monotonic to monotonically increasing.

For fretting fatigue damage applications, distinct crack initiation and growth contributions have been established both numerically and experimentally, involving respectively Crossland's criterion and Paris' relation. The nucleation – growth transition has been determined to calibrate a critical distance, used as nucleation criterion location and initial crack size in order to establish the nucleation and growth lifetime (Gandiolle et al., 2016).

The multiple mechanisms in high- and very high cycle fatigue require strategies bridging multi-scale experiments and higher fidelity models. Approaches have been discussed paying particular attention to modelling of microstructure sensitive driving forces and thresholds, including challenges to predict the transition of failure mechanisms at different response levels (Castelluccio et al., 2016). Applying full-field calorimetric measurements, cyclic slip-induced microplasticity – the primary damage mechanism in the very high cycle fatigue region – has been evaluated based on an experimental energy balance. A relation to fatigue life has been established using the Manson-Coffin relation (Wang et al., 2017b).

An elastoplastic strain energy based fatigue damage model has been proposed, involving the atom dislocation movement induced crack initiation- as well as crack growth energy terms. Loading & response ratio effects are incorporated, adopting Walker's model. Using a variety of different metals with initiation and growth data available in literature the model has been validated. Damage estimates are in agreement with experimental results, although at very low strain levels some inaccuracies have been observed (Huffman, 2016).

Over the past decades, strain energy (density) has been used as fatigue damage criterion for both crack initiation- and crack growth dominated lifetimes separately. A generalized energy relationship has been developed and can be used to estimate initiation as well as growth dominated fatigue (Mohammadi et al., 2016a).

3.6 Multi-scale criteria

Additional macro-, meso- and micro-fatigue damage mechanism information – physics at a smaller scale – can be used to enhance an engineering based model, providing a multi-scale fatigue damage criterion. Following the macro-scale developments from global to local fatigue

damage criteria during the time the continuum mechanics lower bound is approaching and a correlation to the 'netherworld' (i.e. to meso- or even micro-scale physics) is a next step (Den Besten, 2019), for both base and polymer composite materials.

Numerical multi-scale models have been introduced in a new class of finite element methods, involving nodal or element enrichment, respectively X-FEM and E-FEM, meant to alleviate some of the continuum damage mechanics model limitations. To describe both short and long crack growth behaviour, a cohesive zone model and a 2D elemental enriched finite element model have been coupled. Element enrichment allows for the displacement jump over the crack front, meaning no special interface elements are required in contrast to traditional finite element modelling. Following calibration of the model parameters using the long crack mode-I Paris relation properties, a comparison of the mixed-mode short crack path simulation results and experimental data obtained using electronic backscatter diffraction shows a good correlation (Panwar et al., 2016).

Adopting the Chaboche non-linear continuum damage mechanics model, an intrinsic crack size; a process zone criterion reflecting short crack growth considerations has been derived correcting the linear elastic stress intensity factor expression. The proposed model is applicable for short and long cracks and incorporates loading & response ratio-, amplitude variability- and loading sequence effects including single and multiple overloads. Good correlation with test results has been obtained (Zhang et al., 2016a).

Using the crack density (i.e. effective stress) as a key parameter, a continuum fatigue damage mechanics criterion has been derived, modelling the trans-scale process from nucleation of many short cracks to the growth of a few long cracks, eventually up to fracture. Calibrating the five model parameters using damage evolution curves, good correlation with experimental results have been obtained (Sun et al., 2016).

The fatigue damage process from micro-defect to macro-fracture can be characterized using an energy density zone model involving scale transition functions. Parameter estimates require fatigue resistance information of plane- and notched geometries. The fatigue resistance scatter terms have been shown to be predominantly a consequence of microscopic effects (Zhang et al., 2016b).

Due to the multi-scale architecture of polymer composite materials, a wide variety of failure mechanisms can be observed. Multi-scale modelling approaches have been proposed to estimate high-cycle fatigue, based on weak spots showing visco-elastoplastic material behaviour. Scale transition has been achieved using non-linear mean-field homogenization (Krairi et al., 2016).

Since uncertainties exist in both micro- and macro-scale parameters, the fatigue performance of six commonly used failure criteria has been compared using a multi-scale reliability analysis. Homogenization methods; i.e. rule of mixtures, Mori-Tanaka and computational homogenization are adopted to link the scales and to translate uncertainties from micro- to macro-scale. In a comparison to a single-scale analysis, more accurate reliability estimates can be obtained (Zhou et al., 2016).

A new stress-based multi-scale criterion has been proposed, involving fiber as well as matrix induced failure at a microscopic level. For engineering purposes, interface-related failure has been ignored meaning the fiber size should be carefully determined. As soon as the finite (shell) element based macroscopic stress distribution has been obtained, the microscopic stresses are calculated using representative volume elements at a set of reference points; i.e. maximum stress points for different elementary loading conditions, to establish the damage evolution. Validation using open-hole off-axis tension tests show good agreement between experimental results numerical estimates (Li et al., 2014b).

A cohesive zone- and two-scale continuum damage model are coupled to estimate delamination induced fatigue of polymer composites. At macro-scale, the response is considered to be elastic; at micro-scale elastoplasticity is involved and obtained using representative volume elements (Amiri-Rad et al., 2015).

Decomposition of several signals, such as mechanical vibration and acoustic signals, into multi-scale intrinsic mode functions by the empirical mode decomposition technique has been conducted and a new adaptive multi-scale spectral features selection approach has been proposed, based on a sphere criterion which was applied to the intrinsic mode function frequency spectra (Tang et al., 2016).

3.7 Damage criterion statistics

At a materials level, crack initiation is typically related to plasticity at the micro- and mesoscale w.r.t. grain boundaries, dislocations, corrosion pits, manufacturing induced defects as well as inclusions, voids and pores. However, their character is random in terms of size, orientation, number and location. Concerning growth, the governing material bulk properties of Young's modulus are random as well. At a structures level, (weld) geometry parameters are random variables, meaning that the character of fatigue resistance information is essentially stochastic. Because of the random nature of the wind and wave induced loading, the response as well as the fatigue damage assessment involves reliability and confidence.

The weakest link theory has been related to the effective notch stress criterion to include both the (weld) volume induced- and response gradient induced size effects for different welded joint geometries. Using fatigue test data the most likely model parameter values are obtained and lifetime estimates are obtained in the data scatter band (Blacha & Karolczuk, 2016).

By integrating rough set theory; a tool to deal with uncertain knowledge, and neural network technology with particle swarm optimization to establish the fatigue resistance relation, hybrid intelligent technology has been established to obtain lifetime estimates. Simulation results show that estimates are more accurate than conventional neural network technology based ones (Yang et al., 2015).

4. CRACK GROWTH APPROACHES

Fatigue damage development includes initiation and growth contributions. Fatigue crack growth assessment has become increasingly used as an important part of Engineering Critical Assessment (ECA) for demonstrating fitness for service of the ship and offshore structures like FPSO's, maintenance or any need for repair (Song & Dong, 2016). Furthermore, manufacturing and construction quality acceptance are increasingly relying on ECA-based quantitative assessment methodologies as well to establish acceptance manufacturing defects or discontinuities below which fatigue crack propagation lives are deemed adequate to meet lifetime requirements. In contrast to fatigue damage accumulation approaches, crack growth approaches are based on the theory of fracture mechanics assuming that structures and materials inevitably contain defects that may develop during manufacturing and construction or during a certain period of service. Therefore, crack growth approaches have become an important tool for preventing fatigue failure of engineering structures, as has been discussed by numerous researchers over the last two decades for applications in the ship and offshore structures.

4.1 Defects and initial cracks

Welded structures contain various forms of defects such as porosities, inclusions, micro-cracks resulted from welding processes, often serving as the origin for fatigue crack development under service loading and environment. The effects of such initial crack-like defects or quantifiable initial cracks caused by service loading on remaining structural lives require fracture mechanics based crack propagation approaches to ensure safe operation of the ship and offshore structures. However, fracture mechanics applications in the ship and offshore structures are

complicated for complex structural details which are typically exposed to complex stress concentration behaviours at hot spot positions with sudden geometrical changes as holes or corners where fatigue cracks are typically found during regular inspection intervals. This means that crack-like defects much larger than those implicit in fatigue design curves, once found during inspections must be quantitatively evaluated to demonstrate a structural detail that contains such crack-like defects is fit for continued service. For fracture mechanics treatment, these crack-like defects can be characterized by surface cracks, through-thickness cracks and embedded cracks (Yeter et al., 2015b). Further discussions on applications in the various ship and offshore structures are given in (Yan et al., 2016), for pressure vessels in (Ding et al., 2015), pipelines in (Zhang et al., 2016c), some offshore structure details in (Lotsberg et al., 2016) among others.

4.2 Crack sizing during in-service inspection

Fatigue crack growth analysis can be carried out to demonstrate that a structure containing a flaw fits for a continued operation to a required lifespan, which must be accompanied by in-service inspection measures to mitigate any uncertainties in fracture mechanics based crack growth assessment. In-service inspection to detect fatigue cracks and determine their sizes is normally performed to ensure that potential cracks in the structure, which may have been present from the initial delivery or have arisen at a later stage during service, do not exceed a critical size determined from a fracture instability evaluation such as those given in BS 7910 in terms of failure assessment diagrams. A well-established reliability of a non-destructive testing (NDT) is typically applied, which characterizes the method's ability to detect an existing crack as a function of the crack size and uncertainty associated with the sizing of a crack of interest. Often, further calibration of a given NDT method may be required to improve the probability of detection and minimize uncertainty. An analysis methodology with calibrated initial defects was presented to make inspection planning less time consuming and less complex to perform (Lotsberg et al., 2016).

4.3 Modelling

Crack growth approaches based on fracture mechanics is then adopted as a basis to determine the detection curves. When planning inspection, it is important to assess the consequence of a potential fatigue crack at a considered hot spot.

Approaches based on fracture mechanics principles are implemented in the form of a Paris type of empirically observed power relationship between the stress intensity factor range and crack growth rate, which allows an estimation of crack propagation life from an initial crack size to a final crack size. The final crack size is often determined through fracture instability or global structural collapse analysis, based on the FAD (failure assessment diagrams) approach in well-established FFS (fitness-for-service) or ECA (engineering critical assessment) procedures, e.g., BS 7910 or API 579 RP-1/ASME FFS-1. There exist various crack growth models as reported in the literature, most of which represent somewhat extended or modified versions of the original Paris relation. Over the last three years, some models are further assessed and some extended to accommodate important parameters identified. These parameters include those related to material, structure, environment, loading etc. In this section, the current applications of crack growth rate models in fatigue and fracture analysis of ship and offshore structures as reported in the recent literature are reviewed and discussed.

4.3.1 Paris relations

The Paris relation is still a widely-accepted formula (Ilman et al., 2016, Ji et al., 2016, Soliman et al., 2016, Zhang et al., 2016c). Although this model includes only region-II of the crack growth rate curve, it is widely used because region-II represents the majority of the fatigue life for many structural components (Branco et al., 2015). A multi-objective optimization problem and solved it to simultaneously provide an effective and reliable decision-making approach, in

which the Paris relation is used to describe the crack growth rate was formulated in (Soliman et al., 2016).

The Paris relation with the stress intensity factor range replaced with a normalized strain energy release rate range, i.e., $da/dN=C(\triangle G/G_C)^m$. was adopted in (Harper & Hallett, 2015). The same reference also proposed a method for determining the constants C and m through a linear variation in the form of $C=(G_1/G_T)C_I+(G_2/G_T)C_{II}$ and $m=(G_1/G_T)m_I+(G_2/G_T)m_{II}$ for applications in composite tidal turbine blades. Here, G_I and G_{II} are the model I and mode II components of the total strain energy release rate, G_T, which is extracted from the numerical model and m_I, C_I, m_{II}, C_{II} are the pure model I and the mode II Paris relation constants extracted from experimental data. Further improvement to the current Paris relation fatigue model may be possible if mixed mode fatigue data becomes available.

A similar fatigue crack growth relation, $da/dN=C\Delta G^m$, is adopted in (Zhang et al., 2016c) when conducting fatigue analysis on offshore pipelines with embedded cracks. From the point of view of energy consumption, the mixed mode theory is adopted to calculate the equivalent fracture energy release rate G_{eqivC}. One of the mixed-mode models is expressed as $G_{eqivC}= G_{IC}+(G_{IIC}-G_{IC})[(G_{II}+G_{III})/(G_I+ G_{II}+ G_{III})]^{\eta}$.

Under non-proportional mixed mode loading conditions, most recent developments in introducing a moment of load path or MLP method seem to show great promise, as discussed in (Wei & Dong, 2014), which is further proven by evaluating a large amount of crack growth rate test data under non-proportional loading conditions (Mei & Dong, 2017b). The validity of such an approach has been validated using non-proportional multiaxial loading test data as given in (Mei & Dong, 2016, 2017a). The MLP method can be used for arbitrary variable amplitude multiaxial loading conditions through a multiaxial cycle counting procedure given in (Wei & Dong, 2014).

It is pointed out in (Lotsberg et al., 2016) in demonstrating probabilistic methods for the planning of inspection for fatigue cracks in offshore structures that small changes in basic assumptions for fatigue analysis can have a significant influence on the predicted crack propagation lives. Analysis results from fracture mechanics are dependent on factors such as crack growth parameters, initial crack size, and stress intensity factors. The Paris and Erdogan equation at any point along the crack front is used to calculate the fatigue crack growth per stress cycle.

4.3.2 Modified relations

Some new formulae are proposed. However, most of the new formulae added more parameters, or changed the original parameters of the Paris relation, with the result that a large amount of experimental C and m data cannot be directly used. To remedy this, the unique curve model, $da/dN=C[(\Delta K_{eq0})^m-(\Delta K_{th0})^m]$ and $\Delta K_{eq0}=M_R M_P \Delta K$ was proposed in (Huang et al., 2016), which is used in recent years for prediction of fatigue crack growth in a ship detail under wave-induced loading (Yan et al., 2016), taking advantage of the existing C and m database and at the same time taking the stress ratio and loading sequence into consideration. The determination of all parameters in the model is explained sufficiently. This model combines simplicity and practicability and has the potential for future use. To consider the effect of residual stress, the nominal stress intensity factor and the stress ratio are changed to $\Delta K_{eff}=(K_{max}+K_{res})-(K_{min}+K_{res})$ and $R_{eff}=(K_{min}+K_{res})/(K_{max}+K_{res})$ respectively, as adopted in (Ilman et al., 2016). The fatigue life of cruciform welded joints by considering both the effect of residual stresses and the influence of the weld toe geometry was estimated in (Tchoffo Ngoula et al., 2017). Fatigue crack growth analyses are performed by using the node release technique, together with the finite element program ABAQUS. The effective cyclic J-integral is used as crack tip parameter in a relation like the Paris equation for the calculation of the fatigue life. An analytical model to determine CTOD for a cracked component subjected to cyclic axial in-plane loading was proposed in (Dong et al., 2016). A simple fracture mechanism-based model for fatigue crack

growth assumes a linear correlation between the CTOD and the crack growth rate da/dN. The effects of stress ratio and crack closure were investigated by elastic-plastic finite element stress-strain analysis of a cracked component. The crack opening displacement can characterize the crack tip state at large scale yielding constant amplitude fatigue crack growth.

Variable amplitude loading history should be considered for fatigue analysis of ship and offshore structures. To explain variable amplitude loading effects, the Space-state model and the generalized Willenborg model were applied in (Maljaars et al.) by comparing them with the fatigue tests on welded, thick-walled C-Mn steel specimens subjected to CA (constant amplitude) loads with and without OL (overload) and of two types of VA (variable amplitude) loads. The Space-state model is found to be a relatively simple and useful tool for simulation of VA fatigue loads and VA sequences, but in the case of 'wave' load, the model was unable to predict the fatigue life. It shows that the Willenborg model provides good predictions of retardation effects in case of single overloads but when underloads exist, the model is not able to predict the fatigue life accurately. The modified Paris relation, $da/dN=C(\Delta Keff)^m$, was adopted in (Hodapp et al., 2015) when performing nonlinear fatigue crack growth of ship structures under variable amplitude stress by making the value of the stress intensity factor in crack opening level a time-dependent value. When discussing an improved procedure for generating standardized load-time histories for ship and offshore structures, applied the model $da/dN=(AM^m)/[1-(K_{max}/K_C)^n]$ combining the definitions of M and K'_{op}, $M=K_{max}-K'_{op}-\Delta K_{effth}$ and $K'_{op}=øK_{op}=øf_{op}K_{max}$, to consider the load sequence effect by introducing a parameter ø (Li, 2015).

The crack growth approaches accounting for the retardation effect have been applied for the fixed offshore wind turbine support under both constant and variable amplitude loading history (Yeter et al., 2015b, a).

Various approaches have been employed for the fatigue assessment of multiple surface cracks. Fitness-for-service codes, e.g., BS 7910 or API 579 RP-1, usually assume crack propagation of adjacent cracks without interaction and a re-characterization of multiple or complex flaws into a single crack of maximum dimensions after certain proximity conditions are observed. Another accepted concept is the fatigue crack closure (Elber, 1971), which explains how stresses lower than a crack opening stress can be insufficient to propagate the crack (Elber, 1971). However, the predicted life is usually conservative. An improved fatigue life analyses for multiple cracks were developed in (Pang et al., 2017) considering crack coalescence stage and fatigue crack closure. The predicted remaining fatigue life shows similarity with the experimental results.

A corrosion-crack correlation model for fatigue crack growth influenced by the hydrogen embrittlement to be used in pipeline carbon steels under gaseous hydrogen conditions was proposed in (Cheng & Chen, 2017a, b). The model is developed based on the correlation of the environment-affected zone and the plastic zone. In the model, the fatigue crack growth rate considers the influence of fracture toughness by the Forman equation and the stress-driven hydrogen diffusion and the hydrogen-enhanced de-cohesion hypothesis are used to describe the critical frequency and the "transition" stress intensity factor. In addition, the phenomenon of the cracking growth rate plateau is described by an approximation involving the stress ratio and the threshold stress intensity factor range.

A phenomenological fatigue crack propagation model for API-5L X100 pipeline steel exposed to high-pressure gaseous hydrogen was proposed in (Amaro et al., 2014). The material response in hydrogen at $da/dN<3\times10^{-4}$ mm/cycle was observed to be primarily affected by the hydrogen concentration, resulting in a hydrogen-dominated mechanism. The response in hydrogen at $da/dN>3\times10^{-4}$ mm/cycle results from fatigue-dominated mechanisms. The proposed model predicts fatigue crack propagation as a function of applied ΔK and hydrogen pressure.

4.4 Parameter estimates

Fatigue crack growth is dependent on various parameters from structural geometries, stress state, material properties, loading history and environmental conditions. Those parameters are typically incorporated into an appropriate crack growth model for assessing propagation behaviour of a fatigue crack. Stress intensity factor or its range is the most important parameter in commonly-used crack growth models. The stress intensity factor as a function of crack size depends significantly on the local stress field and crack size. The complexity increases when a change in stress distribution during crack growth is to be accounted for. With the aid of advanced computation techniques, the application of crack growth approaches in the ship and offshore structures have become more common in recent years (Yeter et al., 2014a, b, Matic et al., 2015, Yeter et al., 2015b, a, e).

4.5 Experimental data

The crack growth rate model used for fatigue and fracture analysis is derived and supported by basic crack growth data of the material. The crack growth rate database of different materials is enriched gradually by published articles and reports. For example, recently, the experimental crack growth data of pre-cracked 7050, 7075, 5083 and 6061 aluminum plates under fatigue conditions in a corrosive environment as the basis of investigating the effect of composite repair patch was given in (Schubbe et al., 2016). The fatigue crack growth data of AA 5083 metal inert gas (MIG) welded joints under static thermal tensioning by experiments was provided in (Ilman et al., 2016).

4.6 Numerical simulations

With the aid of high-performance computers, the numerical simulation is an alternative way for extensive parametric studies, replacing a large amount of costs on the experimental set up to conduct fatigue crack experimental tests. Progress in the computational modelling of fracture and fatigue with the advent of cohesive zone theory and more recently with the extended finite-element techniques will improve the basic understanding of fracture processes (Matic et al., 2015). The progress of computation techniques such as finite method and meshless methods makes the calculation of stress intensity factors (SIF) and crack shape development easier for ship details and offshore structures. During the last three years, the application of crack growth approaches on fatigue analysis of ship details and offshore structures has mainly been concentrated in the study by the aid of finite element method. Crack growth modelling is concentrated on structural details as tidal turbine blades, cruciform welded joints, pressure vessel steel, multi-planar DX-joint welds, offshore pipelines, aged jacket platforms etc. (Ding et al., 2015, Harper & Hallett, 2015, Ji et al., 2016, Tchoffo Ngoula et al., 2017). For example, a series of numerical analyses on the fatigue properties of multi-planar DX-joint welds were carried out in (Liu et al., 2015). The study mainly covered FE modelling of DX-joints, HSS analysis of DX-joint welds, and SIF study of weld cracks. The SIF of a crack in a ship detail was investigated in (Yan & Huang, 2015).

4.6.1 Loading sequence

One of the most important advantages of numerical simulation is to help to understand the load sequence effect by simulating the load history of the cracked body as real as possible. Stochastic nonlinear fatigue crack growth predictions for simple specimens were made, subject to representative ship structural loading sequences through a time-dependent stress intensity factor, which is based on the evolution of a rate-independent, incremental plasticity model simulating combined nonlinear kinematic and isotropic hardening (Hodapp et al., 2015). The result is a mechanistic rather than phenomenological numerical model requiring only experimentally measured fatigue crack growth rates under constant amplitude cyclic loading and a full material constitutive model defined through experimental push-pull tests for the same material. This

approach permits a consideration of material behaviours which are physically relevant to structural steels, yet necessarily omitted in the similar application of a strip-yield model. Both experimental and numerical studies to follow cracking damage in steel cylinder/plane fretting fatigue contact subjected to variable loading conditions were performed in (Gandiolle et al., 2016). To formalize crack nucleation prediction, the Crossland multiaxial fatigue behaviour was applied at a critical distance to consider the severe fretting fatigue gradients. The crack propagation rate was formalized using the Kujawski's fatigue crack driving force parameter and coupling the Paris relation of the material. Constant fretting fatigue conditions and variable fretting fatigue sequences were investigated. The influence of different plastic laws was investigated. An iterative method to simulate 3D fatigue crack propagation in crystalline materials is proposed based on the computation of a damage indicator based on plastic activity around the crack tip (Proudhon et al., 2015). By post-processing, this quantity after a given loading sequence, local crack direction and growth rate are estimated along the crack path. A Multi-Scale FEM Crack Growth model successfully extends the finite element analysis of plasticity-induced crack closure to variable amplitude, high-cycle fatigue by considering a physically accurate, time-dependent loading sequence (and hence stress intensity factor) applicable to ship structures in the marine environment, capable of considering material constitutive models which are suited to cyclic plasticity in structural steels was proposed in (Li, 2015). A numerical simulation of the fatigue crack propagation under superimposed stress histories containing different frequency components with several mean stress conditions was conducted in (Matsuda & Gotoh, 2015). The numerical simulation of fatigue crack propagation based on an advanced fracture mechanics approach using the RPG (Re-tensile Plastic Zone Generating) stress criterion was improved to enable the extraction of the effective stress history for fatigue crack propagation under superimposed stress histories.

An approach to assess the probabilistic life of mixed-mode FCG by coupling of finite element analysis and Kriging-based reliability methods was used in (He et al., 2015). A simulation program (FCG-System) is developed to simulate the fatigue crack path and to compute the corresponding fatigue life. Numerical applications dealing with FCG are presented to illustrate the numerical efficiency and accuracy of the proposed approach.

4.6.2 Residual stress

The plasticity effects on fatigue growth for a physically short crack was simulated in (Alfredsson et al., 2016). The material description comprised the Drucker-Prager yield surface, non-associated flow rule and non-linear combined hardening. The material's strength differential effect was the key difference explaining why compressive residual stresses instead of crack face closure were responsible for the short crack effect in this material. (Zhou & Jia, 2015) investigated the crack propagation behaviour in cast quenched and tempered steel after one overload cycle in tension as well as in compression on short cracks in deeply notched specimens. The crack propagation after overload cycles is investigated by inspection of the fatigue threshold R-curve and fatigue crack propagation rate. A fatigue crack growth (FCG) model for specimens with well-characterized residual stress fields using experimental analysis and finite element (FE) modelling was studied in (Garcia et al., 2016). The FE FCG models were developed using a linear elastic model, a linear elastic model with crack closure and an elastic-plastic model with crack closure. The results demonstrate that the negative part of the stress cycle with a fully closed crack contributes to the driving force for the FCG and thus should be accounted for in the fatigue life estimates.

4.6.3 Simulation on different crack forms and positions

The residual strength of a pin-loaded lug and a finite plate with semi-elliptical crack emanating from a hole are examined by a new analytical methodology which analyses the crack propagation process in terms of the life estimation and crack front evolution (Boljanovic et al., 2016). The stress field and the stress intensity factor were computed by applying both analytical and

numerical approaches, and the two-parameter driving force model was implemented for the fatigue life estimation and the crack front evolution. A 2D Finite Element model of an edge crack, in which the combined effects of the travelling Hertzian load (the contact pressure which conforms to the Hertzian contact theory) and the lubricant are accounted for, was developed in (Dallago et al., 2016). A pressurization is implemented by applying the external contact pressure acting on the crack mouth to the crack faces and the new fluid pressure inside the crack is found by an iterative procedure based on the condition of constant volume. The contribution of fluid entrapment to the stress intensity factors is investigated through an extensive parametric analysis.

A numerical simulation of crack propagation due to thermal cycling on a circular disc was performed in (Qayyum et al., 2016). The effect of the length of cracks and interaction between adjacent cracks has been investigated. The variation in Stress Intensity Factor (SIF), hoop stress and Crack Mouth Opening Displacement (CMOD) has been plotted as a function of primary/secondary crack lengths and a number of cracks. Results show a significant drop in hoop stress, SIF and CMOD with an increase in the number of cracks, thus limiting the number of cracks possible in a thermal fatigue crack network.

A systematic investigation has been carried out on the fracture resistance behaviour of offshore pipelines containing an elliptical embedded crack under cyclic tension loadings (Zhang et al., 2016c). The extended finite element method (XFEM) is adopted for numerical simulations. The influences of different initial crack lengths and stress ratios on fatigue crack growth are investigated in detail. Furthermore, the comparison between the values obtained from the theoretical analysis, (BS7910, 2005) and current investigation is made on the fatigue crack growth rate, from which it is obvious that the results obtained by XFEM are reasonable and reliable.

4.6.4 Damage mechanics models

Advanced simulation techniques should integrate a proper damage model to judge crack growth. The fish-eye fatigue crack growth after crack nucleation for very high cycle fatigue was investigated in (Nguyen et al., 2015). An iterative procedure based on three-dimensional finite element analyses is developed to conduct crack growth simulations. The stress intensity factors are used to estimate the fatigue crack growth by integrating the fatigue crack relation between the initial and final crack lengths. The formation of short cracks at notched members of super alloy single crystals under high-temperature low cycle fatigue was analysed in (Bourbita & Rémy, 2015). A damage model based on a visco-plastic strain energy density and dilation energy density is used to describe short crack growth and fatigue life of smooth specimens.

The seismic performance of welded joints with different weld access hole geometries and the effect of crack initiation and growth on the load carrying capacity of welded joints was discussed in (Tong et al., 2016). A continuum damage mechanics model used previously for monotonic loading was reformulated to account for the extremely low cycle loading condition.

Crack propagation under mixed-mode loading by means of the finite element method was simulated in (Al-Mukhtar, 2016). The numerical integration of the Paris' equation was carried out. The effect of normal and transverse applied load on crack propagation was presented. The results confirm the use of a fracture mechanics approach in the biaxial fracture.

A fracture mechanics approach to the phenomenon of the fatigue crack propagation in geometries such as plates and sheets was presented in (Toribio et al., 2016). A numerical procedure was designed and implemented starting from a discretization of the crack front and considering a sort of crack advance on the basis of the Paris relation, governed by the stress intensity factor obtained in (Newman & Raju, 1981).

The effect of shapes of circular hole defects on the rolling contact fatigue (RCF) crack initiation and propagation in high strength steel by RCF test and synchrotron radiation micro-computed

tomography (SR micro CT) imaging was clarified in (Makino et al., 2016). The mechanism of RCF crack propagation was discussed by finite element analysis.

Two important aspects of fatigue crack growth at negative stress ratios have been investigated. First, the controlling crack tip loading parameters are discussed (Benz & Sander, 2015) and an alternative stress based parameter has been correlated with the crack tip loading for negative loads. Second, the deformation mechanisms at negative stress ratios are discussed, and a new method is proposed in order to visualize the plastic deformations even at the negative loading part.

The crack growth behaviour of a pressure vessel steel was predicted in (Ding et al., 2015). The approach consists of elastic-plastic finite element stress-strain analysis of a cracked component and application of a multiaxial fatigue damage criterion to access the crack growth. Discussions are made to relate the characteristics of the crack growth behaviour of the material to the cyclic deformation of the material and to the contact of cracked surfaces.

Three-dimensional finite element analyses studied both crack initiation and propagation in a gear tooth. A damage mechanics approach was used to model crack initiation on the surface of a gear tooth due to the Rolling Contact Fatigue (RCF) (Ghaffari et al., 2015). A finite element model was developed to study the effects of friction on the fatigue crack initiation life.

4.6.5 Polymer composites

With the wide application of polymer composite materials in the ship and offshore structures, the study on the failure is ongoing. The advanced numerical modelling techniques of composite tidal turbine blades demonstrate the development of numerical techniques for modelling the growth of interfacial cracks (Harper & Hallett, 2015). The effect of moisture ingress on the bending fatigue of laminated composites was investigated in (Meng et al., 2016). A 2D Finite Element model (FEA) was developed to simulate the fatigue crack propagation based on virtual crack closure technique, while a 3D FEA model was developed to investigate the edge effect on fatigue crack propagation. A 4-step fatigue failure theory was proposed to explain the moisture effects on the crack propagation under bending fatigue.

The traditional phantom node method for crack propagation modelling of composite materials under fatigue loading was extended in (Wang & Xu, 2016). A fatigue damage variable related to experimental crack propagation rate was combined with the static one for interface property degradation, and a bilinear cohesive law considering damage initiation was used for quasi-static cracking modelling.

4.7 Crack growth assessment statistics

Fatigue cracks can appear at various locations along the ship structure and may occur at early stages in the service life of a ship or offshore structure. Due to the presence of significant uncertainties associated with crack initiation and propagation, the planning of inspection, monitoring and/or repair actions should be performed probabilistically.

A probabilistic framework for incorporation of risk and updating in the inspection of fatigue-sensitive details of ship structures, considering that fatigue cracks as a structural deterioration mechanism may lead to unanticipated out of service for naval ships, was developed in (Dong & Frangopol, 2015, 2016). The computation associated with fatigue damage is performed using fracture mechanics and uncertainties are considered within this process. As indicated, the fatigue crack size increases significantly with time and uncertainties are incorporated into the process. The uncertainties are also associated with inspection events. The outcomes of an inspection event are affected by many factors, such as the type of inspection method, human factors, and inspection quality. Consequently, uncertainties should be incorporated into the risk-informed decision making and updating. A useful flowchart for risk-informed inspection planning of fatigue-sensitive details is proposed which is illustrated on fatigue-sensitive details of

an existing tanker. Random variables associated with the fatigue crack limit state are analysed. It is pointed out that future research is needed to include nonlinear fracture mechanics in the damage assessment of fatigue-sensitive details and the effects of multiple fatigue cracks on the structural capacity should be considered in future studies for the risk assessment of fatigue-sensitive structures.

At the same time, a probabilistic approach for inspection, monitoring, and maintenance optimization for ship details under fatigue effects on the basis of the crack growth approach was proposed in (Soliman et al., 2016). Based on the stress profile and the crack geometry at the damaged location, intervention times and types are determined by solving an optimization problem which simultaneously minimizes the life-cycle cost, maximizes the expected service life, and minimizes the expected maintenance delay over the life-cycle.

4.8 Service life extension

Service life extension measures can be taken when cracks are observed. A composite patch repair is gaining popularity as it counters most of the problems faced by conventional renewal repairs. Extensive studies can be found in the literature addressing the efficiency of this novel repair method using techniques which meet higher performance and monitoring standards than these commonly found in naval applications. The efficiency of practices widely used in the ship repair industry for the implementation of composite patch repairing was addressed in (Karatzas et al., 2015). To this end, steel plates repaired with composite patches were tested under fatigue loading. The composite patches consisted of carbon fibers in an epoxy matrix and were directly laminated to the steel surface using the vacuum infusion method. Two different surface preparation methods, namely grit-blasting and mechanical treatment with the use of a needle gun were studied. In addition, to account for the harsh environmental conditions during the operating life of the structure and to study its effect on the repair, two different ageing scenarios were considered. The non-destructive evaluation of the patches was performed so as to assess the quality of the repair, and the evolution of debonding during testing.

An investigation of the performance for a composite repair patch to prolong the service life of pre-cracked 7050, 7075, 5083 and 6061 aluminum plates under fatigue conditions in a corrosive environment was performed in (Schubbe et al., 2016). Both insulated graphite–epoxy and boron–epoxy composite patches were evaluated for the effects of corrosion fatigue. The repair patches consisted of unidirectional plies (laminae) oriented in the loading direction. The improvement of service life and the effect that a corrosive environment had on crack propagation rates for the repaired aluminum plates were examined. The bond durability between the aluminum plates and the boron patch were also assessed. As expected, the introduction of salt water during testing greatly increased crack growth rates and has been quantified for comparison. The graphite patch consistently showed positive results compared to the boron patch for 6061 aluminum samples. The same system on 5083 aluminum had mixed results. Examination of potential 5083 sensitizations due to elevated cure cycles are discussed. The boron–epoxy repairs showed a positive life improvement in both lab air and salt water-exposed environments for 7050 and 7085 aluminums while the graphite–epoxy repair accelerated crack growth rates in the saltwater environment.

A rational method for determining the appropriate size of a stop hole, in which both high-cycle and low-cycle fatigue analyses are carried out according to the long-term and short-term wave-induced loading was proposed in (Chen, 2016). The time to initiate a new crack at a stop hole subjected to the long-term wave induced loading is predicted by the use of characteristic S–N curves and the Palmgren–Miner's rule. The time to initiate a new crack of a stop hole within severe sea conditions is calculated by strain-life methods in terms of the short-term wave loading induced in severe sea conditions. The effects of the return period of the potential severest sea condition, the crack length, and the environmental severity factor on the remaining service life of a stop hole are investigated.

5. FABRICATION, DEGRADATION, IMPROVEMENTS AND REPAIR

Fatigue strength of ship and offshore structures is largely affected by inherent defects and imperfections. More than often, such effects are included in safety (ignorance) factors rather than explicitly assessed. However, the trend is towards a more and more explicit and rational consideration of them in the design practice allowed by modern design procedures.

Two categories of imperfections may be distinguished: fabrication imperfections, existing at different levels in a structure just after construction, and in-service degradations, occurring during the lifetime of the structure.

Fabrication imperfections may be further categorized into misalignments and distortions, weld induced defects and initial crack size. Other imperfections include variations in material properties. In-service degradations also affect fatigue behaviour of structures: while corrosion and other degradation phenomena variously influence fatigue strength and introduce very large uncertainties in the fatigue assessment process, inspection and maintenance techniques are advancing as well. The reader is referred to the reports of Technical Committee V.2 - Experimental Methods and of Technical Committee V.7 - Structural Longevity for further and specific information on the matter. Thus, inspection and monitoring strategies, as well as maintenance issues, are only partially covered in this section and with particular emphasis on fatigue and fracture of the ship and offshore structures. The subject following a risk-based approach to the optimum inspection and maintenance planning for ship structures was recently addressed in (Dong & Frangopol, 2015, 2016).

Fabrication imperfection and in-service degradation countermeasures have been introduced and are continuously developed in construction to minimize detrimental effects on fatigue behaviour. Moreover, besides current recommendations on fabrication tolerances and post-weld improvement techniques (IACS, 2012), steel materials with enhanced fatigue resistance are now available for the shipbuilding industry.

A very comprehensive review paper has been recently published in six parts (Ibrahim, 2015a, b, c, d, 2016a, b), rationally presenting several aspects of structural life assessment of ship structures.

5.1 Fabrication imperfections

5.1.1 Misalignments and distortions

To improve the energy efficiency of the ship and offshore structures, new lightweight solutions are required. This is possible by utilizing thinner plates together with modern laser and laser-hybrid welding technologies. In thin plates ($t<5$mm), the main challenge is their proneness to larger distortions during production because of their lower bending stiffness. As distortions cause secondary bending, which increases the structural stress, the large distortions can lead to significant reduction in fatigue strength. In this regard, the traction structural stress method (Dong, 2005, 2010, Dong et al., 2014) coupled with analytically derived stress concentration factors for two typical distortion modes (Dong et al., 2017a, Dong et al., 2017b) showed rather promising results. Based on the experimental results from small-scale specimens (Lillemae et al., 2017) and numerical welding simulations (Tekgoz et al., 2013a, b, 2014, Garbatov et al., 2016a), the distortions can be larger and also with a different shape in comparison to the thick plate. In addition, the straightening of the thin plate under axial tension loading can result in the non-linear relation between structural stress and nominal stress (Fricke et al., 2015, Remes et al., 2017). The recent full-scale tests prove these findings. Initial distortions in full-scale 4-mm thick laser-hybrid welded ship structures were measured and reported in (Lillemäe et al., 2016, Lillemae et al., 2017). The fatigue test results showed that when initial distortion shape and geometrical nonlinearity are properly considered, the small- and full-scale specimens have equal fatigue strength with small scatter. The geometrical nonlinearity means in practice that the commonly used stress magnification factor given in classification rules is not suitable for

thin-plate structures. Thus, further studies are required to develop new design methods as well as quality limits for the distortions. For thicker plates (t>5 mm), the structural behaviour is linear, and plates are not curved close to welds. Then analytical formulations for stress magnification factors are possible.

However, the consideration of surrounding structures and boundary conditions can cause challenges. New analytical formulations for stress magnification factors were introduced in (Xing & Dong, 2016) for different geometrical configurations and boundary conditions of cruciform joints and discussed the validity of the stress magnification factor equations given in current rules (BS7910, 2005, DNV, 2010b). The authors show that some of the existing solutions are valid under a narrower set of conditions than documented and some seem to be an insignificant error.

The distortion is always related to the residual stress. The tensile residual stress increases the mean stress for fatigue loading and thus, decreases the fatigue strength. Therefore, it is important to develop the welding and manufacturing methods, which at the same time result in small residual stress and distortion. Welding simulations to predict distortions and residual stress are developed by several researchers.

The influence of thermo-mechanical material properties of T-joints made of different steel grades was studied with the conclusion that for the prediction of residual stresses, only the yield stress needs to be temperature-dependent (Bhatti et al., 2015). For the assessment of angular distortions with acceptable accuracy, the heat capacity, yield stress and thermal expansion should be employed as temperature dependent in the welding simulations. Several studies analysed the welding distortions by a nonlinear thermo-elasto-plastic approach and compared them with the experiments, which showed the same trend, but up to 20% higher values (Chen et al., 2014a, Chen et al., 2014b, Hashemzadeh et al., 2014, Hashemzadeh et al., 2015b, a, 2016, Chen et al., 2017, Hashemzadeh et al., 2017a). The development of reliable methods to predict distortions and residual stress in large ship structures still requires a significant amount of further work. At this stage, the simulation methods can provide new ideas for further development of manufacturing. For instance, in (Ilman et al., 2016) a method to mitigate distortions and residual stress by static thermal tensioning was developed and demonstrated the resulting increase in fatigue strength. The weld area was cooled and areas further from the weld were heated to 100, 200 and 300ºC. Out of plane distortion was reduced using a stretching effect generated by static thermal tensioning treatment, which counterbalanced the distortion induced by welding. Also, harmful tensile residual stresses were reduced and to some extent, also beneficial compressive residual stresses could be formed.

A broad research project involving both academia and industry and dealing with naval vessels has been recently reported in (Huang et al., 2014a, Huang et al., 2016): actual measurements were comprehensively analysed and their effect on structure strength estimated.

5.1.2 Welding induced defects

Welded high strength steel and thin plates are more sensitive to dimensional accuracy than thicker plates (Remes & Fricke, 2014, Dong et al., 2017a, Dong et al., 2017b). The fatigue strength of thin laser-hybrid welded butt joints using the notch stress approach and micro-scale measurements of the weld geometry were studied in (Liinalampi et al., 2016). The notch stress was defined using the Neuber's stress averaging approach, where no fictitious rounding of the notch is needed. A significantly smaller averaging length than commonly assumed for welded joints was required to capture the increased notch stress due to sharp notches caused by e.g. axial misalignment. As a result, the scatter in the test results was significantly reduced. In addition to that, the variation in the material properties causes the asymmetrical distribution of welding-induced residual stresses and distortions (Hashemzadeh et al., 2017b).

Plate butt joints made of normal and high strength steels of 4-mm in thickness produced by different welding methods were investigated in (Lillemäe et al., 2016), with the most important factors influencing fatigue strength being the weld height and the flank angle. Also, visible non-continuous undercuts had an important effect, even though the mean values from the weld geometry analysis showed a very small undercut. The correlation between the weld toe radii and fatigue strength was weak, unlike often suggested (Jonson et al., 2011, Jonson et al., 2016a).

Similarly, investigations showed that weld flank angle has a significant influence on the fatigue strength of 10-mm thick high strength steel cruciform joints, while weld toe radius effect seems insignificant, possibly because pre-cracks was found (Tchoffo Ngoula et al., 2017).

The effect of the undercuts on the fatigue strength of 6-mm thick ultra-high-strength steel butt joints was studied in (Ottersbock et al., 2016). They concluded that the fatigue strength of defective specimens is within the scatter band of the non-defective ones if the support effects are considered. Fatigue strength assessment of butt welded specimens whose defect level was found non-conforming to the acceptance criteria was also carried out in (Cosso et al., 2016). After appropriate numerical and experimental analyses by properly considering the fabrication imperfection effects, the specific structures were demonstrated to be safe enough for the intended service.

A dedicated fatigue test on butt welded specimens notched in way of the weld to validate Strain Energy Density SED-N curves was carried out in (Fischer et al., 2016b). Noticeably, the Notch Stress Intensity Factor (N-SIF) based fatigue assessment approaches inherently consider the very local weld notch geometry, hence potentially including notch geometry effects. While stress relieving of residual stress was generally carried out in all tested series, various notch geometries, microstructure (i.e. notch in HAZ, weld or parent material) and steel types were fatigue tested. Namely, the advantages of these tests are that both the exact notch geometry and the local stress range at the notch, including misalignment effects, were carefully identified and considered in experimental data analysis. However, the fabrication imperfections may change the post weld distortions and residual stress leading to a significant impact on fatigue strength (Hashemzadeh et al., 2017c).

When discussing the weld geometry, the question arises how to measure and define the variables of weld geometry such as the toe radii. Three different non-destructive methods to assess the weld geometry were compared in (Harati et al., 2014). All three methods are applicable, but the radius highly depends on the evaluation procedure. Weld Impression analysis is an economic and sufficient option when only the weld toe radius in a single point is needed. If the whole 3D image of the weld profile is needed, the Structured Light Projection is a good choice.

The fact that different operators ended up with different results for the common weld surface evaluation methods was studied in (Stenberg et al., 2015). Therefore, an algorithm was developed which assesses weld bead surface geometry and automatically defines the toe radius and the toe angle along the weld.

Another question is how to include the weld quality in the fatigue assessment. The suitability of the effective notch stress and Battelle's structural stress method for evaluating the fatigue strength of thin and thick normal and thick high quality cruciform and T-joints was studied in (Stenberg et al., 2015). The actual weld geometry was not included, the notches were rounded with fictitious radius: $R = 0.05$ mm for $t = 2$ mm, $R = 0.3$ mm for $t = 4$ mm and $R = 1$ mm for $t > 5$ mm. The authors concluded that both methods work, but the notch stress resulted in smaller scatter. Effective notch stress method was able to consider the increased weld quality by increasing the design curve by 25% for each step in the quality class (STD181-0004). Also, stochastic methods have been recently proposed to evaluate the fatigue strength based on random (Schoefs et al., 2016) or real weld geometries (Lang & Lener, 2016). Finally, high weld quality leads to longer short crack growth periods and this might be the reason for the observed shallower slope of the S-N curve (Remes et al., 2017).

It is well known that the weld quality influences the fatigue strength significantly, but it is not always easy to define what is required for high quality and which parameter has the decisive effect. Existing ISO quality standards (ISO13919-1, 1996, ISO12932, 2013, ISO5817, 2014) define the limiting values for weld size, shape and defects, and divide welds into 3 different categories accordingly. However, these quality levels do not have a straightforward link to the fatigue strength. Efforts have been made to link quality categories with certain fatigue strength (STD181-0004, Barsoum & Jonson, 2011, Jonson et al., 2011, Hobbacher & Kassner, 2012) and based on this the IIW has recently published a guideline (Jonson et al., 2016a). The guideline can be considered as a first draft of the applicability of e.g. thin plates ($t < 5$ mm) has not been validated.

In addition to welded joints, also the cut plate edges are fatigue critical details in the ship and offshore structures. Fatigue critical cut edges are in e.g. window corners of a large passenger ship. The increased fatigue strength for high strength steels with improved surface quality has been demonstrated and the need to update the rule highlighted in (Stenberg et al., 2016).

5.1.3 Initial crack size

One of the main influencing factors on the fatigue performance of materials is the initial crack size, and there have been a large number of research efforts devoted to investigating the impact (Matic et al., 2015, Liu et al., 2016, Reddy et al., 2016). Although there is a need for a unified definition of the fatigue crack initiation and propagation, there is no agreement in which the phases of the fatigue crack growth could be divided with an exact definition: microscopic, small and macroscopic. Generally, cracks with lengths lower than 10^{-1} mm are regarded as microscopic ones, whose growth is dominated by the microstructure texture. The size of the microscopic crack is marked as an initiation size, which is consistent with the first stage of the fatigue process. When the crack length is within the interval of 10^{-1} mm and 1mm, which is the so-called early growth stage, the crack is considered as a small crack. The initiation stage of the fatigue crack is determined by the shortest uni-oriented detectable microscopic crack.

Fatigue tests on six compact tension specimens made of S355J2+N steel (ISO EN 10025 standard, IACS-AH36) in the air and in laboratory-simulated seawater under free corrosion conditions were carried out in (Adedipe et al., 2015). All specimens were pre-cracked in the air at a loading ratio of 0.1 and loading frequency of 5 Hz. Crack lengths in these tests were monitored by four methods in all: Alternating Current Potential Difference (ACPD), the direct current potential difference (DCPD), optical measurements through the StreamPix5 digital camera and travelling microscope, and back face strain (BFS). The BFS method was found particularly effective in the simulated seawater environment, while both DCPD and BFS methods were reliable and cost-effective for the crack growth measurement in the corrosion environment.

A general fatigue life prediction procedure was presented in (Correia et al., 2016), which was based on the CCS crack growth rate model (Blasón et al., 2015) and the proposed approach was used to obtain the fatigue data of a notched plate made of P355NL1 steel, in which the Equivalent Initial Flaw Size (EIFS) concept had been employed. As the EIFS concept assumes that materials had defects acting like initial cracks, this EIFS was usually smaller than the crack initiation concept of the local/Fracture Mechanics integrated approaches.

Fatigue crack growth data of P335NL1 steel using CT specimens under several stress R-ratios, applying the EIFS approach and employing a back-extrapolation calculation was analysed in (Alves et al., 2015). The EIFS concept assumed the material includes intrinsic defects acting like initial flaws, and the equivalent initial size a_i calculation is based on cyclic J-integral, which is used to consider the elastic-plastic deformations in the crack-tip area as $da/dN=f(\Delta J)$, where da/dN is the fatigue crack growth rate, and ΔJ is the range of the cyclic J-integral and the fatigue life N can be estimated by integrating from the final crack size, a_i to the final one a_f.

Generally, the EIFS might be calculated through an inverse analysis, and some endeavour had been made to estimate the EIFS directly adopting the Kitagawa Takahashi diagram (Kitagawa & Takahashi, 1976).

5.2 In-service degradation

Various degradation effects influence fatigue behaviour like surface roughness, crater, groove, linear, spot and common wearing, general and pitting corrosion. However, relatively few papers were found in the surveyed literature on this specific aspect. It should be admitted that it is extremely difficult to obtain data, from both dedicated tests and in situ measurements, about fatigue behaviour of welded structures. On top of this, numerical simulations appear to be extremely difficult to be carried out and examples of research work ongoing in this very challenging field are presented in (Brennan, 2013, Garbatov et al., 2014a, Garbatov et al., 2014b, Garbatov, 2016, Garbatov et al., 2016b).

5.3 Strength improvement

Different strategies have been followed to improve fatigue strength of ship and offshore structures in the past years ranging from new materials to post-welding treatments and other fabrication processes. The IIW has recently updated a booklet on the matter (Haagensen & Maddox, 2013). It provides guidance for the practical use of each method, including equipment, weld preparation and operation and allows a more predictable implementation of the most widely applied improvement methods.

Mostly, improvement methods are intended to improve the fatigue strength of welds. However, parent material too may undergo fatigue failures. Fatigue tests of different strength steel specimens treated by grinding or by grinding followed by sandblasting, i.e. using post-cutting treatments that are suitable for shipyard conditions, were carried out in (Korhonen et al., 2013, Remes et al., 2013). The resulting surface roughness, hardness profile, and residual stress were measured. The investigation shows that post-cutting treatments suitable for shipyard conditions can considerably increase the fatigue strength of the high-strength steel used in opening corners of a large-scale structure. Sandblasting after grinding increases the surface roughness, but reduces the fatigue strength only slightly.

High strength steels have huge potential in enabling new lightweight designs. However, welding introduces stress concentration and initial defects into the material. As higher strength steel is more sensitive to initial defects (de Jesus et al., 2012), a phenomenon called notch sensitivity, the increased fatigue strength is lost. In addition, harmful tensile residual stresses are introduced by welding. By appropriate post-weld treatment of fatigue-critical details, the initial defects, as well as harmful tensile residual stresses, can be removed.

Post-weld treatment methods can be divided into two groups, the ones that improve the weld shape, such as toe grinding and tungsten inert gas (TIG)-dressing, and the ones, which alternate the residual stress state such as the High-Frequency Mechanical Impact (HFMI) treatment. In fact, the local plastic deformation of the impacted material causes changes in microstructure, geometry and the residual stress state. Therefore, the increase of the fatigue strength is a combination of weld geometry improvement as well as the residual stress modification.

The High-Frequency Mechanical Impact (HFMI) has significantly developed as a reliable, effective and user-friendly method for post-weld fatigue strength improvement technique for welded steel structures. One possible approach to fatigue assessment for HFMI-improved joints by analysing several IIW documents reporting HFMI technology results was presented in (Marquis et al., 2013). A companion paper has also been prepared concerning HFMI equipment, proper procedures, safety, training, quality control measures, and documentation in (Marquis & Barsoum, 2014). Lack of standards and guidelines prevent the wide application of improvement methods since their effect is not accurately predicted for the time being.

Tests of 68 available HFMI-improved welds subjected to overloads or pre-fatigue loads at various loading conditions representative of the ship and offshore structures prior to fatigue testing were presented in (Yildirim & Marquis, 2015). A review of current IIW guidelines is also reported. Indeed, class rules are seldom considering the beneficial effect of improvement methods because of uncertainties in quantifying their effect on real structures and in-service conditions. An overview of the recent results on fatigue strength improvement by HFMI-treated high-strength steel welded joints is presented in (Yıldırım, 2016).

The effect of HFMI treatment on the weld toe geometry and the fatigue strength of fillet welded extra high strength steel, σ_y = 1,300 MPa was studied in (Harati et al., 2016b). The weld toe radius did not change noticeably after the treatment, but the profile was more uniform. The fatigue strength increase was not as significant as expected because the quality of the as-welded joints was already quite high. A deeper analysis of the same results, including the effect of residual stress, was presented in (Harati et al., 2016a).

The fatigue strength of hammer peened S690 butt joints was studied in (Lefebre, 1993). The increase in fatigue strength was in accordance with the proposed guideline (Marquis et al., 2013), even though the hammer peening did not improve the local toe geometry as often assumed, but introduced crack-like folds instead. Based on this it seems that compressive residual stresses played the key role.

Various High-Frequency Hammer Peened (HFHP) ultra-high-strength steel (S960, S110 and S1300) joint types with different plate thicknesses were studied in (Berg & Stranghoner, 2016). They show the conservatism of existing design proposals. However, the study included only the constant amplitude loading with the stress ratio of R=0.1.

The high strength steel grades S690 and S960 in as-welded and HFMI-treated condition, both before and after stress-relief annealing was investigated in (Leitner et al., 2015b). Fatigue tests at a stress ratio of R=0.1 showed a significant increase of the fatigue strength due to the HFMI-treatment compared to an as-welded condition. The superimposed post-heat treatment, however, lowers the fatigue strength, but not back to the level of an initial as-welded state. They also discuss the change in mean stress due to clamping of the specimens with considerable angular misalignment. The effect of post-heat treatment on as-welded and HFMI-treated mild steel joints (S355) is discussed in (Leitner et al., 2015a). They show that additional post-weld heat treatment is not beneficial. As no changes in distortions and microstructure were observed, the decrease in fatigue strength can mainly be attributed to the relief of manufacturing induced (as-welded/HFMI-treated) prior compressive residual stresses to an almost zero stress value.

(Deng et al., 2016) studied numerically the effect of HFMI treatment on the stress state close to weld toe of the butt joint made of different material grades. Structural stress approaches with through-thickness and linear surface extrapolation was applied and characteristic fatigue strength values were proposed and compared with the values from literature and available experimental data.

Numerical investigations on the improvement of non-load-carrying welded cruciform joints by ultrasonic impact treatment (UIT) including thermo-mechanical welding simulation and dynamic elastic-plastic FE analysis was performed in (Yuan & Sumi, 2016). A 3D simulation method is based on thermo-mechanical welding simulation, the dynamic elastic-plastic FE analysis and fracture mechanics-based fatigue life assessment. The predicted plastic deformation and residual stress resulting from UIT as well as the fatigue strength under various R-ratios agree relatively well with the experiments. It is found that UIT is beneficial up to R<0.5. The results not only clearly distinguish the fatigue strengths of as-welded and UIT-processed welded joints, but also show the effects of preloads and stress ratios, so that the proposed solution method may provide an effective tool to simulate improvement methods in engineering structures.

Also in (Leitner et al., 2016) a setup of a closed simulation loop including a thermo-mechanical coupled weld simulation, numerical computation of the HFMI-process and fatigue assessment by the local stress/strain and crack propagation approaches were presented. Comparison with experimental residual stresses and fatigue strength show generally reasonable agreement. Linear elastic fracture mechanics-based approach works well for as-welded joints but needs further development to consider the enhanced crack initiation period of HFMI-treated welds properly.

Even though the fatigue improvement methods considered in these papers are available to the industry for quite some years, their simulation testifies the interest in reliably estimating the enhancing effect in the design process.

In case of post-weld treatment methods, where fatigue strength increase is mainly due to beneficial compressive residual stress, the influence of variable amplitude loading, and high-stress ratios becomes extremely important as these might relax the compressive residual stresses.

The effect of loading history on non-load carrying specimens improved by ultrasonic impact treatment was studied in (Polezhayeva et al., 2015a). The investigation aimed to determine whether loading histories specific to marine and offshore structures cause shakedown of compressive residual stress produced by HFMI treatment and therefore affect fatigue resistance of welded joints improved by these methods. A significant relaxation of compressive residual stresses is achieved by application of compressive cycles in fatigue testing, depending on both stress level and number of applied cycles. The beneficial effect of the HFMI is therefore reduced. The influence of the load history on the improvement effects on fatigue strength by the Ultrasonic Peening was confirmed experimentally in (Deguchi et al., 2012) testing several joint type specimens. In addition, they identified some cases that have the possibility of decreasing or increasing the improvement effects on fatigue strength by Ultrasonic Peening and suggested some efficient methods of the Ultrasonic Peening for ship structures.

The influence of spectrum loading including pre- and overloads on the fatigue strength of HFHP-treated S1100 stiffener and butt joint specimens were studied in (Berg et al., 2016). The stress ratio was R=0.1 in both constant and variable amplitude loading, and they observed similar fatigue strength under both loadings, i.e. fatigue strength improvement was not lost under VAL.

The fatigue behaviour of the impact treated mild steel (yield strength 356 MPa) cruciform and lap joints under variable amplitude loading, including effects of high R-ratios and overloads was studied in (Ghahremani et al., 2015). Two types of variable amplitude loading histories and nominal, structural and effective notch stress approaches were used. The results showed fatigue strength improvement under VAL also with stress ratios R>0.4.

A methodology for variable amplitude fatigue analysis of as-welded and HFMI-treated structural steel based on effective strain-life and a strain-based fracture mechanics model was proposed in (Ghahremani et al., 2016). With the proposed method, accurate or in some cases conservative predictions were obtained compared to experiments.

The combined effect of microstructure, geometry and residual stress were systematically studied in (Mikkola & Remes, 2016, Mikkola et al., 2017). They concluded that even if compressive residual stress is completely relaxed at R=0.5 and $S_{min} \leq -0.6\sigma_y$, the post-weld treatment still results in fatigue strength increase due to weld toe geometry improvement and strain hardening. A new recommendation for fatigue design was proposed in (Mikkola et al., 2016). The fatigue strength of HFMI-treated high strength steel joints under constant and variable amplitude block loading with the stress ratio of R=0.1 was studied in (Leitner et al., 2015b). The results showed good accordance with the constant amplitude tests when the equivalent stress range was calculated assuming a damage sum of D=0.5 in finite-life regions and D=0.3 in high-cycle regions.

The lightweight potential of high strength steels treated by HFMI under constant and variable amplitude loading was discussed in (Yıldırım, 2015, 2016). They considered longitudinal attachments made of S700 steel and tested with the stress ratio of R=-1. The fatigue strength was increased under both constant and variable amplitude loading, although the improvement under VAL was smaller. They also discuss the Gassner versus Wöhler lines. The Gassner line involves plotting $\Delta\sigma$max vs. N to failure and allows designers to easily compare fatigue strength with other potential failure modes like global yielding or buckling.

A review of the fatigue data of welds improved by TIG-dressing was presented in (Yildirim & Marquis, 2015, Yıldırım, 2016). The influence of high-stress ratios on the fatigue strength of TIG-dressed ultra-high strength steel fillet welds is studied in (Skriko et al.). They showed a 30% reduction in characteristic fatigue strength when stress ratio was increased from R=0.1 to R≥0.5. They also presented weld toe radius and residual stress measurement results before and after TIG-dressing.

Low transformation temperature filler material is an alternative method to reduce detrimental tensile residual stresses or even induce beneficial compressive residual stresses (Ooi et al., 2014). However, as the weld toe profile is not improved by this technique, the fatigue strength increase is not obtained at high-stress ratios (Bhatti et al., 2013). They reported increased fatigue strength compared to traditional filler material under constant amplitude loading with R=0.1 and variable amplitude loading with R=-1, but no increase under R=0.5. The relative effects of residual stress and weld toe geometry on the fatigue strength of 8-mm thick high strength steel cruciform joints welded with the Low Transformation Temperature filler material were studied in (Harati et al., 2015). Based on the results, the residual stress had higher influence.

Also, the alternative welding methods could be applied to achieve favourable weld shape. (Holmstrand et al., 2014) showed that the extended weld leg and weaved toe line increase the fatigue strength as the flank angle is decreased. The analysis showed that the crack initiated from the undercut. Weaved weld toe is however not suitable for longitudinal loading.

Increased fatigue strength of σ_y = 355 MPa steel obtained with a welding procedure that produces smooth undercut like the one achieved with weld toe grinding or HFMI treatment was presented in (Astrand et al., 2016). When aiming for large weld toe radius, the penetration depth is getting close to the base plate and thus there is an increased chance of harmful cold laps. Therefore, a smooth undercut would be even better than large radius without the undercut. Also, the position of welding with respect to a load carrying fatigue critical notch of the fillet weld influences the fatigue strength (Barsoum & Jonson, 2011). For example, the horizontal welding position creates a sharp transition for the load carrying weld toe because of the gravity, while the vertical position creates a sharper transition for a non-load carrying weld notch and a smooth transition for the load-carrying one.

T-welded joints connecting the web and panel plates made of Q345D steel via CO2 gas shielded arc welding before and after shot peening (SP) was chosen in (Gan et al., 2016). The static loading test and fatigue tests were carried out on peened and unpeened specimens, and the fatigue tested specimens were prepared with different peening intensities (PI). The tests showed: (i) all SP treatments could change the surface residual stresses 1 mm from the weld toe, (ii) the depth of the compressive residual stress field and the maximum compressive residual stresses tended to increase with higher PI, while the fatigue life of the T-weld was not always increased with the PI increasing, (iii) a PI of 0.3 mmA could result in twice the fatigue life.

5.4 Polymer composite patch repairs

Worth mentioning are EU projects like Co-patch (www.co-patch.com), whose objective is to identify design procedures to accept polymer composite patches as permanent repairs and/or reinforcements of steel structures and Mosaic (https://trimis.ec.europa.eu/project/materials-

onboard-steel-advancements-and-integrated-composites#tab-outline), partly devoted to replacement of specific structural parts of the ship with composite materials also in view of better fatigue behaviour.

Among the others, studies were carried out to assess the improvement on fatigue strength at corner openings by adding suitable composite patches to the steel plates. Their effect is not only to locally stiffen the structure but also to obtain a faired and less notched geometry.

Comprehensive strength and fatigue testing of composite patches for ship plating fracture repair were carried out in the frame of a joint research project in the USA and reported in (Karr et al., 2015, Karr et al., 2016).

Experimental investigation of the behaviour of an adhesively bonded, hybrid, composite-to-steel butt joint was carried out in (Karatzas et al., 2015). Two types of joints were tested, e.g. one involving only the adhesive and one involving a combination of the adhesive and bolts. The goal was to obtain lighter and more fatigue resistant structural details compared to metallic ones.

Borrie et al. (2015) studied the combined effect of marine environment and fatigue loading on the bond behaviour between CFRP and steel. The results show that even in short-term exposures, the protection and maintenance of such rehabilitated structures are paramount in ensuring their strength and resilience over time.

Several numerical simulation strategies of the composite to steel bonding were presented in (Tomaso et al., 2014). The aim of the work was to simulate the delamination of interfaces. Theoretical fundamentals of each method were considered identifying the main geometrical, i.e. the overlap length. Numerical results were compared to experimental tests thus benchmarking the simulation quality against the elastic stiffness of the joint and its failure load. Similar simulation strategies were also presented in (Godani et al., 2014, Godani et al., 2015) the numerical and experimental analysis of the interlaminar shear strength of composites and in (Nebbia et al., 2015a, Nebbia et al., 2015b) the numerical and experimental characterization of yacht steel plates coated by fillers.

6. FATIGUE RELIABILITY

The new information that can be derived from fatigue tests and uncertainties related to the previous chapters could be analysed, revealing the overall integral picture including different limit state functions, sensitivity analysis (what factors are more important than others, etc.) to be included here.

Structural reliability is not a new phenomenon now in ship design procedures. Reliability assessment is being used to support engineering, operational and maintenance scheduling decisions using the techniques of the risk assessment in ship structures. Traditionally, the reliability of a structural component is defined as the probability of maintaining its ability to fulfil its design purpose for some time under specified environmental and operational conditions. Time-dependent conditions will have the greatest influence on the reliability outcome. Therefore, it is expected that the ship structure reliability needs to account for the following influencing parameters (i) time-dependent corrosion and fatigue damage accumulation, (ii) uncertainties in strength (fatigue damage accumulation and crack growth), (iii), uncertainties in operational loads, (iii) maintenance periods, (iv) safety and consequences of failure.

In the context of fatigue reliability, in general, two approaches are often considered to describe the fatigue limit state: S-N and fracture mechanics based crack growth approaches. The fatigue reliability assessment considers the uncertainties induced by all parameters involved in the fatigue assessment treating them as basic stochastic variables. Yet, obtaining the correct and reliable statistical information of the stochastic variables is one of the main challenges.

In this chapter, the following sections describe the attention paid towards statistical descriptors involved in the fatigue reliability assessment, limit state functions, reliability index, partial safety factors and their calibration and the fatigue reliability based life prediction assessment.

6.1 Statistical descriptors

The fundamental basis of the fatigue reliability assessment of ship and offshore structures is the probabilistic description of fatigue failure influencing parameters, which account for the uncertainties in strength (fatigue damage accumulation, crack growth) and fatigue load. These uncertainties are to be considered by treating them as basic random variables and are represented in terms of statistical distributions (distribution type, mean and standard deviation, etc.).

There could be various uncertainties in the fatigue failure, such as:

- Current condition of the ship structure
- Time-dependent degradation of strength due to corrosion
- Crack initiation and growth with time
- Quality of construction and maintenance practices
- Weld distortion and residual stresses
- Weld details
- Stress concentration factors
- Material property variability
- S-N curve parameters, etc.

Methodologies developed to account for the uncertainties related to strength and load are described in the following sections.

6.1.1 Fatigue loading

The loads acting on the ship and offshore structures are uncertain due to many factors, including wave height, period and distribution. The uncertainties in the fatigue load are as important as strength uncertainties. Determination of reliable fatigue load considering various influencing factors is still a challenging task. The sources of load uncertainties are:

- Modelling of fatigue loads
- Wave-induced global bending moment
- Slamming loads
- Exposure to a variety of loads
- Operational variations and different operating areas

The uncertainties in the wind and wave-induced loading on an offshore wind turbine supporting structure to evaluate the probability of failure and the dynamic behaviour of the structure was determined based on the finite element method were studied in (Yeter et al., 2015c, d, 2016b, 2017c). The results of the fatigue damage assessment were obtained by employing the S-N, fracture mechanics, and the strain-based approaches. The results of the reliability analysis were presented as a function of the offshore wind turbine operational scenarios in a way to allow determining what operating conditions should be avoided. It was proposed that the narrow-band load may be improved by a proper correction factor accounting for the existence of a wideband loading to achieve close outcomes compared to the rain flow solution in the time domain. The performed sensitivity analysis showed that the uncertainty with respect to the wind loading is substantially important.

The First Order Reliability Method (FORM) and Monte Carlo Simulation (MCS) methods of reliability analysis to compute the fatigue damage in offshore wind turbine to demonstrate that the uncertainties related to fatigue damage estimation of non-linear systems are highly dependent on the tail behaviour and extreme values of the stress range distribution was compared in

(Horn & Jensen, 2016). It has been shown that the standard deviation is reduced up to 30% for load cases where the fatigue damage distribution deviates from the normal distribution.

A fatigue damage estimation procedure for non-linear systems subjected to stochastic load excitations uses a combination of Monte Carlo simulations (MCS) and the FORM was proposed in (Jensen, 2015), where FORM is used to get a more accurate description of the upper tail behaviour of the probability distribution of the rain flow counting damage estimation. The study undertook a specific example dealing with the stresses in a tendon in a tension leg platform subjected to second order wave forces and observed that the coefficient of variation (COV) is reduced by a factor larger than three. Also, the total computational effort for the present example was reduced by one order of magnitude for the same prediction accuracy in the fatigue damage estimation. Stationary conditions are assumed and therefore for a long-term analysis, the proposed calculations have to be done for all pertinent stationary sea states. The FORM analysis does not need to be recalculated if only the significant wave height is changing as the FORM reliability index is strictly inversely proportional to the significant wave and thus the calculation time gets reduced.

In case of stochastic loading & response and non-linear system behaviour, the spectral calculation of fatigue damage estimates can be rather time-consuming. Usually, the Monte Carlo (Hammersley & Handscomb, 1975) simulation is applied, but if the number of simulations is relatively small the coefficient-of-variation can be large because of the sensitivity w.r.t. large simulation values. If the safety index is linearly related to damage, the first order reliability method can be used in addition to obtain a better estimation of the damage distribution tail, reducing the coefficient-of-variation. An example shows that a reduction by a factor 3 is possible (Jensen, 2015).

For the fatigue assessment of containerships, a time efficient response calculation procedure has been proposed. The hull girder finite shell element model could be replaced by a beam model, but the torsion induced response estimates would introduce quite large errors. Using a shell element model, the relation between the loading and the structural response has been established for an arbitrary sea state in a few time steps. The result has been used to estimate the generalized relationship for an arbitrary sea state using linear regression analysis. The procedure is almost as time efficient as for a finite beam element model. General capabilities of the regression method still need to be checked (Mao et al., 2015).

Assessing fatigue of catenary risers, the touchdown point requires attention. One of the challenges is related to riser – seabed interaction. Adopting a non-linear model, the geotechnical parameter sensitivity has been investigated because of the considerable uncertainty. Fatigue reliability is not extensively investigated for riser design and a first-order reliability method has been adopted to estimate the fatigue safety index (Elosta et al., 2014).

6.1.2 Fatigue damage accumulation

The uncertainties in the load determination are transferred to the uncertainties in computed stresses. The uncertainties associated with the fatigue capacity through empirical S-N curves are accounted for by modelling K as a Log-Normal distributed stochastic variable. The experimentally developed S-N curves are the basis of the fatigue damage accumulation methodology. However, S-N curves are developed based on relatively small structures and their failure does not necessarily reflect the actual failure scenario of the ship structure, which is a very large and highly redundant structure.

In the S-N curve based approach to a fatigue reliability assessment, the role of the stress concentration factor (SCF) is very important. Uncertainties in SCF computation was studied in (Ogeman et al., 2014.). They reviewed the different direct calculation procedures for how to obtain the SCF based on fatigue assessment guidelines. The effect of different element types (shell and solid) and local stress extrapolation methods to the fatigue damage estimation was

studied for both longitudinal and bending (vertical and horizontal) load conditions in a container ship of 4,400TEU. It was shown that the use of the solid element or 8 node shell element approach would give conservative results. However, no attempt to verify experimental data has been performed. The authors also pointed out the effect of the bracket thickness and stiffener flange on SCF.

6.1.3 Crack growth

Fatigue crack propagation is also affected by many parameters such as initial crack size, history of local nominal stresses, and load sequence (Dong & Frangopol, 2015). In addition, there are uncertainties related to the crack growth parameters in the Paris Erdogan equation, in geometry functions for the plate solution and the weld notch and in the initial defect distribution. Other uncertainties are the effect of residual stresses and mean stress and threshold value for crack growth. The crack size at fracture is another uncertainty which can be important for the structural reliability as the probability of detecting a crack is increasing with the crack size (Lotsberg et al., 2016).

It is of a significance to evaluate the risk associated with marine vessels to manage the ship routing. A series of factors ranging from weather, sea states, uncertainties in structural capacity and load effects to the decision maker's attitude towards the expected consequences of the ship routing will affect the risk encountered in the travel, and thus play roles in ship routing decisions. A structural reliability approach is suggested in (Dong & Frangopol, 2016), where the support system deals with the uncertainties in the structural capacity and loading to investigate the fatigue damage. In the procedure, four important aspects, related to the repair cost, cumulative fatigue damage, total travel time, and carbon dioxide emissions are treated as the consequences of the decision, and the Multi-Attribute Utility Theory (MAUT) is adopted to reach a balanced combination of various attributes.

A probabilistic approach is proposed for the failure risk assessment of a welded ship structure with respect to the fatigue damage caused by multiple site cracks (Feng et al., 2012b, a, 2014, Huang & Sridhar, 2016). The initiation and propagation of fatigue cracks often occur at weld toes while the welded structure is subjected to alternating loading and to account for the interaction of multiple fatigue cracks and inherent uncertainties in the fatigue crack growth process, a probabilistic model for fatigue crack growth is developed based on the Paris relation. The probabilities of fatigue failure of multiple cracks in the welded structure are estimated by using the reliability analysis. Then, the failure risk assessment for the welded structure with multiple site cracks is performed based on the fatigue reliability estimation. As the service life of ship structures is usually very long, in-service maintenance activities for the locations of critical fatigue damage in ship structures are necessary to ensure the integrity of structures. The failure risk associated with the fatigue crack growth can be updated through inspections and repairs based on the probabilistic model of the damage detection. The effects of the in-service inspection quality and frequency are investigated with respect to the risk assessment of structural fatigue failure.

6.2 Limit state functions

The instantaneous reliability may be obtained by defining the limit state function, which defines the failure domain; safe or unsafe. Failure can be defined considering several criteria depending upon many considered influencing parameters or uncertainties.

6.2.1 Fatigue damage accumulation

Exceeding a certain damage level or fatigue safety ratio (generally equal to one), the fatigue safety levels are some examples of the damage accumulation limit state function. The Palmgren-Miner rule forms the basis of the damage accumulation limit state function. A limit state function to determine the accumulated failure probability was proposed in (Lotsberg et al., 2016) as $M(t) = \Delta - D(t)$, where Δ is a function describing the uncertainty in the Palmgren-

Miner damage accumulation and D(t) is accumulated fatigue damage at time t based on S-N data.

A methodology of the reliability assessment based on a direct finite element analysis of the ship hull structures based on the distribution of structural strains was developed in (Feng et al., 2015). The distributions of ship structural strains in the short and long-term sea states were defined first by using the FE method and further derived the extreme strain accounting for the stochastic origin of the still water and wave-induced loads. The limit state function based on the von Mises stress failure criterion is used. The ship structural response in still water was calculated based on the FE method identifying the structural strain, which was normally distributed. Both the global and local load effects were considered and only the full loading condition of a bulk carrier was analysed.

The fatigue reliability of the fixed offshore wind turbine support structures based on the spectral fatigue damage assessment was studied in (Yeter et al., 2015c, 2017c). The adequate limit state functions are developed accounting for the physical, statistical, measurement, and modelling uncertainties. The developed limit state functions also addressed the narrow-banded approximation. The system reliability was estimated accounting for the correlation between the welded tubular joints of the modular jacket offshore wind turbine structures (Yeter et al., 2016c).

6.2.2 Crack growth

Fatigue cracks can appear at various locations in the ship structure and may occur at early stages in the service life. Due to the presence of significant uncertainties, associated with the crack initiation and propagation, the planning of inspection, monitoring and/or repair actions should be performed probabilistically. The fracture mechanics crack growth based limit state function may include the exceedance of a critical crack size, critical number of cycles or critical stress intensity factor (Ibrahim, 2015a).

A stochastic Gamma process was modelled in (Guida & Penta, 2015), mainly to derive the distribution of the time to reach any crack size. In the model, the proposed time to reach a given crack size is considered a random process over the crack size domain, giving rise to three main advantages: the time to reach any crack size is completely defined by its first-order distribution, the process exactly coincides with the postulated deterministic crack growth rate model, and it can account for the presence of both heterogeneity and load conditions, and it is capable of predicting the main stochastic features of the time to first reach a given crack length as a function of the load conditions.

A probabilistic framework for incorporation of risk and updating in the inspection of fatigue-sensitive details of ship structures, considering that fatigue cracks as a structural deterioration mechanism may lead to unanticipated out of service of naval ships was developed in (Dong & Frangopol, 2015). The computation associated with fatigue damage is performed using the fracture mechanics and uncertainties considered within this process. As indicated, the fatigue crack size increases significantly with time and uncertainties are incorporated into the process. The uncertainties are also associated with inspection events. The outcomes of an inspection event are affected by many factors, such as the type of the inspection method, human factors, and inspection quality. Consequently, uncertainties should be incorporated into the risk-informed decision making and updating. The random variables associated with the fatigue crack limit state are analysed. It is pointed out that future research is needed to include the nonlinear fracture mechanics in the damage assessment of fatigue-sensitive details and the effects of multiple fatigue cracks on the structural capacity have to be taken into account in future studies for the risk assessment of fatigue-sensitive structures.

A probabilistic approach for inspection, monitoring, and maintenance optimization for ship details under fatigue effects on the basis of the crack growth approach was proposed in (Soliman

et al., 2016). Based on the stress profile and the crack geometry at the damaged location, intervention times and types are determined by solving an optimization problem, which simultaneously minimizes the life-cycle cost, maximizes the expected service life, and minimizes the expected maintenance delay over the life-cycle.

An approach to assess the probabilistic life of mixed-mode FCG by coupling of the finite element analysis and the Kriging-based reliability methods was proposed and studied in (He et al., 2015). A simulation program (FCG-System) is developed to simulate the fatigue crack path and to compute the corresponding fatigue life. Numerical applications dealing with FCG are presented to illustrate the numerical efficiency and accuracy of the proposed approach.

The probability of the existence of defects, fatigue damage and crack growths in the offshore wind turbine support structures subjected to abnormal wave and wind-induced loads is very high and may occur at a faster rate in a low cycle fatigue regime and crack growth, leading to a dramatic reduction in the service life of structures. It is therefore vital to assess the safety and reliability of offshore wind turbine support structures in the sea. To this regard, the reliability analysis incorporating low cycle fatigue and crack growth of an offshore wind turbine support structure during the service life was performed in (Yeter et al., 2016b). The analysis includes different loading scenarios and accounts for the uncertainties related to the structural geometrical characteristics, the size of the manufacturing and service life defects, crack growth, material properties, and the model assumed in the numerical analyses. The probability of failure is defined as a serial system of two probabilistic events described by two limit state functions. The first one is related to a crack initiation based on the local strain approach and the second one on the crack growth applying the fracture mechanics approach. The limit state function introduced in (Yeter et al., 2015d) is developed in such way that the critical crack size is estimated based on the failure assessment diagram, which takes into account yielding and fracture failure conditions.

6.3 Calibration factors for design

The purpose of the code calibration based on the reliability assessment is to arrive at codes that give a uniform and acceptable design for the entire scope and the code is intended to cover and avoid unnecessary costly designs.

A reliability-based partial safety factor code will, to a large extent, reflect the variabilities and uncertainties of the governing quantities. It is therefore essential that these variabilities are properly documented. Such information can be used in other contexts than the ones they originally were collected for. The design codes and their partial safety factors cannot be used in other contexts than the ones they originally were intended for, i.e. their validity is generally restricted to the original scope of the code.

In the reliability analysis, design variables are regarded as random variables with certain levels of uncertainties. A basic method of reliability analyses is the partial safety factor method, referred to as a Level I method, where only the characteristic mean value of each uncertain parameter is used. In Level II methods, the mean values and standard deviations for the uncertain parameters are used, assuming normal distributions. Methods based on the first-order reliability index are used in Level II and can be used to calibrate Level I methods. In Level III, uncertain parameters are modelled by their joint distribution functions, and reliability is assessed based on the probability of failure. Level III methods can be used to calibrate Level II methods. In Level IV, the consequence of failure is also accounted for, considering costs and benefits of construction, maintenance and repair.

Fatigue reliability of structures not subject to inspection is typically based on the SN approach and the linear damage summation. When inspections are planned, the fracture mechanics approach is applied, which allows for updating the reliability based on the presence of cracks. This allows accounting for the condition of the structure, and the reliability can be quantified

from the code by a calibration. For a Level I method, this calibration entails analysing the structure for trial design parameters, each resulting in a reliability index and a set of important factors. For each stochastic variable is assigned a safety factor, and these are found when the calculated reliability index matches the target reliability index. The partial safety factor method is based on both engineering judgement and statistical estimates of the characteristic values (when standard deviations can be calculated analytically). The characteristic values are adjusted by division with partial safety factors that take values between 1.0 to 1.5.

A method for calibrating fatigue design factors for a wave energy converter fixed to the seabed was presented in (Ambuhl et al., 2015). Designs based on inspection and without inspection were considered, relying on a crack growth model for the former and SN curves for the latter. Fatigue design factors, ranging from 1.0 to 6.5, were found for a range of inspection intervals and inspection methods.

In Level II methods, each uncertain variable is described by a mean and a variance, in addition to the covariance between the variables. In the reliability index method, the limit state function is transformed into standard space. The transformed variables have a mean value of 0 and a standard deviation of 1. The reliability index, denoted β, is the distance between the design point to the origin in standard space. The probability of failure Pf is found from the reliability index by evaluating the standard normal cumulative distribution function Φ as $Pf=\Phi(-\beta)$.

Level III requires numerical integration or approximate analytical methods. First-order reliability method (FORM) and second-order reliability method (SORM) are widely used to calculate the failure probability by approximating the limit state function by a first-order or second-order function at the design point. These methods give good results for the small probabilities typically applied in the structural reliability analysis. Alternatively, numerical simulations can be used, such as the Monte Carlo, Latin hypercube, and importance sampling, which give the failure probability as the failure ratio of the simulations.

A new methodology to calibrate structural reliability models (prediction models for anodes, coating, corrosion, crack, etc.) output was presented in (Hifi & Barltrop, 2015). The methodology combines data from experience and prediction models to correct the structural reliability models.

The S-N test data represent a total number of stress cycles to failure (defined as through thickness crack) for a known constant stress range. When performing crack growth analysis, it is required that the initial crack size is known. Two different methodologies for calibration of the fracture mechanics to the S-N test data to obtain comparable results were presented in (Lotsberg et al., 2016) as: (i) the S-N fatigue life is a sum of crack initiation and crack growth. This implies a definition of a suitable critical deterministic crack size a_0, and calibration of a suitable distribution of the crack initiation time, N_i, until such a crack size is developed; and further fatigue life can be described by crack growth; (ii) the S-N fatigue life is assumed to be equal to the crack growth life. This implies an assumption that the crack growth starts from the first stress cycle and a suitable distribution of the initial fictitious crack size a_0 is calibrated.

Several authors have proposed methods for reliability updates following inspection (Lassen & Recho, 2015, Luque & Straub, 2016, Soliman et al., 2016, Schneider et al., 2017). Reliability indices can be derived for different inspection outcomes using the Bayesian inference, while the Paris' constants are typically derived from the SN curves. This can also be used for inspection planning, and DNV-GL has recently published a recommended practice on probabilistic methods for inspection planning of offshore structures, as reported in (Lotsberg et al., 2016).

A reliability-based inspection framework for very large crude carriers was proposed in (Doshi et al., 2017). The crack length as found by the visual inspection was treated as both deterministic and normally distributed with two levels of standard deviations. The inspection intervals were

similar for both deterministic and stochastic crack length evaluations, and significantly shorter compared to NDT. Few studies have been published on Level IV methods.

A framework for establishing system reliability of multiple fatigue locations, considering the correlation between these and consequences of failure was presented in (Dong & Frangopol, 2016). Several authors report on improved numerical procedures and generalized approaches that can account for sequence effects or multiple site damage in a system reliability framework. Several methodologies were presented in (Feng et al., 2012b, a, Huang et al., 2012, 2013, Feng et al., 2014, Huang et al., 2014b, c, Feng et al., 2015, Huang & Sridhar, 2016) based on hot-spot calculations from the finite element analyses, where the reliability of the system is modelled as a series of critical hot-spot details.

A method to improve the accuracy of reliability estimates found by Monte Carlo simulations was proposed in (Jensen, 2015). By deriving the fatigue damage from the failure probability, he was able to demonstrate better accuracy in the tail end of the rain flow damage probability distribution.

Computational methods for assessing the fatigue reliability under variable amplitude loading were presented in (Altamura & Straub, 2014). They show that not assuming constant amplitude loading may yield non-conservative results compared to the variable amplitude model where the sequence effects are accounted for.

The fatigue reliability analysis was incorporated in (Yeter et al., 2017b) as a risk-based multi-objective design optimization. The Pareto frontier is adopted to identify the optimal design solutions within the feasible design space the probabilistic evaluation is performed for these optimal design solutions using FORM, and the second-order Ditlevsen bounds are used to solve the multi-dimensional system reliability problem accounting economic criteria. The levelised cost of energy (LCOE) is considered as the top-level objective function. Also, a time-variant probabilistic assessment of the life-cycle of offshore wind turbine support structures accounting for the uncertainties and their propagation in time is studied in (Yeter et al., 2017a). Several scenarios involving different uncertainties were investigated. Under these scenarios, the life-cycle of the OWT support structure is analysed considering a threshold for an offshore wind turbine to be a viable investment. The results aimed to aid to develop a multi-dimensional framework for decision-makers to attain cost-effective and profitable (long-term) offshore wind energy projects.

A method for estimating the fatigue reliability of butt welds in a submarine pressure hull was presented in (Liu et al., 2014). The initial crack size is treated as a random variable, using the probability density evolution method to simplify the problem. This allowed probability distributions to be calculated and the fatigue reliability could be estimated for random loading and uncertain material parameters without the need for numerical simulations. The Monte Carlo simulation and a probabilistic crack propagation approach, accounting for the uncertainty of the residual stresses in stiffened panels were used in (Mahmoud & Riveros, 2014).

6.4 Fatigue service lifetime estimate

Depending on the information available, the ship and offshore structure stage and the aim of the reliability analysis, a fatigue service lifetime estimate can be obtained using either a fatigue damage accumulation or crack growth approach.

6.4.1 Fatigue damage accumulation

At the design stage, the actual state of the structure is not known in general. The material has not been ordered and only information with respect to the fabrication and inspection process may be available. The type of information expected is the probability of economic loss by failure during the expected service lifetime. For this kind of analysis, a model based on the damage

accumulation is generally preferred. The defined probability of failure depends on the kind of risk assessed.

A time-dependent structural reliability methodology involving fatigue and fracture failure modes at component and system level has been developed for marine vessel applications (Ayyub et al., 2015). Corrosion has been accounted for, although corrosion-fatigue interaction is not considered.

Considering the dent size and applied loading, the fatigue reliability as a function of the number of load cycles has been established for pipelines (Garbatov & Guedes Soares, 2017). The model consists of a series of segments, characterized by the fatigue strength properties and reliability descriptors derived from a Weibull model analysis. The developed approach may be used to identify practical scenarios for inspections and repair.

The fatigue damage accumulation consequences for random corrosion characteristics have been investigated (Cui et al., 2016). Assuming the corrosion depth can be modelled using a lognormal distribution, the corrosion induced fatigue damage is lognormal distributed as well. When cracks are discovered, but no reasonable renewal of the cracked part is possible immediately a provisional repair; a crack stopping hole is commonly carried out allowing the structure to continue its operational service. This repair does not belong to the recognized designs and its efficiency has to be demonstrated, in particular, the time lag before a new initiation in the crack stopping hole. Based on the material properties and a mean stress or a maximum stress, it has been shown that the reliability index increases when the radius of the crack stopping hole increases (Chen, 2015).

Offshore wind turbine supporting structures are subjected to both wind and wave induced loads. A fatigue analysis for the installation of a wind turbine in the Aegean Sea was presented (Bilionis et al., 2015). A full wind and wave correlation has been adopted, as it considered the most extreme situation.

6.4.2 Crack growth

During the inspection, the structural state is better known and particularly, possible flaws are carefully investigated at least at the hot spot area. The aim of the probabilistic analysis is to assess the likelihood of a sudden structural collapse by brittle fracture within the period to the next inspection. Considering the consequences of such a kind of collapse, which may involve human fatalities, the crack growth approach combined with brittle fracture criteria may be preferred. The acceptable probability of failure may be different from any previous case as the consequences may be different.

Among the factors affecting the fatigue damage accumulation, the effect of corrosion randomness on the fatigue damage accumulation was analysed in (Cui et al., 2016). If the corrosion depth can be modelled by a lognormal law they analysed the result of the damage accumulation in terms of an additional fatigue damage which can be modelled by a lognormal law. When the cracks are discovered, but no reasonable renewal of the cracked part is possible immediately, a provisional repair is commonly carried out allowing the structure to continue its operational service. This repair does not belong to the recognized designs and its efficiency is to be demonstrated and particularly the time lag before a new initiation in the crack stopping hole.

Chen (2015) carried out an analysis based on the material properties and a mean stress or a maximum stress. Obviously, the model shows that the reliability index increases when the radius of the crack stopping hole increases. Wind turbine supporting structures are also subjected to fatigue due to both wind and waves. An analysis of fatigue in the Aegean Sea on the installation of a wind turbine was presented in (Bilionis et al., 2015). One challenging question is the correlation between the sea states and the wind. As no correct answer is available, the most extreme situation has been considered a full correlation.

Based on the S-N curve approach, a methodology for the time-dependent structural reliability of marine vessels based on fatigue and fracture failure modes for life predictions at the component and system levels was developed in (Ayyub et al., 2015). The proposed method also accounts for the effect of corrosion on the fatigue reliability while predicting the fatigue reliability and life. However, it does not account for corrosion-fatigue interaction.

An interesting approach was presented in (Garbatov & Guedes Soares, 2017) where different failure criteria considering a dent size and applied load are analysed and fatigue reliability as a function of a number of load cycles is defined. The analysed pipeline is modelled as a series of segments, where any of them is characterized by the fatigue strength properties and reliability descriptors derived from the Weibull model analysis. The developed approach may be used to identify practical scenarios for inspections and repair, accounting for the fatigue and corrosion damage tolerance and load subjected to the pipeline.

7. FATIGUE DESIGN AND VERIFICATION BASED ON RULES, STANDARDS, CODES AND GUIDELINES

The primary objective of various Class rules, regulations and codes applicable to ship and offshore structures is to ensure that the design and analysis process results in the construction of the ship and offshore structures that can resist both extreme loads and cyclic operating loads. This section focuses mainly on the design methodologies for fatigue assessments provided by the Classification Societies. Characteristics of the IACS Common Structural Rules for Bulk Carriers and Oil Tankers (CSR) are summarized and compared to the rules of four Classification Societies that are applicable to non-CSR ships. Changes and updates in the class rules of DNV-GL, LR, BV and IRS in the years 2015-2017 are presented here. Furthermore, the main differences to CSR-rules are highlighted.

A comparison of the fatigue life assessment of a deck longitudinal stiffener end connection for a BC-A bulk carrier was carried out accordingly to the five class rules presented in this Chapter. Additionally, a benchmark study was also conducted to compare the fatigue predictions by spectral analysis of a bulk carrier's deck transverse butt-weld joint that involved direct load evaluation by various CFD methods and different rules processing the fatigue damage.

Furthermore, the latest updates in the IGC-Code addressing fatigue are presented.

7.1 Common Structural Rules (CSR)

The Common Structural Rules for Bulk Carriers and Oil Tankers (CSR) recently issued by IACS consolidated the fatigue assessment methodologies already introduced since some years in previous rules of classification societies (Horn et al., 2013, Shijian et al., 2013, IACS, 2015, 2016). Referring to the categorization of fatigue assessment approaches (see Ch.3), the structural stress approach is basically applied, denoted as “hot spot stress” in the rules. The evaluation of the hot spot stress can be carried out according to different procedures; the possible calculation approaches for ship structures are described in full detail in the rules.

It is worth noting that only fatigue cracks initiating from the toe of the weld and propagating into the plate and fatigue cracks initiating from a free edge of non-welded details are assessed while e.g. root cracks are not explicitly checked but covered by a standard design of structural details. However, the scope of fatigue analysis has been expanded with respect to former CSR and other individual class rules.

Fatigue induced by low cycle loads such as cargo variations or impact loads such as sloshing in partially filled tanks which may induce fatigue damage is not explicitly considered. Beside IACS documentation, a summary external paper about CSR was authored by Jiameng et al. (2016) providing some hints of possible impact and consequences on ship scantlings. The margins taken during the rules development regarding the fatigue assessment based on numerous

classification societies' experience by a comparison with direct spectral fatigue assessment for an oil tanker and a bulk carrier was estimated in (Quemener et al., 2015).

In the following, the main items of the CSR assessment procedure are briefly outlined.

7.1.1 Fatigue capacity

In the rule application of the structural stress approach, the hot spot stress value may be calculated by SCF or directly by the FE analysis. Structural details to be checked are listed and hot spot stress range evaluated either by:

- simplified stress analysis, i.e. nominal stress (beam theory) x Tabulated “SCF”
- finite element stress analysis, i.e. very fine mesh FE model
- screening fatigue assessment (50mm x 50mm mesh), i.e. nominal stress (fine mesh FE model) x tabulated "η".

The latter evaluates the hot spot stress using an FE model already available for other limit state verifications and a magnification factor defined on purpose to obtain a screening and to avoid the very fine mesh analysis. Fatigue assessment by very fine mesh analysis can be omitted for standard details listed in rules for which SCFs are available or other details assessed using the screening procedure; as a result, very fine mesh modelling is necessary for critical and non-standard details failing the screening procedure.

Readout points in FE models are carefully defined in the rules either for very fine or fine mesh models.

CSR applies the DEn S-N curves “B”, “C” (free edge) and “D” (welded joints), with modification on slope value for B and C curve, in-air environment. Specific S-N curves in the corrosive environment are also provided with a single slope. The time in the corrosive environment was initially set to 2 and 5 years depending on the structural member location, but that duration was recently doubled by urgent rule amendments (IACS, 2016).

For steel with specified minimum yield stress value higher than 390 N/mm^2 and for steels with improved fatigue performance, the S-N curves to be used are considered on a case-by-case basis. Mean stress effect and thickness effect correction are included following the IIW guidelines format. In particular, the mean stress effect is revised with a lower bound in compression mean stress set to 0.3 and 0.9 at zero mean stress. Additionally, the thickness effect exponent relates to the type of structural detail and is comprised between 0.0 and 0.25 according to IIW recommendations. Finally, surface finishing factors for the base material are also provided.

Noticeably, weld improvement methods are considered as supplementary means of achieving the required fatigue life only and are applicable to corrosion free conditions, albeit with the limitation of the benefit of post-weld treatment by T/1.47 (i.e. 17 years is the minimum required the life of an improved detail). Only weld geometry control and defect removal by burr grinding are considered as the basic methods at the fabrication stage. The application of post-weld fatigue improvement is subject to limitations and adequate workmanship control for construction.

7.1.2 Fatigue Loads

According to IMO-GBS (IMO, 2015), 25 years life is required for ships, which is the target considered in CSR-H rules also for fatigue assessment. Rule quasi-static wave induced loads are based on the North Atlantic wave environment. A Weibull distribution function is used to obtain the stress time history, calibrated at 10^{-2} probability level with shape parameter equal to 1.0 as this is the less sensitive point for calibration of the statistical distribution (Derbanne et al., 2011).

The fatigue stress range for each load case of each loading condition is defined by selecting 5 EDW and obtaining the corresponding load cases but differently, from other limit state checks,

the wave maximizing the heave and pitch accelerations in a head sea and oblique sea respectively are not considered to limit the computational burden. Loading conditions have been defined according to ship commercial practice and recently updated as far as bulk carrier types BC-B and BC-C is concerned (IACS, 2016). Damage is evaluated based on the stress range obtained from the predominant load case in each loading condition (e.g. full load, ballast, …), including all mentioned correction factors.

While a conventional ship speed of 5knots is assumed for extreme loads, for fatigue assessment the speed is ¾ V_{design}.

7.1.3 Fatigue assessment

Apart from detail design standards that provide welding requirements at critical structural details to prevent specific types of fatigue failure, the Palmgren-Miner linear summation of damage is implemented in the rules, duly considering the contribution of ship loading conditions as well as load cases. The hot spot stress range is evaluated by applying different methods and checked against S-N curves based on the structural stress approach. The worst-case principal stress components acting within or outside ±45° of the perpendicular to the weld toe are considered.

Instead of correction factors to account for corrosion effects, S-N curves for the corrosive environment are introduced and the fatigue damage is calculated for in air and corrosive environments, implicitly stating the time period during which the corrosion protection is effective.

It is worth noting that the corrosion is also accounted for when evaluating the acting stress by deducting half of the design corrosion margin from the gross thickness. This net scantling approach enables simply to reproduce the average thickness diminution through the ship's design life.

7.2 DNV·GL regulations

As a consequence of the merger, it became necessary to merge the former DNV (DNV, 2015) and former GL rules (GL, 2015) into one common set of rules. The rules came into force in January 2016, but for a transition time until July 2017 the DNV and GL rules were to be kept valid. The opportunity was used, and many small improvements were introduced. The load concept from Common Structural Rules for Bulk Carriers and Oil Tankers (CSR), which has been developed by the International Association of Classification Societies, (IACS, 2015), has been used as a basis. It has been improved to be applicable also for other ship types, e.g. also for small and slender ships. The fatigue capacity part is also aligned with CSR, but very much based on what has already been used by DNV and GL. Well proven parts from former rules have been kept. The topological structure has been taken from former DNV with a relatively short rule part with fundamental requirements and acceptance criteria and with a supporting class guideline with a detailed description of the fatigue strength assessment methods and approaches. The rules can be found in DNV GL rules for Classification, Ships, Part 3 Hull, Chapter 9 Fatigue (DNV-GL, 2017c) and the class guideline in DNVGL-CG-0129 Fatigue assessment of ship structures (DNV-GL, 2017a).

While in the past 20 years' lifetime was assumed, the design life has now been increased to 25. This is due to nowadays improved coating systems and inspection schemes. However, the corresponding number of load cycles for the calculation of fatigue damage depends on ship length. It is 8.6 10^7 for a ship of about 90 m in length and reduces to, e.g., 6.4 10^7 for 400 m length. This reflects the increase of encounter periods for larger ships in the same wave environment, leading to fewer load cycles at the same time.

Same Weibull distribution function as in CSR is used to obtain the stress time history, calibrated at 10^{-2} probability level with shape parameter equal to 1.0. The background is that the damage contribution of high-stress ranges is rather small due to the associated low number of cycles.

Depending on the S-N curve used, for a straight-line spectrum, the highest damage density fits with or is close to the quarter of the maximum stress range.

As DNV was using the hot-spot stress approach and GL the nominal stress approach, now both can be used, i.e., either the stress concentration factor K for serving the hot-spot concept or the FAT classes serving the nominal stress concept.

A revised thickness and size effect has been introduced where not only the base plate thickness is considered but also the length of transverse attachments, cruciform joints, and butt welds.

For consideration of corrosion a simplification has been done, the effect of which is however small. Other rules and standards use separate SN-curves for corrosive environments. But as measured corrosion progress scatters very much in practice, the related damage contribution is taken as based on the S-N curve in the air and then multiplied by 2.0. The amount of time to be considered in a corrosive environment is defined based on compartment type and content and ranges between 0 and 5 years. For target lifetimes above 25 years, the formulation for the predicted lifetime is made independent of the target lifetime, assuming a regular maintenance regime.

The mean stress effect, which can be important when details are exposed to compression, is handled similarly to how it has been in DNV and in GL. The pronounced effect of residual stresses and its shakedown on the mean stress effect, as it is considered in CSR for bulk carrier and tanker, is not relevant for typical loading conditions of other ship types and accordingly not applied in DNV-GL rules.

All full-scale measurements have confirmed that wave-induced hull girder vibrations, referred to as whipping (transient, e.g., from bow flare impact) and springing (resonant), contribute to the fatigue accumulation. The contribution is represented by applying a minimum equivalent increase to the wave bending moment, which is well correlated with the governing vibration mode of the hull girder. The increase is dependent on the beam of the vessel for both slender and blunt vessels, and in practice has a significant contribution for details in the deck, less in the bottom and close to insignificant in the side shell. For container ships, more ship specific and more sophisticated considerations are possible according to DNV GL class guideline for fatigue and ultimate strength assessment of container ships including whipping and springing (DNV-GL, 2017b).

7.3 Lloyd's Register (LR) regulations

The Lloyd's Register Rules and Regulations for the Classification of Ships (LR, 2016a) indicate that the fatigue performance of the hull structure is to be assessed in accordance with the applicable ShipRight Fatigue Design Assessment (FDA) procedures (LR, 2016c). The ShipRight FDA notation is assigned when the appraisal satisfies the requirement of 20 years' fatigue life based on the LR Fatigue Wave Environment (Worldwide) trading pattern. This assessment is mandatory for new oil tanker and bulk carrier configurations over 190 meters in length which are not constructed in accordance with the IACS Common Structural Rules (CSR), but it is not applicable to ships approved using the CSR.

The ShipRight FDA SPR notation is assigned as a supplement to the FDA notations when the fatigue performance of the hull structure considers the effects of the continuous vibrational response of the hull girder in waves (springing). Details for assessment of fatigue including hull girder springing loads can be found in (LR, 2014).

The ShipRight Fatigue Design Assessment (FDA) procedure (LR, 2016c) applies to oil tankers, LNG and LPG carriers, bulk and ore carriers and container ships and requires three possible levels of assessments:

- FDA Level 1 (LR, 2009): the proposed joint configurations at critical areas are compared with the structural design configurations specified in the Structural Detail Design Guide, which can offer an improved fatigue life performance.
- FDA Level 2 (LR, 2015, 2016b): this is a spectral direct calculation procedure based on parametric databases to compute the wave-induced loads and motions and simplified structural models which utilize LR's PC-Windows based software. This procedure is intended for the analysis of secondary stiffener connections.
- FDA Level 3 (LR, 2016d): this is a full spectral direct calculation procedure based on first principles computational methods, such as hydrodynamic load and ship motion analysis to determine the wave-induced loads and motions, and finite element analysis (global 3D FE model and local zoom FE model) to determine the structural response. It is intended mainly for the analysis of primary structural details.

For the FDA Level 2 and FDA Level 3, the Fatigue Wave Environment trading patterns have been derived for specific ship types using worldwide trading statistics. For all these trading patterns the probability of encountering a particular sea condition and wave heading is obtained from a voyage simulation program which makes use of global wave statistical data and applies seakeeping criteria to modify the ship speed and heading (LR, 2016c). The North Atlantic Wave Environment is based on the route from Norway to USA (East Coast) where the voyage simulator program is also used to obtain the operation probability profile. The simulation of the voyages using anticipated ship's operational profiles together with the hydrodynamic and structural mathematical models determine the stress range and associated number of cycles.

The FDA procedures adopt a unit load approach to estimate the total stress response by combining the results of discrete unit load cases and the applied loads. The unit cases include hull girder global loadings, external hydrodynamic wave pressure loads, and internal cargo/water ballast inertia pressure loads. All these loads are further computed for any loading condition and sea state resulting from the hydrodynamic analysis and voyage simulation. The distribution and magnitude of internal inertia pressure loads are determined by simplified expressions for each ship motion.

Both FDA Level 2 and FDA Level 3 adopt a hot spot stress approach in conjunction with the Palmgren-Miner cumulative damage rule. The LR hot spot reference design S-N curve represents the fatigue strength of the welded material in air, including the stress concentration due to the local notch at the weld toe. It consists of two slopes modified as per the Haibach correction at the 10^7-stress cycle and a reduction factor for corrosive operational environments. Additional stress concentration factors to account for construction tolerances and plate thickness effects may be applied (LR, 2016d). The mean stress correction is included to reduce the overall stress range when the stress cycle is in compression.

7.4 Bureau Veritas (BV) regulations

Bureau Veritas Rules concerning fatigue for steel ships are involved in NR 467 (BV, 2016b). Specific rules have been developed for containerships NR 625 (BV, 2016a). These rules involve a part dedicated to loads including fatigue loads defined in the framework of design load scenarios. In each scenario, Hot Spot Stress ranges are calculated according to a specified spectral approach. In addition, a class notation Whisp NR 583 considers whipping and springing.

NR 445 (BV, 2016c) deals with offshore structure. As dedicated to a structure where the operator specifications are generally very detailed this Classification rule is more focused on the objectives of the assessment including for fatigue than aiming to provide a comprehensive procedure to assess the structure. Within the objectives, different loads are involved due to waves, inertia, vortex shedding, and slamming. Fatigue life is addressed involving linear cumulating

of damage or alternatively fracture mechanics. The rules for each type of ship, ship-shaped offshore structure or tubular structure, fixed or floating, refer to NI 611 for fatigue assessment.

An assessment based on a fracture mechanics approach has been introduced, to assess the validity of inspection planning. Fracture mechanics is applicable from flaw detection up to fracture criterion in terms of a Failure Assessment Diagram. When no crack is detected e.g. at design stage the initial crack assumed is defined by the capacity of NDE implemented during the inspection.

The failure modes considered are detailed, including initiation at the weld toe, initiation at the weld root, initiation on shared surfaces and initiation in bolted assemblies. The stress calculations, particularly in the case of Finite Element Models, are clarified.

The load model involves different levels of refinement; from a simplified rule-based approach to different direct calculation approaches, spectral or time domain. Different methodologies are proposed for long-term simulation such as design sea states, equivalent design waves, spectral approaches, up to direct simulation. Nonlinear effects such as intermittent wetting and whipping are addressed.

In alignment with CSR, the reference stress has been changed from notch stress to hotspot structural stress as well as S-N curves accordingly. The reference fatigue stress incorporates the mean stress effect and plate thickness effect as given in (IACS, 2015). When relevant methods to model weld beads effects are provided. Nevertheless, for some classes of details an alternative definition of stresses is retained, such as structural stress in the weld bead for root initiation or a dedicated stress definition for bolted assemblies.

Fatigue strength corresponding to a cathodic protection condition for welded assemblies is involved. The effect of weld improvement is considered by using S-N curves with a lower slope and higher fatigue limit. For free edges, the applicable S-N curve depends on the treatment of shared surfaces and particularly the treatment of edge corners. The capacity of remaining fatigue life evaluation is addressed with crack propagation analysis. Concerning offshore units, the case of unit conversion is addressed. The fatigue damage of the unit before conversion is to be included in the total damage. The issues related to the impossibility of inspection or impossibility of repair are also addressed in term of increasing the design fatigue life.

7.5 Indian Register of Shipping (IRS) regulations

IRS rule approach for simplified fatigue assessment of ship structures is aligned with the IACS recommendation 56 (IACS, 1999). Based on above approach internal guidance notes are to be utilized for simplified fatigue assessment of ships except CSR ships. For CSR oil tanker and bulk carrier, fatigue analysis is to be performed using the IACS Common Structural Rules (IACS, 2015).

The computation of loads in simplified approach is to be referred to the IRS Rules and Regulations for the Construction and Classification of Steel Ships (IRS, 2016a, b). All the design loads used for fatigue assessment which include local loads (external and internal pressure) and hull girder loads in still water and in waves are based on Equivalent Design Approach (EDW).

The nominal or hot-spot stress based approach can be considered as per the guidance notes. Details mandated for evaluation of the hotspot stress are provided in IRS Rules for Bulk Carriers and Oil Tankers (IRS, 2016a, b). Stresses induced due to applicable loads are to be evaluated using beam theory. The long-term distribution of stress ranges is assumed to be defined by the two-parameter Weibull distribution. These two parameters are scaling factor which is defined by reference stress range and shape parameter which depends on location and probability level of loads. In simplified fatigue assessment, the shape parameter is assumed to equal to one, same as CSR at a given probability level of loads of 10^{-2}. The reference fatigue

stress incorporates the mean stress effect, plate thickness effect and warping effect as given in the rules (IRS, 2016a, b). The total number of cycles for design life is computed by considering the 25 years of ship's life. All the structural properties are computed based on a net thickness approach. Net thickness of local support members is to be obtained by deducting 0.5tc from the gross thickness.

The fatigue damage is computed using the Palmgren-Miner summation rules. The characteristic fatigue strength of structural details is referred from the design S-N curves (UK-HSE, 1990, IACS, 1999). For fatigue damage estimation, both air and corrosive environment are considered in the analysis.

7.6 Comparison of simplified fatigue approaches

Besides the common fatigue approach for oil tankers and bulk carriers in CSR, each Classification Society uses its own simplified procedure for fatigue checks of other ship types. These individual fatigue procedures differ more or less from the CSR approach, although the principal method is similar and in alignment with the Unified Recommendation No. 56 of the International Association of Classification Societies (IACS, 1999).

Most procedures are based on the identification of two critical dynamic load cases for each of the relevant loading conditions. Therefore, in each load case, an evaluation is performed of the stresses induced by global loads of the hull girder and stresses due to local loads (external wave pressure and internal inertial pressure) to identify the cases with the maximum and minimum total stress. On the resulting maximum nominal stress range stress concentration factors are applied to account for the geometry of the investigated structural detail. From the reference stress range and its associated probability, a stress range distribution is derived. This distribution, coupled with the Miner's hypothesis of linear accumulated damage and to S-N curves describing the fatigue strength, provides the background for all verifications, even if the way such verification is formulated, and the type of final output can differ. The various steps of this general framework are analysed in more detail in the following.

The detail selected for comparison of simplified checks in the present chapter is the end connection of the deck stiffener at the same location (y=21.4m, z=24.54m) as considered in the spectral benchmark. The midspan of the stiffener is located at Fr. 154 (x=127.76m, x/L=0.4481) and the investigated end connection cross at Fr. 157 (x=130.34m, x/L=0.4547). The stiffener type is a symmetrical bulb profile corresponding to a T-profile of the size 263*12.0*89*27.0. Connected to the deck plate of t=36mm with a stiffener distance of 700mm. Every 5.16m the deck stiffener is supported by a web frame and connected with a web stiffener FB 110*14. All material properties have a yield strength of 355 N/mm².

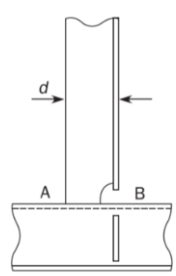

Figure 3: End connection type

Regarding this sample case, formulations of considered class rules in respect of fatigue capacity and fatigue loads have been compared. The LR rules are not considered in this comparison, as the LR procedures FDA Level 2 and FDA Level 3 (see Section 7.3) are based on spectral direct calculations and not a simplified procedure for fatigue checks.

However, the fatigue damage determined by applying the LR FDA Level 2 approach is also given for reference (see Table 7). The LR assessment considers the four loading conditions and it is based on the LR North Atlantic wave environment (LR, 2015, 2016c, b). This operational profile together with the hydrodynamic load motions, obtained from parametric databases, and the structural mathematical models determine the stress range and associated number of cycles (see Section 7.3). Therefore, intermediate calculations of the loads and motions, as well as the associated stress range, cannot be provided here as they will vary for each individual sea state.

7.6.1 Loading

For a sample case in the upper hull, the vertical hull girder bending is the dominating load component. For quantification of the vertical wave bending moment, all class societies refer to the unified requirement S11 (IACS, 1989). Load combinations effected by horizontal bending and torsional moment are not of relevance for the investigated location in the upper hull and accordingly not explicitly considered here.

In IACS unified requirement S11, the wave vertical bending moment (MWV) refers to an exceedance probability of 10-8. For fatigue, it is useful to scale this extreme value, which may occur only once in ship's lifetime, down to a value more representative for fatigue behaviour. In newly developed CSR (IACS, 2015) an exceedance probability of 10-2 was introduced for the fatigue loads and some of the class societies apply this load level for fatigue in their own rules, too. The probability factor in Table 1 describes the ratio between the 10-8 hogging wave bending moment and the considered fatigue amplitude.

Table 1: Hull girder loads at 0.45 x/L

Permissible still water moment						
M_{SW} hog [MNm]		4,300				
M_{SW} sag [MNm]		-4,000				
Vertical wave bending moment		acc. IACS UR S11				
10^{-8} M_{WV} hog [MNm]		6,245				
10^{-8} M_{WV} sag [MNm]		-6,563				
		CSR	DNV GL	LR	BV	IRS
Probability for fatigue		10^{-2}	10^{-2}	Sec 7.6	10^{-8}	10^{-2}
Homogen	Factor probability	0.218	0.218	-	-	0.218
	Factor hull girder vibration	1.0	1.2	-	1.0	1.0
	M_{WV} fatigue amplitude [MNm]	1,362	1,634	Sec 7.6	6,938	1,389
	M_{SW} applied [MNm]	-1,600	-4,000	-1,316	n/a	-1,600
Alternate	Factor probability	0.218	-	-	-	0.218
	Factor hull girder vibration	1.0	-	-	-	1.0
	M_{WV} fatigue amplitude [MNm]	1362	-	Sec 7.6	-	1389
	M_{SW} applied [MNm]	3,225	-	3,272	-	3,225
Normal Bal.	Factor probability	0.223	0.223	-	-	0.223
	Factor hull girder vibration	1.0	1.2	-	1.0	1.0
	M_{WV} fatigue amplitude [MNm]	1,393	1,671	Sec 7.6	6,938	1,420
	M_{SW} applied [MNm]	3,440	4,300	2,969	n/a	3,440
Heavy Ballast	Factor probability	0.221	-	-	-	0.221
	Factor hull girder vibration	1.0	-	-	-	1.0
	M_{WV} fatigue amplitude [MNm]	1,385	-	Sec 7.6	-	1,412
	M_{SW} applied [MNm]	-3,000	-	-1,660	-	-3,000

For the investigated detail, the mean stress is dominated by the assumed still water moment M_{SW}. According to some class rules permissible still water moments are applied. CSR consider reduced still water moments for the different loading conditions.

Local loads are generated on the outer hull by external hydrodynamic pressures and on tank and cargo hold boundaries by inertial pressures exerted in the liquid or bulk cargo by ship's local accelerations. Formulations are provided for combined accelerations at the investigated stiffener location as the sum of ship's translational and rotational accelerations. Listed reference values correspond to the fatigue exceedance probability for the relevant load case of the different loading conditions.

7.6.2 Response

Stresses from global and local loads are summarized in Table 3 to 6 for the considered loading conditions. In all rules, local external loads are not relevant to fatigue strength of deck stiffeners. As per CSR, local internal loads are neglected for fatigue strength of deck stiffeners.

Nominal stress components are multiplied by stress concentration factors (SCF) to get hotspot stresses or notch stresses. These corrections are applied during the evaluation of single components to allow different SCFs for global and local stresses.

Table 2: Combined accelerations at deck stiffener location

Loading Conditions with CSR default values		CSR	DNV GL	LR	BV	IRS
	Probability for fatigue	10^{-2}	10^{-2}	Sec.7.6	10^{-5}	10^{-2}
Homogen T=17.5 m GM =5.59 m k_r = 16.31 m	Relevant EDW	HSM	HSM	Sec.7.6	n/a *	HSM
	Long. acceleration amplitude [m/s²]	-0.245	-0.205		a, b: 0.868 c, d: 0.0	-0.245
	Trans. acceleration amplitude [m/s²]	0.0	0.0		a, b: 0.0 c, d: 5.341	0.0
	Vert. acceleration amplitude [m/s²]	0.421	0.431		a, b: 2.097 c, d: 7.160	0.422
Alternate T=17.5 m GM =9.32 m k_r = 18.64 m	Relevant EDW	HSM	-	Sec.7.6	-	HSM
	Long. acceleration amplitude [m/s²]	-0.245	-		-	-0.245
	Trans. acceleration amplitude [m/s²]	0.0	-		-	0.0
	Vert. acceleration amplitude [m/s²]	0.421	-		-	0.422
Normal Bal. T=9.07 m GM =15.38 m k_r = 20.97 m	Relevant EDW	HSM	HSM	Sec.7.6	n/a *	HSM
	Long. acceleration amplitude [m/s²]	-0.219	-0.143		a, b: 1.056 c, d: 0.0	-0.219
	Trans. acceleration amplitude [m/s²]	0.0	0.0		a, b :0.0 c, d: 5.074	0.0
	Vert. acceleration amplitude [m/s²]	0.162	0.165		a, b: 2.097 c, d :2.493	0.162
Heavy Ballast T=11.51 m GM =11.65 m k_r = 18.64 m	Relevant EDW	HSM	-	Sec.7.6	-	HSM
	Long. acceleration amplitude [m/s²]	-0.220	-		-	-0.220
	Trans. acceleration amplitude [m/s²]	0.0	-		-	0.0
	Vert. acceleration amplitude [m/s²]	0.235	-		-	0.235

* Accelerations acc. BV-rules are provided for four load cases individually

Table 3: Stresses in Homogen Condition

		CSR	DNV GL	LR	BV	IRS
	Relevant EDW	HSM	HSM	Sec 7.6	n/a	HSM
Local stress	Internal pressure range [kPa]	-	-	-		-
	Bending stress per unit pressure	1.799	1.715	Sec 7.6		-
	Nominal bending stress range [MPa]	-	-	-		-
	Stress concentration factor, SCF	1.60	1.60	1.43	1.65	1.40
Global stress	Load combination factor for M_{WV}	1.0	1.0	-	a,b: 0.625 c, d: 0.4	1.0
	Global stress per 10^3 unit M_{WV}	21.01	21.31	Sec 7.6	n/a	21.42
	Nominal global stress range [MPa]	57.24	69.65	-	n/a	58.19
	Stress concentration factor, SCF	1.28	1.28	1.43	1.30	1.28
Total stress incl. SCF						
	Fatigue stress range [MPa]	74.26	89.14	-	a: 290.0 b: 0.0 c: 134.5 d: 97.7	74.49
	Mean stress [MPa]	-43.04	-109.10	Sec 7.6	n/a	-43.87
	Factor mean stress	0.665	0.700	0.700	1.0	0.664

Table 4: Stresses in Alternate Condition

		CSR	DNV GL	LR	BV	IRS
	Relevant EDW	HSM	-	Sec 7.6	-	HSM
Local stress	Internal pressure range [kPa]	-	-	-	-	-
	Bending stress per unit pressure	1.799	-	Sec 7.6	-	-
	Nominal bending stress range [MPa]	-	-	-	-	-
	Stress concentration factor	1.60	-	1.43	-	1.40
Global stress	Load combination factor for M_{WV}	1.0	-	-	-	1.0
	Global stress per 10^3 unit M_{WV}	21.01	-	Sec 7.6	-	21.42
	Nominal global stress range [MPa]	57.24	-	-	-	58.19
	Stress concentration factor	1.28	-	1.43	-	1.28
Total stress incl. SCF						
	Fatigue stress range [MPa]	74.26	-	-	-	74.49
	Mean stress [MPa]	86.76	-	Sec 7.6	-	82.25
	Factor mean stress	1.00	-	1.00	-	1.00

Table 5: Stresses in Normal Ballast

		CSR	DNV GL	LR	BV	IRS
	Relevant EDW	HSM	HSM	Sec 7.6	n/a	HSM
Local stress	Internal pressure range [kPa]	-	0.549	-		1.947
	Bending stress per unit pressure	1.799	1.715	Sec 7.6		1.488
	Nominal bending stress range [MPa]	-	-0.941	-		4.803
	Stress concentration factor	1.60	1.60	1.43	1.65	1.40
Global stress	Load combination factor for M_{WV}	1.0	1.0	-	a, b: 0.625 c, d: 0.4	1.0
	Global stress per 10^3 unit M_{WV}	21.01	21.31	Sec 7.6		21.42
	Nominal global stress range [MPa]	58.50	71.19	-		59.48
	Stress concentration factor	1.28	1.28	1.43	1.30	1.28
Total stress incl. SCF						
	Fatigue stress range [MPa]	74.88	89.84	-	a:291.2 b19.6 c:19.0 d:14.7	78.22
	Mean stress [MPa]	92.54	127.07	Sec 7.6		99.81
	Factor mean stress	1.00	1.00	1.00	1.0	1.00

Table 6: Stresses in Heavy Ballast

		CSR	DNV GL	LR	BV	IRS
	Relevant EDW	HSM	-	Sec 7.6	-	HSM
Local stress	Internal pressure range [kPa]	-	-	-	-	1.956
	Bending stress per unit pressure	1.799	-	Sec 7.6	-	1.488
	Nominal bending stress range [MPa]	-	-	-	-	4.824
	Stress concentration factor	1.60	-	1.43	-	1.40
Global stress	Load combination factor for M_{WV}	1.0	-	-	-	1.0
	Global stress per 10^3 unit M_{WV}	21.01	-	Sec 7.6	-	21.42
	Nominal global stress range [MPa]	58.14	-	-	-	59.11
	Stress concentration factor	1.28	-	1.43	-	1.28
Total stress incl. SCF						
	Fatigue stress range [MPa]	74.40	-	-	-	77.77
	Mean stress [MPa]	-80.71	-	Sec 7.6	-	-76.73
	Factor mean stress	0.466	-	0.700	-	0.505

Table 7: Fatigue assessment

		CSR	DNV GL	LR	BV	IRS
Long term	Probability for fatigue	10^{-2}	10^{-2}	Sec.7.6	10^{-5}	10^{-2}
	Factor environment (NA=1.0 or WW=0.8)	1.0	0.8	1.0	1.0	1.0
	Weibull shape factor for long-term distribution.	1.0	1.0	Sec 7.3		1.0
Capacity	S-N curve in air FAT class [MPa]	90	90	Sec 7.3	90	D
	Factor thickness effect	1.013	1.000	1.030		1.000
Homogen	Fraction of time	0.25	0.50	0.20		0.25
	Number of cycles in 10^6	17.156	34.313	Sec 7.3	a, b: 5.489 c, d: 10.978	17.118
	Reference stress range [MPa]	49.34	49.92	-	a: 290.0 b: 0.0 c: 134.5 d: 97.7	49.49
	Partial damage in air	0.0383	0.0850	-	0.24*	0.0387
	Partial damage (corrosive)	0.0333	0.0425	-	-	0.0336
Alternate	Fraction of time	0.25	-	0.30	-	0.25
	Number of cycles in 10^6	17.156	-	Sec 7.3	-	17.118
	Reference stress range [MPa]	74.20	-	-	-	74.48
	Partial damage in air	0.1799	-	-	-	0.1823
	Partial damage (corrosive)	0.1133	-	-	-	0.1146
Normal Ballast	Fraction of time	0.20	0.50	0.20		0.2
	Number of cycles in 10^6	13.725	34.313	Sec 7.3	a,b,c: 7.318 d: 0.0	13.694
	Reference stress range [MPa]	75.84	71.69	-	a:291.2 b:19.6 c:19.0 d:14.7	78.22
	Partial damage in air	0.1554	0.3344	-	0.25*	0.1732
	Partial damage (corrosive)	0.0968	0.1672	-	-	0.1062
Heavy Ballast	Fraction of time	0.30	-	0.30	-	0.3
	Number of cycles in 10^6	20.588	-	Sec 7.3	-	20.542
	Reference stress range [MPa]	35.132	-	-	-	39.30
	Partial damage in air	0.0106	-	-	-	0.0175
	Partial damage (corrosive)	0.0144	-	-	-	0.0202
Final Result	Total damage	0.642	0.629	0.595	0.49	0.687
	Damage limit	< 1.0	< 1.0	< 1.0	<0.98	<1.0
	Fatigue life [years]	32	40	42	40	31
	Fatigue life limit [years]	>25	>25	> 25	>20	>25

* Corrosion effect is provided by a factor of 1.1 on the damage in the air

7.6.3 Assessment

All fatigue checks presented here are based on a long-term stress range distribution which is used in combination with an S-N curve to compute the damage accumulated according to the Palmgren-Miner's Rule. In most cases, a long-term Weibull distribution is applied. This is identified by a shape parameter and by a reference stress range at the used probability level.

The S-N curves characterize the fatigue strength capacity and are represented by two straight lines in a semi-logarithmic plot with a slope of 3 and 5 for welded details. The change of slope is usually at 10^7 cycles and the reference FAT class at $2 \cdot 10^6$ cycles. The fatigue strength is to assess with S-N curve in the air and in corrosive environments. Design life is divided into two intervals corresponding to unprotected (corrosive) and protected (dry air) environment.

Finally, a check is performed on the detail to assess if it satisfies a minimum fatigue strength requirement. While the general background of checks is the same, the way they are formulated can be a comparison against limit values of the predicted damage and/or respectively fatigue life or a comparison of the reference stress range with an allowable value.

7.7 International Gas Carrier (IGC) code

The resolution of the Maritime Safety Committee MSC.370(93) 'Amendments to the international code for the construction and equipment of ships carrying liquefied gases in bulk, IGC code (IGC, 2014), adopted on 22 May 2014, replaces the resolution MSC.5(48), referred here as 'old IGC code'. While the amendments affected all chapters of the IGC code, the interest here is on Chapter 4 'Cargo Containment' which goal is 'to ensure the safe containment of cargo under all design and operating conditions having regard to the nature of the cargo carried'. Chapter 4 has been completely reorganized, covering general requirements for all types of containment systems and for individual tanks. The main changes related to fatigue design assessment are summarized next.

Part A 'Cargo Containment' initially provides details of the functional requirements. Of interest is that the design life of the containment system shall not be less than the design life of the ship and that it shall be designed for North Atlantic environmental conditions and relevant long-term sea state scatter diagrams for unrestricted navigation.

Part A also covers new requirements for the inspection/survey plan for the cargo containment system, and how it shall be designed and built to ensure safety during operation, inspection and maintenance. This relates closely to the section 'Fatigue design conditions' which contains requirements for tank members where leakage monitoring systems do not work until cracks reach a critical state, and in-service inspection plans do not show visual detection of cracks.

In this case, the fatigue design criterion Cw (maximum allowable cumulative fatigue damage) is reduced to 0.1 or the crack propagation period is increased to three times the lifetime of the tank. However, for tank members where the in-service inspection plan can demonstrate cracks are visually detectable in service, Cw can be increased to 0.5, and the crack propagation period can be decreased to three times the inspection interval.

Regarding the design of the secondary barrier, the acceptance in-service will require the critical defect sizes of the secondary barrier to be defined.

In Part C 'Structural Integrity', under section 4.18.2 'Fatigue design conditions', it is indicated that the S-N curves shall be based on a 97.6 % probability of survival corresponding to the mean-minus-two-standard-deviation curves of relevant experimental data up to final failure (paragraph 4.18.2.4.2). This introduces clear design S-N curves for initial crack calculation.

Also, it is introduced clear design criteria for crack propagation analysis to determine (1) crack propagation paths in the structure, (2) crack growth rate, (3) the time required for a crack to cause a leakage from the tank, (4) the size and shape of through-thickness cracks, and (5) the time required for detectable cracks to reach a critical state.

For locations of the tank where the effective defect or crack development detection cannot be assured, an enhanced Cw of 0.1 or less is required for some areas of the containment system, particularly the attachment of the pump tower base support to the inner bottom (Cw was before 0.5). This requirement covers the primary members of prismatic Type B containment systems.

Part E 'Tank Types' introduces a clear design philosophy for Type C independent tanks, where the fatigue stress range is less than the fatigue limit. Here, the tanks' design is based on pressure vessel criteria modified to include fracture mechanics and crack propagation criteria.

For membrane tanks, it is also indicated that structural elements not accessible for in-service inspection, and where a fatigue crack can develop without warning, shall satisfy fatigue and fracture mechanics requirements. This means it may be necessary to assess crack propagation for the weld junction of the pump tower base support and the inner hull.

8. CONCLUSIONS AND RECOMMENDATIONS

The recent developments in fatigue and fracture of ships and offshore structures have been revised here. The major concern was the fatigue crack initiation and growth under cyclic loading as well as the unstable crack propagation in the ship and offshore structures.

Special attention was paid to load-induced fatigue, material properties and testing related to fatigue and fracture. Revision of the advances in the fatigue damage accumulation and crack growth approaches was also made.

Due attention was dedicated to the fabrication, improvements and in-service maintenance with respect to the suitability and uncertainty of physical models and testing. Consideration was given to fatigue design and verification based on Rules, standard and guidelines and reliability assessment performed in three benchmark studies (Garbatov et al., 2017, Lillemäe-Avi et al., 2017, Rörup et al., 2017) that will be presented and discussed in the third volume of the Proceedings of the 20th International Ship and Offshore Structures Congress.

462 references, covering the last four years, were reviewed and discussed in the report. The references discussed in the report originate from 2017 - 11%, 2016 - 37%, 2015 - 31%, 2014 - 10% and 2013 - 6%.

The reference list includes publications from 46 international journals, many book chapters, conference proceedings, rules, guidelines and standards. The first most cited journals are International Journal of Fatigue - 32%, Marine Structures - 11%, Engineering Fracture Mechanics, 10%, Fatigue and Fracture of Engineering Materials and Structures, 7%, Welding in the World, 4%, Ocean Engineering, 3%, Engineering Failure Analysis, 3%, Journal of Ship Production and Design, 3%, Theoretical and Applied Fracture Mechanics, 2%, Materials and Design, 2%, Composite Structures, 2%, Engineering Structures, 2%, Journal of Constructional Steel Research, 2%, Structural Safety, 2% and Ships and Offshore Structures, 2%.

The most discussed topics translated into key-words are: fatigue, 36%, strength, 15%, weld, 11%, crack, 10%, fracture, 8%, steel, 7%, ship, 6%, experiment, 6%, load, 6%, mechanics, 5%, offshore, 4%, reliability, 3%, damage, 2%, numerical, 2%, energy, 2%, residual, 2%, rules, 2%, corrosion, 2%, failure, 2%.

Several discussions and conclusions were derived and presented here, according to the already revised topics in different report chapters.

8.1 Fatigue and fracture loading

Fatigue loads are very complex and case dependent. They depend on either the environmental actions or the ability to obtain correct efforts from environmental conditions. Design metocean description is in principle solved for the loads in situ as the location is well known and metocean description analyses are generally undertaken before the operation. Design metocean description is more questionable for ships or offshore structure during transportation. Recommendation

34 of IACS propose a scatter diagram close to the North Atlantic condition to be associated with a speed equal to ¾ of maximum speed for calculation of fatigue loads. Especially for common cargo ships, it is likely to be a conservative approach. As fatigue damage is more sensitive to frequent sea states encountered by a ship than to the extreme sea states, fatigue analyses based on the actual trading pattern rather than on the worst conditions may provide better information on the predicted fatigue experienced by a fleet and knowledge on the scatter of fatigue loads on common ships, allowing a rational judgment on the suitability of the present approach for fatigue load determination and then allowing estimating/setting a reasonable safety margin. Fatigue loading due to navigation in ice conditioned e.g. navigation in the Arctic Ocean should be addressed as not currently considered in the ship design.

8.2 Material properties and testing

For fatigue and fracture assessment of materials, components and structures, material testing is virtually indispensable for calibrating material models and verifying simulations. More accurate consideration of material properties is an important topic for the future since numerical tools are developing rapidly, enabling more accurate modelling of manufacturing, e.g. welding, and strength properties under more complex loading paths. It is realized that both the fracture resistance and criteria depend on the stress state, which may be different in the standard test specimens and in actual structures. Failure strain also depends on the strain path and strain rate. Cyclic material properties of various zones of the welded joints are also a topic for research, recently especially for HFMI-treated weld toes. In fatigue testing, the friction stir welded steel joints have received increasing attention with the hope of application to marine, offshore and pipeline structures soon. New results have also been published for very high cycle fatigue of base material, fatigue in a corrosive environment or under temperature loads and for full-scale testing of structures. Digital image correlation during fatigue and fracture testing is not anymore, an alternative method but has become a new norm. Future research probably brings more experimental evidence for the fatigue crack initiation and short crack growth at microstructural levels as such test methods become more available.

8.3 Fatigue damage accumulation approaches

Joints connecting ship and offshore structural members are typically fatigue sensitive. In this respect welded joint fatigue assessment concepts developed over time have been classified and evaluated regarding the type of information, geometry, parameter and process zone as well as plane and life region annotations (Section 3.1). Fatigue involves several resistance dimensions, distinct contributions in different stages of the damage process as well as physics over a range of scales and the concept overview, as well as the concept criteria advances (Section 3.2), show that from modelling perspective, not all (governing) physics are incorporated explicitly.

Continuum or discrete damage mechanics criteria can be adopted to estimate the initiation and growth of lifetime contributions. Without being complete, it should be mentioned that damage mechanics criteria can be adopted as well to model fatigue phenomena. The same physics can be incorporated and may even provide better opportunities to obtain more accurate lifetime estimates (Section 3.3).

The fatigue damage criterion defines in terms of resistance the fatigue strength scatter and can be improved. Modelling developments and trends of fatigue damage criteria towards complete strength, total life and multi-scale criteria are identified (Section 3.4). The interacting material, geometry, loading & response (multiaxiality and amplitude variability, mean- and residual stress, time or frequency domain formulation) and environment resistance dimensions become explicitly incorporated, specifying the fatigue strength as well as initiation, growth and propagation induced damage process contributions and physics at different scales.

Material and geometry typically define the reference resistance; loading & response and environment are involved as influence factors. Most modelling and assessment publications paying

attention to fatigue damage criteria advances are (still) related to uniaxial response conditions, since the ship and the offshore structural response is predominantly Mode-I defined, even if the loading is multiaxial. Fatigue damage criteria developments are ongoing in this respect – focus seems to be on critical plane approaches – and comparisons to the available guidelines have been made (Section 3.4.1). Consistency with experimental results for different loading & response conditions is typically lacking. A rather broad range of mean and residual mean stress models are available and developments in this respect involve mainly the application of existing ones rather than introducing modelling advances (Section 3.4.2). Frequency domain approaches are considered less reliable but more efficient. Time domain approaches, on the other hand, are more accurate but computationally expensive. To combine the advantages of time and frequency domain approaches, hybrid approaches are under development (Section 3.4.3). Corrosion and gaseous hydrogen induced environmental fatigue damage consequences are under investigation and modelling start to allow for quantification (Section 3.4.4).

To quantify the relative initiation, growth and propagation contributions to fatigue lifetime, correlation of intact and crack damaged geometry parameters are required. Typically, either an intact or crack damaged geometry parameter is adopted and if both are incorporated separately, the transition is predefined. An important challenge seems to be the development of a loading & geometry dependent correlation of intact and crack damaged geometry parameters without predefined transition (Section 3.5).

Additional macro-, meso- and micro-fatigue damage mechanism information – physics at a smaller scale – can be used to enhance fatigue damage criteria, providing a multi-scale fatigue damage criterion (Section 3.6). Following the macro-scale developments from global to local fatigue damage criteria over time, the continuum mechanics lower bound is approaching and a correlation to the 'netherworld' (i.e. to meso- or even micro-scale physics) is the next step. Developments involve typically numerical modelling.

Fatigue damage accumulation is typically a random process. Reliability and confidence with respect to fitting parameters and lifetime can be established, but some contributors (e.g. size effects) can be explicitly incorporated in the fatigue damage criterion in order to provide more accurate lifetime estimates (Section 3.7).

8.4 Crack growth approaches

Fatigue crack growth approaches based on the theory of Fracture Mechanics have become an important tool for preventing fatigue failure of the ship and offshore structures during certain periods of service. The application of fatigue crack growth approaches on evaluation of the failure of ship and offshore structural details such as tidal turbine blades, cruciform welded joints, pressure vessel steel, multi-planar DX-joint welds, offshore pipelines, and aged jacket platforms have been discussed by many researchers in the last few years by using some extended crack growth models considering variable influential factors, which is typically realized by combining the theories with new simulation techniques.

However, some newly developed methods and theories in the field of fatigue and fracture have not been applied to ship and offshore structures, and fatigue crack growth approaches are still not well documented in the specifications for the ship and offshore structures.

8.5 Fabrication, degradation, improvements and repair

There is a clear gap between structural modelling and reality due to several assumptions and approximations introduced to make practically feasible and cost-efficient the design process. As far as fatigue strength is concerned, fabrication induced imperfections, as well as in-service degradation effects, are far to be considered in structural analyses explicitly, duly considering their actual quantification. Rather, safety/correction factors are generally adopted.

Nevertheless, it is already time to fully consider them in the design process and the trend outlined by the literature presented in this chapter and in the benchmark studies carried out by the Committee is clear: suitable technologies are available to adequately collect necessary data and, if properly applied, they largely improve the final design.

Two main categories of fabrication-induced imperfections have been identified: geometrical and welding induced. In both cases, applications leading to improved design have been found. It can be underlined that fatigue assessment approaches need to be improved to be able to consider these more accurate input data. The most recent developments of fatigue assessment approach as described in previous chapters of this report are probably driven also by the above trends.

Certainly, corrosion degradation is an issue. However, it is considered only marginally in this chapter if it can only be settled with the availability of sound experimental data. This remains an open issue and a significant gap to be filled in the next years.

It is noted that fatigue improvement and repair methods are nowadays emerging fast and more and more widely applied. It is, however, necessary to develop rules and regulations to create a common playground for their adequate development.

8.6 Fatigue reliability

It has been noticed from the recent publications in the field of fatigue reliability that the research investigations are favouring the fracture mechanics based approaches rather than the SN based approaches. Therefore, the reliability analysis and service life prediction based on the fracture mechanics approach is more frequently used. While doing so, there are relatively fewer investigations in the review period of this report pertaining to the corrosion-fatigue interaction. Future studies need to focus on the understanding of the interaction mechanism between the fatigue damage and corrosion degradation and their effect on the reliability and risk-based structural assessments. Certainly, the reliability techniques are becoming mature and well understood and software are being made available.

8.7 Fatigue design and verification based on rules, standards, codes and guidelines

With the introduction of CSR for bulk carrier and oil tanker in 2015, the classification societies are aligning their own fatigue regulations more with CSR. Although a complete harmonization is not expected and some regulations were already aligned before, a progress for the examined class rules in this report is identified by following observations:

- 25-year fatigue life is the minimum design lifetime for all societies.
- A minimum time in corrosive environments is considered by all rules.
- In principle for all rules, the thickness effect is adopted from CSR with an exponent, which relates to the type of structural detail.
- Three of the four considered class societies (DNVGL, BV and IRS) analyse stiffener end connections on the basis of the S-N curve “D” respectively FAT90 in conjunction with a simplified stress analysis, i.e. Nominal stress x Tabulated “SCF”.
- Two class societies (DNVGL and IRS) adopt the fatigue load concept with 10^{-2} probability level and equivalent design waves (EDW). A third (BV) introduced it too, but at this time for container ships only.

The pronounced effect of residual stresses and its shakedown on the mean stress effect, as it is considered in CSR for bulk carriers and tankers, is not relevant for typical loading conditions of other ship types and consequently not adopted by any other class rules in general.

The two benchmark studies carried out for this report, demonstrate for the simplified assessment as well as for the stochastic spectral approach, comparable results for the combined fatigue

damage. Nevertheless, in case of the spectral approach single loading conditions exhibit obvious differences in the fatigue damage mainly due to different hydrodynamic loads and mean stress effects and give an identification for further harmonization efforts.

REFERENCES

Adedipe, O., Brennan, F. & Kolios, A. 2015. Corrosion fatigue load frequency sensitivity analysis. *Marine Structures,* 42**,** 115-136.

Adepipe, O., Brennan, F. & Kolios, A. 2016. A relative crack opening time correlation for corrosion fatigue crack growth in offshore structures. *Fatigue & Fracture of Engineering Materials & Structures,* 39**,** 395-411.

Al-Mukhtar, A. M. 2016. Mixed-Mode Crack Propagation in Cruciform Joint using Franc2D. *Journal of Failure Analysis and Prevention,* 16**,** 326-332.

Albinmousa, J. 2016. Investigation on multiaxial fatigue crack path using polar stress-strain representation. *International Journal of Fatigue,* 92**,** 406-414.

Alderliesten, R. C. 2016. How proper similitude can improve our understanding of crack closure and plasticity in fatigue. *International Journal of Fatigue,* 82**,** 263-273.

Alfredsson, B., Arregui, I. L. & Hazar, S. 2016. Numerical analysis of plasticity effects on fatigue growth of a short crack in a bainitic high strength bearing steel. *International Journal of Fatigue,* 92**,** 36-51.

Altamura, A. & Straub, D. 2014. Reliability assessment of high cycle fatigue under variable amplitude loading: Review and solutions. *Engineering Fracture Mechanics,* 121**,** 40-66.

Alves, A. S. F., Sampayo, L. M. C. M. V., Correia, J. A. F. O., De Jesus, A. M. P., Moreira, P. M. G. P. & Tavares, P. J. S. 2015. Fatigue life prediction based on crack growth analysis using an equivalent initial flaw size model: Application to a notched geometry. *ICSI 2015, the 1st International Conference on Structural Integrity Funchal,* 114**,** 730-737.

Amaro, R. L., Rustagi, N., Findley, K. O., Drexler, E. S. & Slifka, A. J. 2014. Modelling the fatigue crack growth of X100 pipeline steel in gaseous hydrogen. *International Journal of Fatigue,* 59**,** 262-271.

Ambuhl, S., Ferri, F., Kofoed, J. P. & Sorensen, J. D. 2015. Fatigue reliability and calibration of fatigue design factors of wave energy converters. *International Journal of Marine Energy,* 10**,** 17-38.

Amiri-Rad, A., Mashayekhi, M., van der Meer, F. P. & Hadavinia, H. 2015. A two-scale damage model for high cycle fatigue delamination in laminated composites. *Composites Science and Technology,* 120**,** 32-38.

Andrews, B. J. & Potirniche, G. P. 2015. Constitutive creep-fatigue crack growth methodology in two steels using a strip yield model. *Engineering Fracture Mechanics,* 140**,** 72-91.

ANSYS 2009. Online Manuals, Release 12.

Astrand, E., Stenberg, T., Jonson, B. & Barsoum, Z. 2016. Welding procedures for fatigue life improvement of the weld toe. *Welding in the World,* 60**,** 573-580.

Aydin, H. & Nelson, T. W. 2013. Microstructure and mechanical properties of hard zone in friction stir welded X80 pipeline steel relative to different heat input. *Materials Science and Engineering a-Structural Materials Properties Microstructure and Processing,* 586**,** 313-322.

Ayyub, B. M., Stambaugh, K. A., McAllister, T. A., de Souza, G. F. & Webb, D. 2015. Structural Life Expectancy of Marine Vessels: Ultimate Strength, Corrosion, Fatigue, Fracture, and Systems. *ASME Journal of Risk and Uncertainty in Engineering Systems Part B-Mechanical Engineering,* 1**,** 1-13.

Bandara, C. S., Siriwardane, S. C., Dissanayake, U. I. & Dissanayake, R. 2016. Full range S-N curves for fatigue life evaluation of steels using hardness measurements. *International Journal of Fatigue,* 82**,** 325-331.

Baptista, C., Reis, A. & Nussbaumer, A. 2017. Probabilistic S-N curves for constant and variable amplitude. *International Journal of Fatigue,* 101**,** 312-327.

Barile, C., Casavola, C., Pappalettera, G. & Pappalettere, C. 2016. Analysis of crack propagation in stainless steel by comparing acoustic emissions and infrared thermography data. *Engineering Failure Analysis,* 69**,** 35-42.

Barsoum, Z. & Jonson, B. 2011. Influence of weld quality on the fatigue strength in seam welds. *Engineering Failure Analysis,* 18**,** 971-979.

Baumgartner, J., Schmidt, H., Ince, E., Melz, T. & Dilger, K. 2015. Fatigue assessment of welded joints using stress averaging and critical distance approaches. *Welding in the World,* 59**,** 731-742.

Benasciutti, D., Sherratt, F. & Cristofori, A. 2016. Recent developments in frequency domain multi-axial fatigue analysis. *International Journal of Fatigue,* 91**,** 397-413.

Benz, C. & Sander, M. 2015. Reconsiderations of fatigue crack growth at negative stress ratios: Finite element analyses. *Engineering Fracture Mechanics,* 145**,** 98-114.

Berg, J., Stranghoener, N., Kern, A. & Hoevel, M. 2016. Variable amplitude fatigue tests at high-frequency hammer peened welded ultra-high strength steel S1100. *21st European Conference on Fracture, (Ecf21),* 2**,** 3554-3561.

Berg, J. & Stranghoner, N. 2016. Fatigue behaviour of high-frequency hammer peened ultra-high strength steels. *International Journal of Fatigue,* 82**,** 35-48.

Berg, T., von Ende, S. & Lammering, R. 2017. Calibration of potential drop measuring and damage extent prediction by Bayesian filtering and smoothing. *International Journal of Fatigue,* 100**,** 337-346.

Berto 2015a. A criterion based on the local SED for the fracture assessment of cracked and V-notched components. *Theoretical and Applied Fracture Mechanics,* 76.

Berto, F. 2015b. Crack initiation at V-notch tip subjected to in-plane mixed mode loading: An application of the fictitious notch rounding concept. *Frattura Ed Integrita Strutturale,* 34**,** 169-179.

Besten, J. H. d. 2015. *Fatigue resistance of welded joints in aluminium high-speed craft: a total stress concept.* PhD.

Beyer, F., Choisnet, T., Kretschmer, M. & Cheng, P.-W., 2015, Coupled MBS-CFD Simulation of the IDEOL Floating Offshore Wind Turbine Foundation Compared to Wave Tank Model Test Data, Proceedings of the 25th International Ocean and Polar Engineering Conference, Hawaii, USA, Paper ISOPE-I-15-272.

Bhatti, A. A., Barsoum, Z., Murakawa, H. & Barsoum, I. 2015. Influence of thermo-mechanical material properties of different steel grades on welding residual stresses and angular distortion. *Materials & Design,* 65**,** 878-889.

Bhatti, A. A., Barsoum, Z., van der Mee, V., Kromm, A. & Kannengiesser, T. 2013. Fatigue strength improvement of welded structures using new low transformation temperature filler materials. *Fatigue Design.* 192-201.

Bigot, F., Mahérault-Mougin, S. & Derbanne, Q., 2016, Comparison of different models for the fatigue analysis of details subject to side shell intermittent wetting effect, Proceedings of the 13th International Symposium on Practical design of ships and other floating structures, Copenhagen, Denmark.

Bilionis, D., V., B. & Vamvatsikos, D., 2015, Probabilistic Fatigue Life Assessment of an Offshore Wind Turbine in Greece, Proceedings of the 25th International Ocean and Polar Engineering Conference, Kona, Hawaii, USA, 684-691.

Blacha, L. & Karolczuk, A. 2016. Validation of the weakest link approach and the proposed Weibull based probability distribution of failure for fatigue design of steel welded joints. *Engineering Failure Analysis,* 67**,** 46-62.

Blasón, S., Rodríguez, C. & Fernández-Canteli, A., 2015, Fatigue characterization of a crankshaft steel: use and interaction of new models, Proceedings of the 5th International Conference on Crack Paths, Ferrara, Italy.

Boljanovic, S., Maksimovic, S. & Djuric, M. 2016. Fatigue strength assessment of initial semi-elliptical cracks located at a hole. *International Journal of Fatigue,* 92**,** 548-556.

Borrie, D., Liu, H. B., Zhao, X. L., Raman, R. K. S. & Bai, Y. 2015. Bond durability of fatigued CFRP-steel double-lap joints pre-exposed to marine environment. *Composite Structures,* 131**,** 799-809.

Bourbita, F. & Rémy, L. 2015. A combined critical distance and energy density model to predict high-temperature fatigue life in notched single crystal super alloy members. *International Journal of Fatigue,* 84**,** 17-27.

Branco, R., Antunes, F. V. & Costa, J. D. 2015. A review on 3D-FE adaptive remeshing techniques for crack growth modelling. *Engineering Fracture Mechanics,* 141**,** 170-195.

Brandão, C. S., Correa, F. N. & Jacob, B. P., 2015, Generation of Multiple Equivalent Regular Waves for Preliminary Analyses of Floating Production Systems, Proceedings of the 25th International Ocean and Polar Engineering Conference, Hawaii, USA, Paper ISOPE-I-15-073.

Branner, K., Berring, P. & Haselbach, P. U., 2016, Subcomponent testing of trailing edge panels in wind turbine blades, Proceedings of the 17th European Conference on Composite Materials.

Brennan, F. P., 2013, The need for variable amplitude corrosion fatigue materials data for Offshore Wind & Marine Renewable energy steel support structures, Proceedings of the 3rd International Conference of Engineering Against Failure, 745-751.

Brugger, C., Palin-Luc, T., Osmond, P. & Blanc, M. 2017. A new ultrasonic fatigue testing device for biaxial bending in the gigacycle regime. *International Journal of Fatigue,* 100**,** 619-626.

BS7910 2005. *British Standard BS7910, Guide to methods for assessing the acceptability of flaws in metallic structures,* London, BSI.

Bufalari, G., Kaminski, M. L., Van Lieshout, P. S. & Den Besten, J. H., 2017, Numerical comparative study of multiaxial fatigue methods applied to welded joints in a container vessel, Proceedings of the Symposium on Structural Durability in Darmstadt, Germany.

BV 2015. Rules Notes NR 583 Whipping and Springing Assessment. Paris: Bureau Veritas.

BV 2016a. Rules Note NR 625 Structural Rules for Container Ships. Paris: Bureau Veritas.

BV 2016b. Rules Notes 467 Rules for the Classification of Steel Ships. Paris: Bureau Veritas.

BV 2016c. Rules Notes NR 445 Rules for the Classification of Offshore Units. Paris: Bureau Veritas.

Calle, M. A. G., Verleysen, P. & Alves, M. 2017. Benchmark study of failure criteria for ship collision modelling using purpose-designed tensile specimen geometries. *Marine Structures,* 53**,** 68-85.

Campagnolo, A., Meneghetti, G. & Berto, F. 2016. Rapid finite element evaluation of the averaged strain energy density of mixed-mode (I plus II) crack tip fields including the T-stress contribution. *Fatigue & Fracture of Engineering Materials & Structures,* 39**,** 982-998.

Carpinteri, A., Fortese, G., Ronchei, C., Scorza, D. & Vantadori, S. 2016. Spectral fatigue life estimation for non-proportional multiaxial random loading. *Theoretical and Applied Fracture Mechanics,* 83**,** 67-72.

Carrion, P. E., Shamsaei, N. & Daniewicz, S. R. 2017. Fatigue Behaviour of Ti-6Al-4V ELI Including Mean Stress Effects. *International Journal of Fatigue,* 99**,** 87-100.

Castelluccio, G. M., Musinski, W. D. & Mcdowell, D. L., 2016, 93:387-396. 2016. Computational micromechanics of fatigue of microstructures in the HCF-VHCF regimes[J]. *International Journal of Fatigue,* 93**,** 387-396.

CEN 2005. Eurocode 3: design of steel structures. European Committee for Standardisation.

Chakherlou, T. N., Taghizadeh, H., Mirzajanzadeh, M. & Aghdam, A. B. 2012. On the prediction of fatigue life in double shear lap joints including interference fitted pin. *Engineering Fracture Mechanics,* 96**,** 340-354.

Chandran, K. S. R. 2016. A constitutive equation for the S-N fatigue behaviour of metal single crystals and validation by the physical definition of fatigue endurance limit. *International Journal of Fatigue,* 91**,** 21-28.

Chattopadhyay, A., Glinka, G., El-Zein, M., Qian, J. & Formas, R. 2011. Stress analysis and fatigue of welded structures. *Welding in the World,* 35**,** 2-21.

Chen, B. Q., Hashemzadeh, M., Garbatov, Y. & Guedes Soares, C. 2014a. Numerical and parametric modelling and analysis of weld-induced residual stresses. *International Journal of Mechanics and Materials in Design,* 11**,** 439-453.

Chen, B. Q., Hashemzadeh, M. & Guedes Soares, C. 2014b. Numerical and experimental studies on temperature and distortion patterns in butt-welded plates. *International Journal of Advanced Manufacturing Technology,* 72**,** 1121-1131.

Chen, B. Q., Hashemzadeh, M. & Guedes Soares, C. 2017. Validation of numerical simulations with X-ray diffraction measurements of residual stress in butt-welded steel plates. *Ships and Offshore Structures***,** 1-10.

Chen, N.-Z., 2015, Reliability-Based Low-Cycle Fatigue Assessment for Crack-Stopping Hole., Proceedings of the 25th International Ocean and Polar Engineering Conference, Kona, Hawaii, USA, 503-507.

Chen, N. Z. 2016. A stop-hole method for marine and offshore structures. *International Journal of Fatigue,* 88**,** 49-57.

Chen, X., Lados, D. A., Pettit, R. G. & Dudzinski, D. 2016. A physics-based model for evaluating hot compressive dwell effects on fatigue crack growth in 319 cast aluminium alloys. *International Journal of Fatigue,* 90**,** 222-234.

Cheng, A. K. & Chen, N. Z. 2017a. Corrosion fatigue crack growth modelling for subsea pipeline steels. *Ocean Engineering,* 142**,** 10-19.

Cheng, A. K. & Chen, N. Z. 2017b. Fatigue crack growth modelling for pipeline carbon steels under gaseous hydrogen conditions. *International Journal of Fatigue,* 96**,** 152-161.

Choung, J., Nam, W., Lee, D. & Song, C. Y. 2014. Failure strain formulation via average stress triaxiality of an EH36 high strength steel. *Ocean Engineering,* 91**,** 218-226.

Corigliano, P., Epasto, G., Guglielmino, E. & Risitano, G. 2017. Fatigue analysis of marine welded joints by means of DIC and IR images during static and fatigue tests. *Engineering Fracture Mechanics,* 183**,** 26-38.

Correia, J. A. F. O., Blason, S., De Jesus, A. M. P., Canteli, A. F., Moreira, P. M. G. P. & Tavares, P. J. 2016. Fatigue life prediction based on an equivalent initial flaw size approach and a new normalized fatigue crack growth model. *Engineering Failure Analysis,* 69**,** 15-28.

Cosso, G. L., Rizzo, C. M. & Servetto, C. 2016. Fitness-for-service assessment of defected welded structural details by experimental evaluation of the fatigue resistance S-N curve. *Welding in the World,* 60**,** 847-858.

Cui, J., Wang, D. & Ma, N., 2016, Spectral Fatigue Analysis Considering Probabilistic Corrosion Effects: A Case Study of Container Ship's Hatch Coaming Detail, Proceedings of the 35th International Conference on Ocean, Offshore and Arctic Engineering, Busan, South Korea.

D'Angelo, L. & Nussbaumer, A. 2017. Estimation of fatigue S-N curves of welded joints using advanced probabilistic approach. *International Journal of Fatigue,* 97**,** 98-113.

Dallago, M., Benedetti, M., Ancellotti, S. & Fontanari, V. 2016. The role of lubricating fluid pressurization and entrapment on the path of inclined edge cracks originated under rolling-sliding contact fatigue: Numerical analyses vs. experimental evidences. *International Journal of Fatigue,* 92**,** 517-530.

Darcis, P., Lassen, T. & Recho, N. 2006. Fatigue behaviour of welded joints part 2: Physical modelling of the fatigue process. *Welding Journal,* 85**,** 19s-26s.

de Jesus, A., Matos, R., Fontoura, B., Rebelo, C., Simões da Silva, L. & Veljkovic, M. 2012. A comparison of the fatigue behaviour between S355 and S690 steel grades. *Journal of Constructional Steel Research,* 79**,** 140-150.

Deguchi, T., Mouri, M., Hara, J., Kano, D., Shimoda, T., Inamura, F., Fukuoka, T. & Koshio, K. 2012. Fatigue strength improvement for ship structures by Ultrasonic Peening. *Journal of Marine Science and Technology,* 17**,** 360-369.

Den Besten, J. H. 2018. Fatigue damage criteria classification, modelling developments and trends for welded joints in marine structures. *Ships and Offshore Structures*, https://doi.org/10.1080/17445302.2018.1463609.

Deng, C. Y., Liu, Y., Gong, B. M. & Wang, D. P. 2016. Numerical implementation for fatigue assessment of butt joint improved by high-frequency mechanical impact treatment: A structural hot spot stress approach. *International Journal of Fatigue,* 92**,** 211-219.

Derbanne, Q., Rezende, F., de Hauteclocque, G. & Chen, X. B., 2011, Evaluation of Rule-Based Fatigue Design Loads Associated at a New Probability Level, Proceedings of the 21st International Ocean and Polar Engineering Conference, Maui, Hawaii, USA.

Desmorat, R., Angrand, L., Gaborit, P., Kaminski, M. & Rakotoarisoa, C. 2015. On the introduction of a mean stress in kinetic damage evolution laws for fatigue. *International Journal of Fatigue,* 77**,** 141-153.

Ding, Z. Y., Gao, Z. L., Wang, X. G. & Jiang, Y. Y. 2015. Modelling of fatigue crack growth in a pressure vessel steel Q345R. *Engineering Fracture Mechanics,* 135**,** 245-258.

DNV-GL 2015. Rotor blades for wind turbines. DNV-GL.

DNV-GL 2017a. Class Guideline DNVGL-CG-0129: Fatigue Assessment of Ship Structures. Oslo: DNV GL.

DNV-GL 2017b. Class Guideline DNVGL-CG-0153: Fatigue and Ultimate Strength Assessment of Container Ships including Whipping and Springing. Oslo: DNV GL.

DNV-GL 2017c. DNVGL-RU-9111:2015-7, Rules for Classification. Oslo: DNV GL.

DNV 2010a. Dynamic Risers. *DNV-OS-F201.* Det Norske Veritas.

DNV 2010b. *Recommended Practice, Fatigue Design of Offshore Steel Structures*.

DNV 2015. Rules for Classification of Ships, Part 3 Hull and Equipment -Main Class, Chapter 1, Hull structural design -Ships with length 100 metres and above, Section 16 Fatigue Control. Oslo: Det Norske Veritas.

Dong, P. 2001. A Practical Stress Definition and Numerical Implementation for Fatigue Analyses. *International Journal of Fatigue,* 23**,** 865-876.

Dong, P. 2005. A robust structural stress method for fatigue analysis of offshore/marine structures. *Journal of Offshore Mechanics and Arctic Engineering-Transactions of the ASME,* 127**,** 68-74.

Dong, P. 2010. The Master SN Curve Method an Implementation for Fatigue Evaluation of Welded Components in the ASME B&PV Code. *Section VIII, Division 2 and API 579-1/ASME FFS-1.*

Dong, P., Pei, X., Xing, S. & Kim, M. H. 2014. A structural strain method for low-cycle fatigue evaluation of welded components. *International Journal of Pressure Vessels and Piping,* 119**,** 39-51.

Dong, P., Xing, S. & Zhou, W. 2017a. Analytical treatment of welding distortion effects on fatigue in thin panels: Part I – closed-form solutions and implications. *In:* Guedes Soares, C. & Teixeira, A. (eds.) *Maritime Transportation and Harvesting of Sea Resources.*

Dong, P., Zhou, W. & Xing, S. 2017b. Analytical treatment of welding distortion effects on fatigue in thin panels: Part II – applications in test data analysis. *In:* Guedes Soares, C. & Teixeira, A. (eds.) *Maritime Transportation and Harvesting of Sea Resources.*

Dong, P. S., Wei, Z. G. & Hong, J. K. 2010. A path-dependent cycle counting method for variable-amplitude multi-axial loading. *International Journal of Fatigue,* 32**,** 720-734.

Dong, Q., Yang, P., Xu, G. & Deng, J. L. 2016. Mechanisms and modelling of low cycle fatigue crack propagation in a pressure vessel steel Q345. *International Journal of Fatigue,* 89**,** 2-10.

Dong, Y. & Frangopol, D. M. 2015. Risk-informed life-cycle optimum inspection and maintenance of ship structures considering corrosion and fatigue. *Ocean Engineering,* 101**,** 161-171.

Dong, Y. & Frangopol, D. M. 2016. Incorporation of risk and updating in inspection of fatigue-sensitive details of ship structures. *International Journal of Fatigue,* 82**,** 676-688.

Dong, Y. & Guedes Soares, C., 2015a, Estimation of effective notch strain for fatigue strength assessment of welded structures under multiaxial stress state, *In:* Guedes Soares, C., Dejhalla, R. & Pavletic, D., eds., Towards Green Marine Technology and Transport, Taylor & Francis Group, London, UK, 397-406.

Dong, Y. & Guedes Soares, C., 2015b, On the fatigue crack initiation point of load-carrying fillet welded joints, *In:* Guedes Soares, C., Dejhalla, R. & Pavletic, D., eds., Towards Green Marine Technology and Transport, Taylor & Francis Group, London, UK, 407-406.

Dong, Y. & Guedes Soares, C. 2017. Uncertainty analysis of local strain and fatigue crack initiation life of welded joints under plane strain condition. *In:* Guedes Soares, C. & Garbatov, Y. (eds.) *Progress in the Analysis and Design of Marine Structures.* Taylor & Francis Group, London, UK.

Doremus, L., Nadot, Y., Henaff, G., Mary, C. & Pierret, S. 2015. Calibration of the potential drop method for monitoring small crack growth from surface anomalies - Crack front marking technique and finite element simulations. *International Journal of Fatigue,* 70**,** 178-185.

Doshi, K., Roy, T. & Parihar, Y. S. 2017. Reliability-based inspection planning using fracture mechanics based fatigue evaluations for ship structural details. *Marine Structures,* 54**,** 1-22.

Dragt, R. C., Maljaars, J. & Tuitman, J. T., 2016, Including Load Sequence Effects in the Fatigue Damage Estimation of an Offshore Wind Turbine Substructure, Proceedings of the 26th International Ocean and Polar Engineering Conference Rhodes, Greece, Paper ISOPE-I-16-653.

Du, J. F., Li, H. J., Zhang, M. & Wang, S. Q. 2015. A novel hybrid frequency-time domain method for the fatigue damage assessment of offshore structures. *Ocean Engineering,* 98**,** 57-65.

Dubey, G. & Kumar, S. 2016. Improvement in the numerical method for integrating weight function of pre-cracked specimen. *Engineering Fracture Mechanics,* 154**,** 83-91.

Dubois, J., Thieken, K., Terceros, M., Schaumann, P. & Achmus, M., 2016, Advanced Incorporation of Soil-Structure Interaction into Integrated Load Simulation, Proceedings of the 26th International Ocean and Polar Engineering Conference, Rhodes, Greece, Paper ISOPE-I-16-570.

Durodola, J. F., Li, N., Ramachandra, S. & Thite, A. N. 2017. A pattern recognition artificial neural network method for random fatigue loading life prediction. *International Journal of Fatigue,* 99**,** 55-67.

Eder, M. A., Branner, K., Berring, P., Belloni, F., Toft, H. S., Sørensen, J. D., Corre, A., Lindby, T., Quispitup, A. & Petersen, T. K. 2015. Experimental Blade Research - phase 2. DTU Wind Energy.

Elber, W. 1971. The Significance of Fatigue Crack Closure. *Damage and Tolerance in Aircraft Structure,* 485**,** 230-242.

Elosta, H., Huang, S. & Incecik, A. 2014. Wave loading fatigue reliability and uncertainty analyses for geotechnical pipeline models. *Ships and Offshore Structures,* 9**,** 450-463.

Erice, B., Roth, C. C. & Mohr, D. 2017. Stress-state and strain-rate dependent ductile fracture of dual and complex phase steel. *Mechanics of Materials,* Article in press.

Ewest, D., Almroth, P., Sjodin, B., Simonsson, K., Leidermark, D. & Moverare, J. 2016. A modified compliance method for fatigue crack propagation applied on a single edge notch specimen. *International Journal of Fatigue,* 92**,** 61-70.

Ezanno, A., Doudard, C., Moyne, S., Calloch, S., Millot, T. & Bellevre, D. 2015. Validation of a high-cycle fatigue model via calculation/test comparisons at structural scale: Application to copper alloy sand-cast ship propellers. *International Journal of Fatigue,* 74**,** 38-45.

Feng, G., Wang, D., Garbatov, Y. & Guedes Soares, C. 2015. Reliability analysis based on a direct ship hull strength assessment. *Journal of Marine Science and Application,* 14**,** 389-398.

Feng, G. Q., Garbatov, Y. & Guedes Soares, C. 2012a. Fatigue reliability of a stiffened panel subjected to correlated crack growth. *Structural Safety,* 36-37**,** 39-46.

Feng, G. Q., Garbatov, Y. & Guedes Soares, C. 2012b. Probabilistic model of the growth of correlated cracks in a stiffened panel. *Engineering Fracture Mechanics,* 84**,** 83-95.

Feng, G. Q., Garbatov, Y. & Guedes Soares, C. 2014. Fatigue reliability of deck structures subjected to correlated crack growth. *Journal of Marine Science and Application,* 12**,** 413-421.

Feng, M. L., Ding, F. & Jiang, Y. Y. 2006. A study of loading path influence on fatigue crack growth under combined loading. *International Journal of Fatigue,* 28**,** 19-27.

Ferro, P. 2014. The local strain energy density approach applied to pre-stressed components subjected to cyclic load. *Fatigue & Fracture of Engineering Materials & Structures,* 37**,** 1268-1280.

Fischer, C. & Fricke, W. 2015. Influence of local stress concentrations on the crack propagation in complex welded components. *Frattura Ed Integrita Strutturale,* 38**,** 99-108.

Fischer, C., Fricke, W. & Rizzo, C. M. 2015. Fatigue assessment of joints at bulb profiles by local approaches. *In:* Guedes Soares, C. & Shenoi, A. (eds.) *Analysis and Design of Marine Structures.* London, UK: Taylor & Francis Group.

Fischer, C., Fricke, W. & Rizzo, C. M. 2016a. Experiences and recommendations for numerical analyses of notch stress intensity factor and averaged strain energy density. *Engineering Fracture Mechanics,* 165**,** 98-113.

Fischer, C., Fricke, W. & Rizzo, C. M. 2016b. Fatigue tests of notched specimens made from butt joints at steel. *Fatigue & Fracture of Engineering Materials & Structures,* 39**,** 1526-1541.

Fischer, C., Fricke, W. & Rizzo, C. M. 2016c. Review of the fatigue strength of welded joints based on the notch stress intensity factor and SED approaches. *International Journal of Fatigue,* 84**,** 59-66.

Fitzka, M. & Mayer, H. 2016. Constant and variable amplitude fatigue testing of aluminum alloy 2024-T351 with ultrasonic and servo-hydraulic equipment. *International Journal of Fatigue,* 91**,** 363-372.

Flore, D. & Wegener, K. 2016. Modelling the mean stress effect on fatigue life of fibre reinforced plastics. *International Journal of Fatigue,* 82**,** 689-699.

Formica, G. & Milicchio, F. 2016. Crack growth propagation using standard FEM. *Engineering Fracture Mechanics,* 165**,** 1-18.

Fricke, W. 2003. Fatigue analysis of welded joints: state of development. *Marine Structures,* 16**,** 185-200.

Fricke, W. 2015. Recent developments and future challenges in fatigue strength assessment of welded joints. *Proceedings of the Institution of Mechanical Engineers Part C-Journal of Mechanical Engineering Science,* 229**,** 1224-1239.

Fricke, W., Remes, H., Feltz, O., Lillemae, I., Tchuindjang, D., Reinert, T., Nevierov, A., Sichermann, W., Brinkmann, M., Kontkanen, T., Bohlmann, B. & Molter, L. 2015. Fatigue strength of laser-welded thin-plate ship structures based on nominal and structural hot-spot stress approach. *Ships and Offshore Structures,* 10**,** 39-44.

Fricke, W., Robert, C., Peters, R. & Sumpf, A. 2016. Fatigue strength of laser-stake welded T-joints subjected to combined axial and shear loads. *Welding in the World,* 60**,** 593-604.

Gan, J., Sun, D., Wang, Z., Luo, P. & Wu, W. G. 2016. The effect of shot peening on fatigue life of Q345D T-welded joint. *Journal of Constructional Steel Research,* 126**,** 74-82.

Gandiolle, C., Fouvry, S. & Charkaluk, E. 2016. Lifetime prediction methodology for variable fretting fatigue loading: Plasticity effect. *International Journal of Fatigue,* 92**,** 531-547.

Garbatov, Y. 2016. Fatigue strength assessment of ship structures accounting for a coating life and corrosion degradation. *International Journal of Structural Integrity,* 7**,** 305-322.

Garbatov, Y., Dong, Y., Rörup, J., Vhanmane, S. & Villavicencio, R. 2017. Fatigue reliability of butt-welded joints based on spectral fatigue damage assessment. *In:* Guedes Soares, C. & Teixeira, A. (eds.) *Maritime Transportation and Harvesting of Sea Resources.* London: Taylor & Francis, 611-617.

Garbatov, Y. & Guedes Soares, C. 2017. Fatigue reliability of dented pipeline based on limited experimental data. *International Journal of Pressure Vessels and Piping,* 155**,** 15-26.

Garbatov, Y., Guedes Soares, C. & Masubuchi, K. 2016a. Residual Stresses and Distortion in Welds. *Reference Module in Materials Science and Materials Engineering.* Elsevier, 1-30.

Garbatov, Y., Guedes Soares, C. & Parunov, J. 2014a. Fatigue strength experiments of corroded small-scale steel specimens. *International Journal of Fatigue,* 59**,** 137-144.

Garbatov, Y., Guedes Soares, C., Parunov, J. & Kodvanj, J. 2014b. Tensile strength assessment of corroded small-scale specimens. *Corrosion Science,* 85**,** 296-303.

Garbatov, Y., Parunov, J., Kodvanj, J., Saad-Eldeen, S. & Guedes Soares, C. 2016b. Experimental assessment of tensile strength of corroded steel specimens subjected to sandblast and sandpaper cleaning. *Marine Structures,* 49**,** 18-30.

Garcia, C., Lotz, T., Martinez, M., Artemev, A., Alderliesten, R. & Benedictus, R. 2016. Fatigue crack growth in residual stress fields. *International Journal of Fatigue,* 87**,** 326-338.

Gates, N. & Fatemi, A. 2014. Notched fatigue behaviour and stress analysis under multiaxial states of stress. *International Journal of Fatigue,* 67**,** 2-14.

Gates, N. & Fatemi, A. 2016. Multiaxial variable amplitude fatigue life analysis including notch effects. *International Journal of Fatigue,* 91**,** 337-351.

Gaur, V., Doquet, V., Persent, E., Mareau, C., Roguet, E. & Kittel, J. 2016. Surface versus internal fatigue crack initiation in steel: Influence of mean stress. *International Journal of Fatigue,* 82**,** 437-448.

Ghaffari, M. A., Pahl, E. & Xiao, S. P. 2015. Three-dimensional fatigue crack initiation and propagation analysis of a gear tooth under various load conditions and fatigue life extension with boron/epoxy patches. *Engineering Fracture Mechanics,* 135**,** 126-146.

Ghahremani, K., Walbridge, S. & Topper, T. 2015. High cycle fatigue behaviour of impact treated welds under variable amplitude loading conditions. *International Journal of Fatigue,* 81**,** 128-142.

Ghahremani, K., Walbridge, S. & Topper, T. 2016. A methodology for variable amplitude fatigue analysis of HFMI treated welds based on fracture mechanics and small-scale experiments. *Engineering Fracture Mechanics,* 163**,** 348-365.

GL 2015. Rules for Classification and Construction, I - Ship Technology, Part 1: Seagoing Ships, Chapter 1 - Hull Structures. Hamburg: Germanischer Lloyd.

Godani, M., Gaiotti, M. & Rizzo, C. M. 2014. Interlaminar shear strength of marine composite laminates: Tests and numerical simulations. *Composite Structures,* 112**,** 122-133.

Godani, M., Gaiotti, M. & Rizzo, C. M., 2015, Influence of air inclusions on the marine composites inter-laminar shear strength, Proceedings of the 25th International Ocean and Polar Engineering Conference, Kona, Hawaii Big Island.

Gonzales, G. L. G., Gonzalez, J. A. O., Castro, J. T. P. & Freire, J. L. F. 2017. A J-integral approach using digital image correlation for evaluating stress intensity factors in fatigue cracks with closure effects. *Theoretical and Applied Fracture Mechanics,* 90**,** 14-21.

Gotoh, K., Niwa, T. & Anai, Y. 2015. Numerical simulation of fatigue crack propagation under biaxial tensile loadings with phase differences. *Marine Structures,* 42**,** 53-70.

Greaves, P. R., Dominy, R. G., Ingram, G. L., Long, H. & Court, R. 2011. Evaluation of dual-axis fatigue testing of large wind turbine blades. *Journal of Mechanical Engineering Science,* 226**,** 1693-1704.

Greaves, P. R., Prieto, R., Gaffing, J., van Beveren, C., Dominy, R. & Ingram, G. 2016. A novel method of strain - bending moment calibration for blade testing. *Journal of Physics: Conference Series 753*.

Gruben, G., Morin, D., Langseth, M. & Hopperstad, O. S. 2017. Strain localization and ductile fracture in advanced high-strength steel sheets. *European Journal of Mechanics a-Solids,* 61**,** 315-329.

Guida, M. & Penta, F. 2015. A gamma process model for the analysis of fatigue crack growth data. *Engineering Fracture Mechanics,* 142**,** 21-49.

Haagensen, P. J. & Maddox, S. J. 2013. *IIW Recommendations on methods for improving the fatigue strength of welded joints: doc. IIW-2142-110,* Paris (France), International Institute of Welding, Woodhead Publishing.

Hammersley, J. & Handscomb, D. 1975. *Monte Carlo Methods,* London, Methuen.

Hao, H., Ye, D. Y., Chen, Y. Z., Mi, F. & Liu, J. Z. 2015. A study on the mean stress relaxation behaviour of 2124-T851 aluminum alloy during low-cycle fatigue at different strain ratios. *Materials & Design,* 67**,** 272-279.

Harati, E., Karlsson, L., Svensson, L. E. & Dalaei, K. 2015. The relative effects of residual stresses and weld toe geometry on fatigue life of weldments. *International Journal of Fatigue,* 77**,** 160-165.

Harati, E., Ottosson, M., Karlsson, L. & Svensson, L. E., 2014, Non-destructive measurement of weld toe radius using Weld Impression Analysis, Laser Scanning Profiling and Structures Light Projection methods, Proceedings of the First International Conference of Welding Non-destructive Testing, Teheran, Iran.

Harati, E., Svensson, L., Karlsson, L. & Widmark, M. 2016a. Effect of high-frequency mechanical impact treatment on fatigue strength of welded 1300MPa yield strength steel. *International Journal of Fatigue***,** 96-106.

Harati, E., Svensson, L. E., Karlsson, L. & Hurtig, K. 2016b. Effect of HFMI treatment procedure on weld toe geometry and fatigue properties of high strength steel welds. *21st European Conference on Fracture, (Ecf21),* 2**,** 3483-3490.

Harkegard, G. 2015. Short-crack modelling of the effect of corrosion pits on the fatigue limit of 12% Cr steel. *Fatigue & Fracture of Engineering Materials & Structures,* 38**,** 1009-1016.

Harper, P. W. & Hallett, S. R. 2015. Advanced numerical modelling techniques for the structural design of composite tidal turbine blades. *Ocean Engineering,* 96**,** 272-283.

Hashemzadeh, M., Chen, B. Q. & Guedes Soares, C. 2014. Numerical and experimental study on butt weld with dissimilar thickness of thin stainless steel plate. *The International Journal of Advanced Manufacturing Technology,* 78**,** 319-330.

Hashemzadeh, M., Garbatov, Y. & Guedes Soares, C. 2015a. Numerical Investigation of the Thermal Fields due to the Welding Sequences of Butt-welds. *In:* Guedes Soares, C. & Santos, T. A. (eds.) *Maritime Technology and Engineering.* London, UK: Taylor & Francis Group, 533-543.

Hashemzadeh, M., Garbatov, Y. & Guedes Soares, C. 2015b. Reduction in weld induced distortions of butt welded plates subjected to preventive measures. *In:* Guedes Soares, C. & Shenoi, A. (eds.) *Analysis and Design of Marine Structures V.* London, UK: Taylor & Francis Group, 581-588.

Hashemzadeh, M., Garbatov, Y. & Guedes Soares, C. 2016. Reduction in welding induced residual stresses and distortions of butt welded plates subjected to heat treatments. *In:* Guedes Soares, C. & Santos, T. (eds.) *Maritime Technology and Engineering.* London: Taylor & Francis Group, 481-488.

Hashemzadeh, M., Garbatov, Y. & Guedes Soares, C. 2017a. Analytically based equations for distortion and residual stress estimations of thin butt-welded plates. *Engineering Structures,* 137**,** 115-124.

Hashemzadeh, M., Garbatov, Y. & Guedes Soares, C. 2017b. Assessment of distortion and residual stresses in butt-welded plates made of different steels. *In:* Guedes Soares, C. & Teixeira, A. (eds.) *Maritime Transportation and Harvesting of Sea Resources.* 617-625.

Hashemzadeh, M., Garbatov, Y. & Guedes Soares, C. 2017c. Distortions and residual stress analysis of thin butt welded plates accounting for manufacturing imperfections. *In:* Guedes Soares, C. & Garbatov, Y. (eds.) *Progress in the Analysis and Design of Marine Structures.* London: Taylor & Francis Group, 623-630.

Hauteclocque, G., Monroy, C. & Bigot, F., 2016, New rules for container-ships Formulae for wave Loads, Proceedings of the 13th International Symposium on Practical design of ships and other floating structures, Copenhagen, Denmark.

He, W. T., Liu, J. X. & Xie, D. 2015. Probabilistic life assessment on fatigue crack growth in mixed-mode by coupling of Kriging model and finite element analysis. *Engineering Fracture Mechanics,* 139**,** 56-77.

Hifi, N. & Barltrop, N. 2015. Correction of prediction model output for structural design and risk-based inspection and maintenance planning. *Ocean Engineering,* 97**,** 114-125.

Hobbacher, A. 2009. *Recommendations for Fatigue Design of Welded Joints and Components, IIW doc.1823-07, Welding Research Council Bulletin 520,* New York, International Institute of Welding.

Hobbacher, A. 2010. New developments at the recent update of the IIW recommendations for fatigue of welded joints and components. *Steel Construction,* 4**,** 231-242.

Hobbacher, A. 2013. IIW recommendations for fatigue design of welded joints and components, IIW-doc. XIII-2460-13.

Hobbacher, A. 2016. *Recommendations for fatigue design of welded joints and components,* Switzerland, Springer International.

Hobbacher, A. & Kassner, M. 2012. On Relation between Fatigue Properties of Welded Joints, Quality Criteria and Groups in ISO 5817. *Welding in the World,* 56**,** 153-169.

Hodapp, D. P., Collette, M. D. & Troesch, A. W. 2015. Stochastic nonlinear fatigue crack growth predictions for simple specimens subject to representative ship structural loading sequences. *International Journal of Fatigue,* 70**,** 38-50.

Hogben, N., Da Cunha, L. F. & Ollivier, H. N. 1986. *Global Wave Statistics*, Urwin Brothers Limited.

Holmstrand, T., Mrdjanov, N., Barsoum, Z. & Astrand, E. 2014. Fatigue life assessment of improved joints welded with alternative welding techniques. *Engineering Failure Analysis,* 42**,** 10-21.

Horn, G. E., Arima, T., Baumans, P., Bøe, A. & Ocakli, H., 2013, IACS Summary of the IMO GBS and the Harmonised Common Structural Rules, TSCF 2013 Shipbuilders Meeting.

Horn, H. & Jensen, J., 2016, Reducing uncertainty of Monte Carlo estimated fatigue damage in offshore wind turbines using FORM, Proceedings of the 13th International Symposium on Practical design of ships and other floating structures, Copenhagen, Denmark.

Hos, Y., Freire, J. L. F. & Vormwald, M. 2016. Measurements of strain fields around crack tips under proportional and non-proportional mixed-mode fatigue loading. *International Journal of Fatigue,* 89**,** 87-98.

Hosdez, J., Witz, J. F., Martel, C., Limodin, N., Najjar, D., Charkaluk, E., Osmond, P. & Szmytka, F. 2017. Fatigue crack growth law identification by Digital Image Correlation and electrical potential method for ductile cast iron. *Engineering Fracture Mechanics,* 182**,** 577-594.

Huang, T. D., Harbison, M., Kvidahl, L., Niolet, D., Walks, J., Christein, J. P., Smitherman, M., Phillippi, M., Dong, P. S., DeCan, L., Caccese, V., Blomquist, P., Kihl, D., Wong, R., Sinfield, M., Nappi, N., Gardner, J., Wong, C., Bjornson, M. & Manuel, A. 2016. Reduction of Overwelding and Distortion for Naval Surface Combatants. Part 2: Weld Sizing Effects on Shear and Fatigue Performance. *Journal of Ship Production and Design,* 32**,** 21-36.

Huang, T. D., Harbison, M., Kvidahl, L., Niolet, D., Walks, J., Stefanick, K., Phillippi, M., Dong, P., DeCan, L., Caccese, V., Blomquist, P., Kihl, D., Wong, R., Nappi, N., Gardner, J., Wong, C., Bjornson, M. & Manuel, A. 2014a. Reduction of Overwelding and Distortion for Naval Surface Combatants, Part 1: Optimized Weld Sizing for Lightweight Ship Structures. *Journal of Ship Production and Design,* 30**,** 184-193.

Huang, W., Garbatov, Y. & Guedes Soares, C. 2012. Fatigue damage assessment of stiffener-frame structures. *In:* Guedes Soares, C., Garbatov, Y., Sutulo, S. & Santos, T. (eds.) *Maritime Technology and Engineering.* London, UK: Taylor & Francis Group.

Huang, W., Garbatov, Y. & Guedes Soares, C. 2013. Fatigue reliability assessment of a complex welded structure subjected to multiple cracks. *Engineering Structures,* 56**,** 868-879.

Huang, W., Garbatov, Y. & Guedes Soares, C. 2014b. Fatigue reliability assessment of correlated welded web-frame joints. *Journal of Marine Science and Application,* 13**,** 23-31.

Huang, W., Garbatov, Y. & Guedes Soares, C. 2014c. Fatigue reliability of a web frame subjected to random non-uniform corrosion wastage. *Structural Safety,* 48**,** 51-62.

Huang, W. & Sridhar, N. 2016. Fatigue Failure Risk Assessment for a Maintained Stiffener-Frame Welded Structure with Multiple Site Cracks. *International Journal of Applied Mechanics,* 8.

Huffman, P. J. 2016. A strain energy based damage model for fatigue crack initiation and growth. *International Journal of Fatigue,* 88**,** 197-204.

Hughes, S., Musial, W. & Stensland, T., 1999, Implementation of two axes servo-hydraulic system for full-scale testing of wind turbine blades., Proceedings in Windpower, 67–76.

Hwang, M.-R., Lee, T.-K., Kang, D.-H. & Suh, Y. S., 2016, A Study on Ice-induced Fatigue Life Estimation Based on Measured Data of the AR-AON, Proceedings of the 26th International Ocean and Polar Engineering Conference, Rhodes, Greece, Paper ISOPE-I-16-486.

Hyunchul, J., Kyoung, J., Kim, J. W., Yan, H. & Wu, G., 2017, CFD of fully coupled mooring and riser effects on vortex-induced motion of semi-submersible Proceedings of the 36th International Conference on Ocean, Offshore and Arctic Engineering, Trondheim, Norway, Paper OMAE2017-62433.

IACS 1989. Longitudinal Strength Standard, IACS Unified Requirement S11. London: International Association of Classification Societies.

IACS 1999. Fatigue assessment of ship structures IACS Recommendation No. 56. London: International Association of Classification Societies.

IACS 2001. Standard Wave Data. *Recommendation 34.*

IACS 2012. Common Structure Rules for Double Hull Oil Tankers, Consolidated version, July 2012.

IACS 2014a. Equivalent Design Wave (EDW) for Fatigue Loads, *Technical Background report for the Harmonized Common Structural Rules.*

IACS 2014b. Hull girder vibration. *Technical Background report for the development of the CSR.*

IACS 2015. Common Structural Rules for Bulk Carriers and Oil Tankers. London: International Association of Classification Societies.

IACS. 2016. *Technical Background Documents for CSR* [Online]. http://www.iacs.org.uk/publications/. [Accessed 1 October 2016.

Ibrahim, R. A. 2015a. Overview of Structural Life Assessment and Reliability, Part I: Basic Ingredients of Fracture Mechanics. *Journal of Ship Production and Design,* 31**,** 1-42.

Ibrahim, R. A. 2015b. Overview of Structural Life Assessment and Reliability, Part II: Fatigue Life and Reliability Assessment of Naval Ship Structures. *Journal of Ship Production and Design,* 31**,** 100-128.

Ibrahim, R. A. 2015c. Overview of Structural Life Assessment and Reliability, Part III: Impact, Grounding, and Reliability of Ships under Extreme Loading. *Journal of Ship Production and Design,* 31**,** 137-169.

Ibrahim, R. A. 2015d. Overview of Structural Life Assessment and Reliability, Part IV: Corrosion and Hydrogen Embrittlement of Naval Ship Structures. *Journal of Ship Production and Design,* 31**,** 241-263.

Ibrahim, R. A. 2016a. Overview of Structural Life Assessment and Reliability, Part V: Joints and Weldments. *Journal of Ship Production and Design,* 32**,** 1-20.

Ibrahim, R. A. 2016b. Overview of Structural Life Assessment and Reliability, Part VI: Crack Arresters. *Journal of Ship Production and Design,* 32**,** 71-98.

IEC-61400-23 2014. Wind turbines - Part 23: Full-scale structural testing of rotor blades. Geneva, Switzerland.

IGC 2014. Annex 6 Resolution MSC.370(93): Amendments to the International code for the construction and equipment of ships carrying liquefied gases in bulk IGC Code.

Ilman, M. N., Kusmono, Muslih, M. R., Subeki, N. & Wibowo, H. 2016. Mitigating distortion and residual stress by static thermal tensioning to improve fatigue crack growth performance of MIG AA5083 welds. *Materials & Design,* 99**,** 273-283.

Im, H.-I., Vladimir, N., Malenica, S., Ryu, H. R. & Cho, D. S., 2015, Fatigue Analysis of HHI Sky Bench 19000 TEU ultra-large container ship with springing effect included, Proceedings of the 7th International Conference on Hydroelasticity in Marine Technology, Split, Croatia.

IMO. 2015. *Focus on IMO - International goal-based ship construction standards for bulk carriers and oil tankers* [Online]. http://www.imo.org/en/OurWork/Safety/SafetyTopics/Pages/Goal-BasedStandards.aspx. [Accessed 1 October 2016.

Ince, A. & Glinka, G. 2016. Innovative computational modelling of multiaxial fatigue analysis for notched components. *International Journal of Fatigue,* 82**,** 134-145.

IRS 2016a. Rules and Regulation for the construction and classification of steel ships. Mumbai: IRS.

IRS 2016b. Rules for Bulk carriers and Oil tankers. Mumbai: IRS.

ISO5817 2014. Welding - Fusion-welded joints in steel, nickel, titanium and their alloys (beam welding excluded) - Quality levels for imperfections.

ISO12932 2013. Welding. Laser-arc hybrid welding of steels, nickel and nickel alloys. Quality levels for imperfections.

ISO13919-1 1996. Welding - Electron and laser-beam welded joints - Guidance on quality levels for imperfections - Part 1: Steel.

Jandejsek, I., Gajdos, L., Sperl, M. & Vavrik, D. 2017. Analysis of standard fracture toughness test based on digital image correlation data. *Engineering Fracture Mechanics,* 182**,** 607-620.

Jaouën, F., Waals, O., Jong, M. d., Hout, A. v. d. & Christou, M., 2016, Methodology for the Design on LNG Terminals in Nearshore Environment, Proceedings of the 35th International Conference on Ocean, Offshore and Arctic Engineering, Busan, Korea, Paper OMAE2016-54724.

Jensen, J. J. 2015. Fatigue damage estimation in nonlinear systems using a combination of Monte Carlo simulation and the First Order Reliability Method. *Marine Structures,* 44**,** 203-210.

Ji, C. Y., Xue, H. Z., Shi, X. H. & Gaidai, O. 2016. Experimental and numerical study on collapse of aged jacket platforms caused by corrosion or fatigue cracking. *Engineering Structures,* 112**,** 14-22.

Jiameng, W., Gang, W. & Shijian, C., 2016, Ramification Study on IACS Harmonized Common Structural Rules: Impact on Structural Design and Scantlings, SNAME Maritime Convention, Houston Texas (USA), SNAME, 124-143.

Jiang, C., Liu, Z. C., Wang, X. G., Zhang, Z. & Long, X. Y. 2016. A structural stress-based critical plane method for multiaxial fatigue life estimation in welded joints. *Fatigue & Fracture of Engineering Materials & Structures,* 39**,** 372-383.

Jones, R. 2014. Fatigue crack growth and damage tolerance. *Fatigue & Fracture of Engineering Materials & Structures,* 37**,** 463-483.

Jonson, B., Dobmann, G., Hobbacher, A., Kassner, M. & Marquis, G. 2016a. *IIW guidelines on weld quality in relationship to fatigue strength,* IIW Paris, IIW Collection.

Jonson, B., Dobmann, G., Hobbacher, A., Kassner, M. & Marquis, G. 2016b. *IW Guidelines on Weld Quality in Relationship to Fatigue Strength*, Springer.

Jonson, B., Samuelsson, J. & Marquis, G. B. 2011. Development of Weld Quality Criteria Based on Fatigue Performance. *Welding in the World,* 55**,** 79-88.

Kahl, A., Fricke, W., Paetzold, H. & von Selle, H. 2015. Whipping Investigations Based on Large-Scale Measurements and Experimental Fatigue Testing. *International Journal of Offshore and Polar Engineering,* 25**,** 247-254.

Kainuma, S., Yang, M. Y., Jeong, Y. S., Inokuchi, S., Kawabata, A. & Uchida, D. 2016. Experiment on fatigue behaviour of rib-to-deck weld root in orthotropic steel decks. *Journal of Constructional Steel Research,* 119**,** 113-122.

Karatzas, V. A., Kotsidis, E. A. & Tsouvalis, N. G. 2015. Experimental Fatigue Study of Composite Patch Repaired Steel Plates with Cracks. *Applied Composite Materials,* 22**,** 507-523.

Karlsson, J., Podgorski, K. & Rychlik, I. 2016. The Laplace multi-axial response model for fatigue analysis. *International Journal of Fatigue,* 85**,** 11-17.

Karolczuk, A., Kluger, K. & Lagoda, T. 2016. A correction in the algorithm of fatigue life calculation based on the critical plane approach. *International Journal of Fatigue,* 83**,** 174-183.

Karr, D., Baloglu, P., Cao, T., Douglas, A., K., N., Ong, K. T., Rohrback, B. & N., S. 2015. *Strength and fatigue testing of composite patches for ship plating fracture repair,* www.shipstructures.org.

Karr, D., Douglas, A., Ferrari, C., Cao, T., Ong, K., Si, N., He, J., Baloglu, C., White, P. & Parra-Montesinos, G. 2016. Fatigue testing of composite patches for ship plating fracture repair. *Ships and Offshore Structures*.

Kennedy, S., Kong, J. S. K., Notaro, G., Brinchmann, K., Kaur, J., Hwang, O., Lim, J., Khoo, C. & Chow, W. H., 2016, Dropped Object SPS Impact Protection Deck for Well Bay Area, Proceedings of the 13th International Symposium on Practical design of ships and other floating structures, Copenhagen, Denmark.

Khalij, L., Gautrelet, C. & Guillet, A. 2015. Fatigue curves of a low carbon steel obtained from vibration experiments with an electrodynamic shaker. *Materials & Design,* 86**,** 640-648.

Khurshid, M., Barsoum, Z., Barsoum, I. & Dauwel, T. 2016. The multiaxial weld root fatigue of butt welded joints subjected to uniaxial loading. *Fatigue & Fracture of Engineering Materials & Structures,* 39**,** 1281-1298.

Kim, Y., Oh, J. S. & Jeon, S. H. 2015. Novel hot spot stress calculations for welded joints using 3D solid finite elements. *Marine Structures,* 44**,** 1-18.

Kitagawa, H. & Takahashi, S., 1976, Applicability of fracture mechanics to very small cracks or cracks in the early stage, Proceedings of the 2nd International Conference on Mechanical Behaviour of Materials, ASM, 627-631.

Koop, A., de Wilde, J., Condino Fujarra, A. L., Rijken, O., Linder, S., Lennblad, J., Haug, N. & Phadke, A., 2016, Investigation on the reasons for possible difference between VIM response in the field and in model tests, Proceedings of the 35th International Conference on Ocean, Offshore and Arctic Engineering, Busan, Korea, Paper OMAE2016-54746.

Kõrgesaar, M., Romanoff, J. & Remes, H. 2017. Influence of material non-linearity on load carrying mechanism and strain path in stiffened panel. *Procedia Structural Integrity,* 5**,** 713-720.

Korhonen, E., Remes, H., Romanoff, J., Niemela, A., Hiltunen, P. & Kontkanen, T. 2013. Influence of surface integrity on the fatigue strength of high strength steel in balcony openings of cruise ship structures. *In:* Guedes Soares, C. & Shenoi, A. (eds.) *Analysis and Design of Marine Structures* London, UK: Taylor & Francis Group, 255-261.

Krairi, A., Doghri, I. & Robert, G. 2016. Multiscale high cycle fatigue models for neat and short fiber reinforced thermoplastic polymers. *International Journal of Fatigue,* 92**,** 179-192.

Krewerth, D., Lippmann, T., Weidner, A. & Biermann, H. 2015. Application of full-surface view in situ thermography measurements during ultrasonic fatigue of cast steel G42CrMo4. *International Journal of Fatigue,* 80**,** 459-467.

Krzyzak, D., Robak, G. & Lagoda, T. 2015. Determining fatigue life of bent and tensioned elements with a notch, with use of fictitious radius. *Fatigue & Fracture of Engineering Materials & Structures,* 38**,** 693-699.

Lahuerta, F., de Ruiter, M. J., Espinosa, L., Koorn, N. & Smissaert, D., 2017, Assessment of wind turbine blade trailing edge failure with sub-component tests, Proceedings of the 21st International Conference on Composite Materials.

Lang, R. & Lener, G. 2016. Application and comparison of deterministic and stochastic methods for the evaluation of welded components' fatigue lifetime based on real notch stresses. *International Journal of Fatigue,* 93**,** 184-193.

Lassen, T. 1990. The Effect of the Welding Process on the Fatigue Crack-Growth. *Welding Journal,* 69**,** S75-S81.

Lassen, T. & Recho, N., 2015, Risk-Based Inspection Planning for Fatigue Damage in Offshore Steel Structures, Proceedings of the International Conference on Offshore Mechanics and Arctic Engineering.

Lee, C. H., Chang, K. H. & Do, V. N. V. 2016. Modelling the high cycle fatigue behaviour of T-joint fillet welds considering weld-induced residual stresses based on continuum damage mechanics. *Engineering Structures,* 125**,** 205-216.

Lee, Y., White, N., Wang, Z., Tong, J., Xiao, Y. & Qihua, L., 2014, Springing Loads and Fatigue Assessment on Large Container Ships, Proceedings of the 24th International Ocean and Polar Engineering Conference Busan Korea, Paper ISOPE-I-14-339.

Lefebre, G., 1993 1993, Extra-High-Strength Grades: The Steel for Tomorrow Offshore Application?, Proceedings of the 12th International Conference on Offshore Mechanics and Arctic Engineering, ASME, New York, USA, 199-205.

Leitner, M., Gerstbrein, S., Ottersbock, M. & Stoschka, M. 2015a. Fatigue strength of HFMI-treated and stress-relief annealed high-strength steel weld joints. *Fatigue Design.* 477-484.

Leitner, M., Gerstbrein, S., Ottersbock, M. J. & Stoschka, M. 2015b. Fatigue strength of HFMI-treated high-strength steel joints under constant and variable amplitude block loading. *3rd International Conference on Material and Component Performance under Variable Amplitude Loading, Val 2015,* 101**,** 251-258.

Leitner, M., Khurshid, M. & Barsoum, Z. 2017. Stability of high-frequency mechanical impact (HFMI) post-treatment induced residual stress states under cyclic loading of welded steel joints. *Engineering Structures,* 143**,** 589-602.

Leitner, M., Simunek, D., Shah, S. & Stoschka, M. 2016. Numerical fatigue assessment of welded and HFMI-treated joints by notch stress/strain and fracture mechanical approaches. *Advances in Engineering Software*.

Li, B. 2015. A new approach of fatigue life prediction for metallic materials under multiaxial loading. *International Journal of Fatigue,* 78.

Li, B. C., Jiang, C., Han, X. & Li, Y. 2014a. A new path-dependent multiaxial fatigue model for metals under different paths. *Fatigue & Fracture of Engineering Materials & Structures,* 37**,** 206-218.

Li, H., Yuan, H. & Li, X. 2015a. Assessment of low cycle fatigue crack growth under mixed-mode loading conditions by using a cohesive zone model. *International Journal of Fatigue,* 75**,** 39-50.

Li, W., Deng, H. L., Sun, Z. D., Zhang, Z. Y., Lu, L. T. & Sakai, T. S. 2015b. Subsurface inclusion-induced crack nucleation and growth behaviours of high strength steels under very high cycle fatigue: Characterization and microstructure-based modelling. *Materials Science and Engineering a-Structural Materials Properties Microstructure and Processing,* 641**,** 10-20.

Li, X., Guan, Z. D., Li, Z. S. & Liu, L. 2014b. A new stress-based multi-scale failure criterion of composites and its validation in open hole tension tests. *Chinese Journal of Aeronautics,* 27**,** 1430-1441.

Li, Y., Chen, Y., Shi, Z., Xie, W. & Ni, K., 2015c, Study on Global Fatigue Analysis for Deep-water Tension-Leg Platform Based on Simplified Spectral Method, Proceedings of the 25th International Ocean and Polar Engineering Conference Hawaii, USA, Paper ISOPE-I-15-229.

Liao, P. K., Lee, Y. J., Lin, H. J., Tsai, S. C., Chien, H. L., Chang, B. C. & Luo, G. M. 2015. Springing effect on the fatigue life of an 8000 TEU container ship. *In:* Shenoi, G. S. (ed.) *Analysis and Design of Marine Structures.* UK.

Liinalampi, S., Remes, H., Lehto, P., Lillemae, I., Romanoff, J. & Porter, D. 2016. Fatigue strength analysis of laser-hybrid welds in thin plate considering weld geometry in microscale. *International Journal of Fatigue,* 87**,** 143-152.

Lillemäe-Avi, I., Remes, H., Dong, Y., Garbatov, Y., Quéméner, Y., Eggert, L., Sheng, Q. & Yue, J. 2017. Benchmark study on considering welding-induced distortion in structural stress analysis of thin-plate structures. *In:* Guedes Soares, C. & Garbatov, Y. (eds.) *Progress in the Analysis and Design of Marine Structures.* London: Taylor & Francis Group, 387-394.

Lillemäe, I., Liinalampi, S., Remes, H., Avi, E. & Romanoff, J., 2016, Influence of welding distortion on the structural stress in thin deck panels, Proceedings of the 13th International Symposium on Practical design of ships and other floating structures, Copenhagen, Denmark.

Lillemae, I., Liinalampi, S., Remes, H., Itavuo, A. & Niemela, A. 2017. Fatigue strength of thin laser-hybrid welded full-scale deck structure. *International Journal of Fatigue,* 95**,** 282-292.

Liu 2015. A multiaxial HCF life evaluation model for notched structural components. *International Journal of Fatigue,* 80.

Liu, B., Garbatov, Y. & Guedes Soares, C. 2015. Non-linear finite element analysis of crashworthy shields of offshore wind turbine supporting structures. *In:* Guedes Soares, C. & Shenoi, A. (eds.) *Analysis and Design of Marine Structures.* London, UK: Taylor & Francis Group, 693-702.

Liu, G. J., Zhong, B. L., Tian, X. J., Chen, P. F. & Mu, W. L. 2016. Numerical analysis on the HSS and SIF of multi-planar DX-joint welds for offshore platforms. *Ocean Engineering,* 127**,** 258-268.

Liu, Y., Yi, H. & Chen, L. Y. 2014. Submarine pressure hull butt weld fatigue life reliability prediction method. *Marine Structures,* 36**,** 51-64.

Lopez-Crespo, P., Moreno, B., Lopez-Moreno, A. & Zapatero, J. 2015a. Characterisation of crack-tip fields in biaxial fatigue based on high-magnification image correlation and electro-spray technique. *International Journal of Fatigue,* 71**,** 17-25.

Lopez-Crespo, P., Moreno, B., Lopez-Moreno, A. & Zapatero, J. 2015b. Study of crack orientation and fatigue life prediction in biaxial fatigue with critical plane models. *Engineering Fracture Mechanics,* 136**,** 115-130.

Lotsberg, I. 2016. *Fatigue design of marine structures,* New York, United States, Cambridge University Press.

Lotsberg, I., Sigurdsson, G., Fjeldstad, A. & Moan, T. 2016. Probabilistic methods for planning of inspection for fatigue cracks in offshore structures. *Marine Structures,* 46**,** 167-192.

Lou, B., Zhang, S., Tong, J., Wong, S., Cheng, F. & Hirdaris, S. 2015. A fracture mechanics-based approach for the analysis of crack growth at weld joints of ship structures. *In:* Guedes Soares, C. & Shenoi, A. (eds.) *Analysis and Design of Marine Structures.* London, UK: Taylor & Francis Group.

LR 2009. ShipRight Design and Construction: Fatigue Design Assessment - Level 1 Procedure Structural Detail Design Guide. London, UK: Lloyd's Register Group Limited.

LR 2014. ShipRight Design and Construction: Structural Design Assessment - Guidance Notes on the Assessment of Global Design Loads of Large Container Ships and Other Ships Prone to Whipping and Springing. *DRAFT version.* London, UK: Lloyd's Register Group Limited.

LR 2015. ShipRight 2014.2 User Guide FDA Level 2 Spreadsheet. London, UK: Lloyd's Register Group Limited.

LR 2016a. Rules and Regulations for the Classification of Ships. Part 3 Ship Structures (General), Chapter 16 ShipRight Procedures for the Design, Construction and Lifetime Care of Ships. London, UK: Lloyd's Register Group Limited.

LR 2016b. ShipRight 2014.2 User Guide FDA Level 2 Assessment. London, UK: Lloyd's Register Group Limited.

LR 2016c. ShipRight Design and Construction: Fatigue Design Assessment - Application and Notations (Notice 1 and Notice 2). London, UK: Lloyd's Register Group Limited.

LR 2016d. ShipRight Design and Construction: Fatigue Design Assessment - Level 3 Procedure Guidance on Direct Calculations (Notice 1). London, UK: Lloyd's Register Group Limited.

Luque, J. & Straub, D. 2016. Reliability analysis and updating of deteriorating systems with dynamic Bayesian networks. *Structural Safety,* 62**,** 34-46.

Madia, M., Zerbst, U., Beier, H. T. & Schork, B. 2017. The IBESS model - Elements, realisation and validation. *Engineering Fracture Mechanics,* Article in press.

Maheswaran, J. & Siriwardane, S. C. 2016. Fatigue life estimation of tubular joints - a comparative study. *Fatigue & Fracture of Engineering Materials & Structures,* 39**,** 30-46.

Mahmoud, H. & Riveros, G. 2014. Fatigue reliability of a single stiffened ship hull panel. *Engineering Structures,* 66**,** 89-99.

Mahtabi, M. J. & Shamsaei, N. 2016. A modified energy-based approach for fatigue life prediction of super elastic NiTi in presence of tensile mean strain and stress. *International Journal of Mechanical Sciences,* 117**,** 321-333.

Makino, T., Neishi, Y., Shiozawa, D., Kikuchi, S., Okada, S., Kajiwara, K. & Nakai, Y. 2016. Effect of defect shape on rolling contact fatigue crack initiation and propagation in high strength steel. *International Journal of Fatigue,* 92**,** 507-516.

Malikoutsakis, M. & Savaidis, G. 2014. Fatigue assessment of thin-welded joints with pronounced terminations. *Fatigue & Fracture of Engineering Materials & Structures,* 37**,** 782-799.

Malikova, L., Vesely, V. & Seitl, S. 2015. Estimation of the crack propagation direction in a mixed-mode geometry via multi-parameter fracture criteria. *Frattura Ed Integrita Strutturale,* 33**,** 25-32.

Malikova, L., Vesely, V. & Seitl, S. 2016. Crack propagation direction in a mixed mode geometry estimated via multi-parameter fracture criteria. *International Journal of Fatigue,* 89**,** 99-107.

Maljaars, J., Pijpers, R. & Slot, H. 2015. Load sequence effects in fatigue crack growth of thick-walled welded C-Mn steel members. *International Journal of Fatigue,* 79**,** 10-24.

Mao, W. G., Li, Z. Y., Ogeman, V. & Ringsberg, J. W. 2015. A regression and beam theory-based approach for fatigue assessment of containership structures including bending and torsion contributions. *Marine Structures,* 41**,** 244-266.

Marquis, G. & Barsoum, Z. 2014. Fatigue strength improvement of steel structures by high-frequency mechanical impact: proposed procedures and quality assurance guidelines. *Welding in the World,* 58**,** 19-28.

Marquis, G. B., Mikkola, E., Yildirim, H. C. & Barsoum, Z. 2013. Fatigue strength improvement of steel structures by high-frequency mechanical impact: proposed fatigue assessment guidelines. *Welding in the World,* 57**,** 803-822.

Matic, P., Geltmacher, A. & Rath, B. 2015. Computational aspects of steel fracturing pertinent to naval requirements. *Philos Trans A Math Phys Eng Sci,* 373**,** 321-325.

Matsuda, K. & Gotoh, K. 2015. Numerical simulation of fatigue crack propagation under superimposed stress histories containing different frequency components with several mean stress conditions. *Marine Structures,* 41**,** 77-95.

Maximiano, A., Koop, A., de Wilde, J. & Gonçalves, R. T., 2017, Experimental study on the vortex-induced motions (VIM) of a semi-submersible floater in waves, Proceedings of the 36th International Conference on Ocean, Offshore and Arctic Engineering, Trondheim, Norway, Paper OMAE2017-61543.

May, M., Saintier, N., Palin-Luc, T. & Devos, O. 2015. Non-local high cycle fatigue strength criterion for metallic materials with corrosion defects. *Fatigue & Fracture of Engineering Materials & Structures,* 38**,** 1017-1025.

Mayer, H., Fitzka, M. & Schuller, R. 2014. Variable amplitude loading of Al 2024-T351 at different load ratios using ultrasonic equipment. *International Journal of Fatigue,* 60**,** 34-42.

Mei, J. F. & Dong, P. S. 2016. A new path-dependent fatigue damage model for non-proportional multi-axial loading. *International Journal of Fatigue,* 90**,** 210-221.

Mei, J. F. & Dong, P. S. 2017a. An equivalent stress parameter for multi-axial fatigue evaluation of welded components including non-proportional loading effects. *International Journal of Fatigue,* 101**,** 297-311.

Mei, J. F. & Dong, P. S. 2017b. Modelling of path-dependent multi-axial fatigue damage in aluminum alloys. *International Journal of Fatigue,* 95**,** 252-263.

Meneghetti 2015. Averaged SED evaluated rapidly from the singular peak stresses by FEM - cracked components under mixed mode loading. *Theoretical and Applied Fracture Mechanics,* 79.

Meneghetti, G., Campagnolo, A. & Berto, F. 2015. Fatigue strength assessment of partial and full-penetration steel and aluminium butt-welded joints according to the peak stress method. *Fatigue & Fracture of Engineering Materials & Structures,* 38**,** 1419-1431.

Meneghetti, G. & Ricotta, M. 2016. Evaluating the heat energy dissipated in a small volume surrounding the tip of a fatigue crack. *International Journal of Fatigue,* 92**,** 605-615.

Meneghetti, G., Ricotta, M. & Atzori, B. 2016. A two-parameter, heat energy-based approach to analyse the mean stress influence on axial fatigue behaviour of plain steel specimens. *International Journal of Fatigue,* 82**,** 60-70.

Meng, M. Z., Le, H. R., Grove, S. & Rizvi, M. J. 2016. Moisture effects on the bending fatigue of laminated composites. *Composite Structures,* 154**,** 49-60.

Mikheevskiy, S., Glinka, G. & Cordes, T., 2015, Total life approach for fatigue life estimation of welded structures, Proceedings of the 3rd International Conference on Material and Component Performance under Variable Amplitude Loading, Prague, Czech Republic.

Mikkola, E., Marquis, G., Lehto, P., Remes, H. & Hanninen, H. 2016. Material characterization of high-frequency mechanical impact (HFMI)-treated high-strength steel. *Materials & Design,* 89**,** 205-214.

Mikkola, E., Murakami, Y. & Marquis, G. 2015. Equivalent crack approach for fatigue life assessment of welded joints. *Engineering Fracture Mechanics,* 149**,** 144-155.

Mikkola, E. & Remes, H. 2016. Allowable stresses in high-frequency mechanical impact (HFMI)-treated joints subjected to variable amplitude loading. *Welding in the World.*

Mikkola, E., Remes, H. & Marquis, G. 2017. A finite element study on residual stress stability and fatigue damage in high-frequency mechanical impact (HFMI)-treated welded joint. *International Journal of Fatigue,* 94**,** 16-29.

Millwater, H., Wagner, D., Baines, A. & Montoya, A. 2016. A virtual crack extension method to compute energy release rates using a complex variable finite element method. *Engineering Fracture Mechanics,* 162**,** 95-111.

Minoura, M., 2016, Stochastic Sea State Model based on Fourier Series Expansion, Proceedings of the 26th International Ocean and Polar Engineering Conference Rhodes, Greece, Paper ISOPE-I-16-325.

Mohammadi, M., Zehsaz, M., Hassanifard, S. & Rahmatfam, A. 2016a. An evaluation of total fatigue life prediction of a notched shaft subjected to cyclic bending load. *Engineering Fracture Mechanics,* 166**,** 128-138.

Mohammadi, S. F., Galgoul, N. S., Starossek, U. & Videiro, P. M. 2016b. An efficient time-domain fatigue analysis and its comparison to spectral fatigue assessment for an offshore jacket structure. *Marine Structures,* 49**,** 97-115.

Mokhtarishirazabad, M., Lopez-Crespo, P., Moreno, B., Lopez-Moreno, A. & Zanganeh, M. 2017. Optical and analytical investigation of overloads in biaxial fatigue cracks. *International Journal of Fatigue,* 100**,** 583-590.

Nebbia, G., Gaiotti, M., Rizzo, C. M. & Caleo, A. 2015a. Mechanical characterization of yachts and pleasure crafts fillers. *In:* Guedes Soares, C. & Shenoi, A. (eds.) *Analysis and Design of Marine Structures.* London, UK: Taylor & Francis Group, 627-635.

Nebbia, G., Gaiotti, M., Rizzo, C. M., Caleo, A. & Ivaldi, A., 2015b, Mechanical behaviour of fillers: tests and comparisons, Proceedings of Design & Construction of Super & Mega Yachts, Genoa, Italy, Royal Institution of Naval Architects.

Newman, J. C. & Raju, I. S. 1981. An Empirical Stress-Intensity Factor Equation for the Surface Crack. *Engineering Fracture Mechanics,* 15**,** 185-192.

Nguyen, H. Q., Gallimard, L. & Bathias, C. 2015. Numerical simulation of fish-eye fatigue crack growth in very high cycle fatigue. *Engineering Fracture Mechanics,* 135**,** 81-93.

Niesłony, A. & Böhm, M. 2016. Frequency-domain fatigue life estimation with mean stress correction. *International Journal of Fatigue,* 91**,** 373-381.

Nykanen, T. & Bjork, T. 2015. Assessment of fatigue strength of steel butt-welded joints in as-welded condition - Alternative approaches for curve fitting and mean stress effect analysis. *Marine Structures,* 44**,** 288-310.

O'Connor, S. J., Nowell, D. & Dragnevski, K. I. 2016. Measurement of fatigue crack deformation on the macro- and micro-scale: Uniform and non-uniform loading. *International Journal of Fatigue,* 89**,** 66-76.

Ogeman, V., Mao, W. & Ringsberg, J., 2014., Uncertainty in Stress Concentration Factor Computation for Ship Fatigue Design, Proceedings of the 33rd International Conference on Ocean, Offshore and Arctic Engineering, San Francisco, California, USA.

Oh, D. J., Lee, J. M. & Kim, M. H. 2014. Fatigue strength assessment of Invar alloy weld joints using the notch stress approach. *Engineering Failure Analysis,* 42**,** 87-99.

Okada, H., Koya, H., Kawai, H., Li, Y. S. & Osakabe, K. 2016. Computations of stress intensity factors for semi-elliptical cracks with high aspect ratios by using the tetrahedral finite element (fully automated parametric study). *Engineering Fracture Mechanics,* 158**,** 144-166.

Ooi, S. W., Garnham, J. E. & Ramjaun, T. I. 2014. Review: Low transformation temperature weld filler for tensile residual stress reduction. *Materials & Design,* 56**,** 773-781.

Ormberg, H. & Bachynski, E. E., 2015, Sensitivity of Estimated Tower Fatigue to Wind Modeling for a Spar Floating Wind Turbine, Proceedings of the 25th International Ocean and Polar Engineering Conference, Hawaii, USA, Paper ISOPE-I-15-385.

Ottersbock, M. J., Leitner, M., Stoschka, M. & Maurer, W. 2016. Effect of weld defects on the fatigue strength of ultra-high-strength steels. *Xviii International Colloquium on Mechanical Fatigue of Metals (Icmfm Xviii),* 160**,** 214-222.

Pahlavan, L. & Blacquiere, G. 2016. Fatigue crack sizing in steel bridge decks using ultrasonic guided waves. *NDT & E International,* 77**,** 49-62.

Pang, J. H. L., Hoh, H. J., Tsang, K. S., Low, J., Kong, S. C. & Yuan, W. G. 2017. Fatigue crack propagation analysis for multiple weld toe cracks in cut-out fatigue test specimens from a girth welded pipe. *International Journal of Fatigue,* 94**,** 158-165.

Pansart, S., 2015, A new rotor blade standard for high product quality and flexible certification, European Wind Energy Association, Paris, France.

Panwar, S., Sun, S. & Sundararaghavan, V. 2016. Modelling fatigue failure using the variational multiscale method. *Engineering Fracture Mechanics,* 162**,** 290-308.

Park, D.-Y., Tyson, W. & Gravel, J.-F. 2017. CANMET SENT test method, updates and applications. *International Jornal of Pressure Vessels and Piping,* Article in press.

Pedersen, M. M. 2016. Multiaxial fatigue assessment of welded joints using the notch stress approach. *International Journal of Fatigue,* 83**,** 269-279.

Peng, B.-F., Chen, C.-Y. & Llorente, C., 2015, Time History and Spectral Fatigue Analyses of Deepwater Offshore Truss-Spar Platform under In-service and Trans-ocean Tow Conditions, Proceedings of the 25th International Ocean and Polar Engineering Conference, Hawaii, USA, Paper ISOPE-I-15-741.

Polezhayeva, H., Howarth, D., Kumar, M., Ahmad, B. & Fitzpatrick, M. E. 2015a. The effect of compressive fatigue loads on fatigue strength of non-load carrying specimens subjected to ultrasonic impact treatment. *Welding in the World,* 59**,** 713-721.

Polezhayeva, H., Toumpis, A. I., Galloway, A. M., Molter, L., Ahmad, B. & Fitzpatrick, M. E. 2015b. Fatigue performance of friction stir welded marine grade steel. *International Journal of Fatigue,* 81**,** 162-170.

Post, N. 2014. Fatigue Test Design: Scenarios for Biaxial Fatigue Testing of a 60-Meter Wind Turbine Blade. National Renewable Energy Laboratory, NREL/TP-5000-65227.

Proudhon, H., Li, J., Wang, F., Roos, A., Chiaruttini, V. & Forest, S. 2015. 3d simulation of short fatigue crack propagation by finite element crystal plasticity and remeshing. *International Journal of Fatigue,* 82.

Qayyum, F., Shah, M., Shakeel, O., Mukhtar, F., Salem, M. & Rezai-Aria, F. 2016. Numerical simulation of thermal fatigue behaviour in a cracked disc of AISI H-11 tool steel. *Engineering Failure Analysis,* 62**,** 242-253.

Quemener, Y., Liao, P.-K., Lee, C.-F. & Chen, K.-C., 2015, Load uncertainties effects on the fatigue life evaluation by the Common Structural Rules, Proceedings of the 34th International Conference on Ocean, Offshore and Arctic Engineering, Newfoundland, Canada.

Radaj, D. 2015. State-of-the-art review on the local strain energy density concept and its relation to the J-integral and peak stress method. *Fatigue & Fracture of Engineering Materials & Structures,* 38**,** 2-28.

Radaj, D., Lazzarin, P. & Berto, F. 2009a. *Fatigue assessment of welded joints under slit-parallel loading based on strain energy density or notch rounding.*

Radaj, D., Sonsino, C. M. & Fricke, W. 2006. *Fatigue assessment of welded joints by local approaches*, Woodhead publishing.

Radaj, D., Sonsino, C. M. & Fricke, W. 2009b. Recent developments in local concepts of fatigue assessment of welded joints. *International Journal of Fatigue,* 31**,** 2-11.

Reddy, S., Jaswanthsai, V., Madhavan, M. & Kumar, V. 2016. Notch stress intensity factor for center cracked plates with crack stop hole strengthened using CFRP: A numerical study. *Thin-Walled Structures,* 98**,** 252-262.

Remes, H. & Fricke, W. 2014. Influencing factors on fatigue strength of welded thin plates based on structural stress assessment. *Welding in the World,* 58**,** 915-923.

Remes, H., Korhonen, E., Lehto, P., Romanoff, J., Niemelä, A., Hiltunen, P. & Kontkanen, T. 2013. Influence of surface integrity on the fatigue strength of high-strength steels. *Journal of Constructional Steel Research,* 89**,** 21-29.

Remes, H., Peltonen, M., Seppänen, T., Kukkonen, A., Liinalampi, S., Lillemäe, I., Lehto, P., Hänninen, H. & Romanoff, J. 2015. Fatigue strength of welded extra high-strength and thin steel plates. *In:* Guedes Soares, C. & Shenoi, A. (eds.) *Analysis and Design of Marine Structures.* London, UK: Taylor & Francis Group.

Remes, H., Romanoff, J., Lillemae, I., Frank, D., Liinalampi, S., Lehto, P. & Varsta, P. 2017. Factors affecting the fatigue strength of thin-plates in large structures. *International Journal of Fatigue,* 101**,** 397-407.

Rizzo, C. M. 2011. Application of advanced notch stress approaches to assess fatigue strength of ship structural details: literature review. *Report 655, Schriftenreihe Schiffbau.* Hamburg, Germany.: Technische Universität Hamburg-Harburg.

Ronevich, J. A., Somerday, B. P. & Feng, Z. 2017. Hydrogen accelerated fatigue crack growth of friction stir welded X52 steel pipe. *International Journal of Hydrogen Energy,* 42**,** 4259-4268.

Rörup, J., Garbatov, Y., Dong, Y., Uzunoglu, E., Parmentier, G., Andoniu, A., Quéméner, Y., Chen, K.-C., Vhanmane, S., Negi, A., Parihar, Y., Villavicencio, R. & Yue, J. 2017. Round robin study on spectral fatigue assessment of butt-welded joints. *In:* Guedes Soares, C. &

Teixeira, A. (eds.) *Maritime Transportation and Harvesting of Sea Resources.* London: Taylor & Francis, 663-671.

Rosemeier, M., Basters, G. & Antoniou, A., 2017, Benefits of sub-component over full-scale blade testing elaborated on a trailing edge bond line design validation, Proceedings of Wind Energy Science Conference.

Roth, C. C. & Mohr, D. 2016. Ductile fracture experiments with locally proportional loading histories. *International Journal of Plasticity,* 79**,** 328-354.

Rother, K. & Rudolph, J. 2011. Fatigue assessment of welded structures: practical aspects for stress analysis and fatigue assessment. *Fatigue & Fracture of Engineering Materials & Structures,* 34**,** 177-204.

Ruggieri, C. 2017. Low constraint fracture toughness testing using SE(T) and SE(B) specimens. *International Journal of Pressure Vessels and Piping,* Article in press.

Sadeghirad, A., Chopp, D. L., Ren, X., Fang, E. & Lua, J. 2016. A novel hybrid approach for level set characterization and tracking of non-planar 3D cracks in the extended finite element method. *Engineering Fracture Mechanics,* 160**,** 1-14.

Sander, M., Muller, T. & Stacker, C. 2016. Very high cycle fatigue behaviour under constant and variable amplitude loading. *21st European Conference on Fracture, (Ecf21),* 2**,** 34-41.

Savaidis, G. & Malikoutsakis, M. 2016. Advanced notch strain based calculation of S-N curves for welded components. *International Journal of Fatigue,* 83**,** 84-92.

Schneider, N., Bodecker, J., Berger, C. & Oechsner, M. 2016. Frequency effect and influence of testing technique on the fatigue behaviour of quenched and tempered steel and aluminium alloy. *International Journal of Fatigue,* 93**,** 224-231.

Schneider, R., Thons, S. & Straub, D. 2017. Reliability analysis and updating of deteriorating systems with subset simulation. *Structural Safety,* 64**,** 20-36.

Schoefs, F., Chevreuil, M., Pasqualini, O. & Cazuguel, M. 2016. Partial safety factor calibration from stochastic finite element computation of welded joint with random geometries. *Reliability Engineering & System Safety,* 155**,** 44-54.

Schubbe, J. J., Bolstad, S. H. & Reyes, S. 2016. Fatigue crack growth behaviour of aerospace and ship-grade aluminum repaired with composite patches in a corrosive environment. *Composite Structures,* 144**,** 44-56.

Schwartzkopff, A. K., Xu, C. S. & Melkoumian, N. S. 2016. Approximation of mixed mode propagation for an internally pressurized circular crack. *Engineering Fracture Mechanics,* 166**,** 218-233.

Šebek, F., Kubík, P., Hůlka, J. & Petruška, J. 2016. Strain hardening exponent role in phenomenological ductile fracture criteria. *European Journal of Mechanics-A/Solids,* 57**,** 149-164.

Shen, F., Voyiadjis, G. Z., Hu, W. & Meng, Q. 2015. Analysis on the fatigue damage evolution of notched specimens with consideration of cyclic plasticity. *Fatigue & Fracture of Engineering Materials & Structures,* 38**,** 1194-1208.

Shi, K. K., Cai, L. X., Qi, S. & Bao, C. 2016. A prediction model for fatigue crack growth using effective cyclic plastic zone and low cycle fatigue properties. *Engineering Fracture Mechanics,* 158**,** 209-219.

Shijian, C., Yiqian, L. & Weiqiang, Q., 2013, Comparison Analysis between CSR-OT and CSR-H for Corrugated Bulkhead of Large Product Tanker, TSCF 2013 Shipbuilders Meeting.

Shin, H. K., Lee, D. W., Park, J. & Cho, S.-R., 2016, Damage of plates due to repeated impulsive pressure loadings, Proceedings of the 13th International Symposium on Practical design of ships and other floating structures, Copenhagen, Danmark.

Skriko, T., Ghafouri, M. & Bjork, T. 2017. Fatigue strength of TIG-dressed ultra-high-strength steel fillet weld joints at high-stress ratio. *International Journal of Fatigue,* 94**,** 110-120.

Snowberg, D., Dana, S., Hughes, S. & Berling, P. 2014. Implementation of a Biaxial Resonant Fatigue Test Method on a Large Wind Turbine Blade.: National Renewable Energy Laboratory, NREL/TP-5000- 61127.

Socie, D. F., Morrow, J. & Chen, W. 1979. A procedure for estimating the total fatigue life of notched and cracked members. *Engineering Fracture Mechanics,* 11**,** 851-859.

Soliman, M., Frangopol, D. M. & Mondoro, A. 2016. A probabilistic approach for optimizing inspection, monitoring, and maintenance actions against fatigue of critical ship details. *Structural Safety,* 60**,** 91-101.

Song, S. & Dong, P. 2016. Residual stresses at weld repairs and effects of repair geometry. *Science and Technology of Welding and Joining,* 22.

Sørensen, J. D., Branner, K. & Toft, H. S. 2013. Milestone 6: Recommendations for future sub component tests. *EUDP: Experimental Blade Research - Phase 2.* Aalborg University & DTU.

Sowards, J. W., Gnaupel-Herold, T., McColskey, J. D., Pereira, V. F. & Ramirez, A. J. 2015. Characterization of mechanical properties, fatigue-crack propagation, and residual stresses in a microalloyed pipeline-steel friction-stir weld. *Materials & Design,* 88**,** 632-642.

Stanzl-Tschegg, S. 2014. Very high cycle fatigue measuring techniques. *International Journal of Fatigue,* 60**,** 2-17.

STD181-0004 Volvo Group Weld Quality Standard.

Stenberg, T., Barsoum, Z. & Balawi, S. O. M. 2015. Comparison of local stress based concepts-Effects of low-and high cycle fatigue and weld quality. *Engineering Failure Analysis,* 57**,** 323-333.

Stenberg, T., Lindgren, E., Barsoum, Z. & Barmicho, I. 2016. Fatigue assessment of cut edges in high strength steel - Influence of surface quality. *Engineering Failure Analysis*.

Storhaug, G. & Kahl, A., 2015, Full-Scale Measurements of Torsional Vibration on Post-Panamax container ships Proceedings of the 7th International Conference on Hydroelasticity in Marine Technology, Split, Croatia.

Strach-Sonsalla, M. & Muskulus, M., 2016, Dynamics and Design of Floating Wind Turbines Proceedings of the 26th International Ocean and Polar Engineering Conference, Rhodes, Greece, ISOPE -I-16-702.

Sun, B., Xu, Y. L. & Li, Z. X. 2016. Multi-scale model for linking collective behaviour of short and long cracks to continuous average fatigue damage. *Engineering Fracture Mechanics,* 157**,** 141-153.

Sung, S. J. & Pan, J. 2016. Further investigation of stress intensity factor solutions for similar and dissimilar welds in lap-shear specimens under clamped loading conditions. *Engineering Fracture Mechanics,* 166**,** 60-81.

Szabo, B., Actis, R. & Rusk, D. 2016. Predictors of fatigue damage accumulation in the neighbourhood of small notches. *International Journal of Fatigue,* 92**,** 52-60.

Tan, C., Lu, Y. S. & Zhang, X. T. 2016. Life extension and repair decision-making of ageing offshore platforms based on DHGF method. *Ocean Engineering,* 117**,** 238-245.

Tang, J., Yu, W., Chai, T. Y., Liu, Z. & Zhou, X. J. 2016. Selective ensemble modelling load parameters of ball mill based on multi-scale frequency spectral features and sphere criterion. *Mechanical Systems and Signal Processing,* 66-67**,** 485-504.

Tao, Z. Q., Shang, D. G., Liu, H. & Chen, H. 2016. Life prediction based on weight-averaged maximum shear strain range plane under multiaxial variable amplitude loading. *Fatigue & Fracture of Engineering Materials & Structures,* 39**,** 907-920.

Taylor, D. 2007. *The Theory of Critical Distances; A New Perspective in Fracture Mechanics,* Linacre House, Jordan Hill, Oxford, United Kingdom, Elsevier.

Tchoffo Ngoula, D., Beier, H. T. & Vormwald, M. 2017. Fatigue crack growth in cruciform welded joints: Influence of residual stresses and of the weld toe geometry. *International Journal of Fatigue,* 101**,** 253-262.

Tekgoz, M., Garbatov, Y. & Guedes Soares, C. 2013a. Finite element modelling of the ultimate strength of stiffened plates with residual stresses. *In:* Guedes Soares, C. & Romanoff, J. (eds.) *Analysis and Design of Marine Structures.* London, UK: Taylor & Francis Group, 309-317.

Tekgoz, M., Garbatov, Y. & Guedes Soares, C., 2013b, Ultimate strength assessment of a stiffened plate accounting for welding sequences, *In:* Chang-Sup Lee, S.-H. V., ed., Proceedings of the 11th International Symposium on Practical Design of Ships and other Floating Structures, Changwon City, Korea, CECO, 1089-1095.

Tekgoz, M., Garbatov, Y. & Guedes Soares, C. 2014. Strength assessment of a stiffened panel based on the modified stress curve approach. *In:* Guedes Soares, C. & Santos, T. A. (eds.) *Maritime Technology and Engineering.* London, UK: Taylor & Francis Group, 503-510.

Thompson, I. 2016. Validation of naval vessel spectral fatigue analysis using full-scale measurements. *Marine Structures,* 49 256-268.

Tomaso, E., Risso, G., Gaiotti, M. & Rizzo, C. M., 2014, Numerical Simulation Strategies of Single Lap Joints, Proceedings of the 24th International Ocean and Polar Engineering Conference, Busan, Korea.

Tong, L. W., Huang, X. W., Zhou, F. & Chen, Y. Y. 2016. Experimental and numerical investigations on extremely-low-cycle fatigue fracture behaviour of steel welded joints. *Journal of Constructional Steel Research,* 119**,** 98-112.

Toribio, J., Matos, J. C. & Gonzalez, B. 2016. Aspect ratio evolution associated with surface cracks in sheets subjected to fatigue. *International Journal of Fatigue,* 92**,** 588-595.

Tumanov, A. V., Shlyannikov, V. N. & Kishen, J. M. C. 2015. An automatic algorithm for mixed-mode crack growth rate based on drop potential method. *International Journal of Fatigue,* 81**,** 227-237.

UK-HSE 1990. Offshore installations: guidance on design and construction. London.

Ulveseter, J. V. & Sævik, S., 2017, In-Line vibrations of flexible pipes, Proceedings of the 36th International Conference on Ocean, Offshore and Arctic Engineering, Trondheim, Norway, Paper OMAE2017-61325.

Van Lieshout, P. S., Den Besten, J. H. & Kaminski, M. L. 2016. Comparative study of multiaxial fatigue methods applied to welded joints in marine structures. *Frattura Ed Integrita Strutturale,* 37**,** 173 – 192.

Vasco-Olmo, J. M. & Diaz, F. A. 2016. Experimental evaluation of the effect of overloads on fatigue crack growth by analysing crack tip displacement fields. *Engineering Fracture Mechanics,* 166**,** 82-96.

Verreman, Y. & Nie, B. 1996. Early development of fatigue cracking at manual fillet welds. *Fatigue & Fracture of Engineering Materials & Structures,* 19**,** 669-681.

Vesely, V., Sobek, J., Frantik, P. & Seitl, S. 2016. Multi-parameter approximation of the stress field in a cracked body in the more distant surroundings of the crack tip. *International Journal of Fatigue,* 89**,** 20-35.

Vettor, R. & Guedes Soares, C. 2015. Detection and Analysis of the Main Routes of Voluntary Observing Ships in the North Atlantic. *Journal of Navigation,* 68**,** 397-410.

Vieira, M., Reis, L., Freitas, M. & Ribeiro, A. 2016. Strain measurements on specimens subjected to biaxial ultrasonic fatigue testing. *Theoretical and Applied Fracture Mechanics,* 85**,** 2-8.

Voie, P., Wu, J., Resvanis, T. L., Larsen, C. M., Vandiver, J. K., Triantafyllou, M. & Baarholm, R., 2017, Consolidation of empirics for calculation of VIV responses, Proceedings of the 36th International Conference on Ocean, Offshore and Arctic Engineering, Trondheim, Norway, Paper OMAE2017-61362.

Vormwald, M. 2015. Multi-challenge aspects in fatigue due to the combined occurrence of multiaxiality, variable amplitude loading, and size effects. *Frattura Ed Integrita Strutturale,* 33**,** 253-261.

Wallin, K., Pallaspuro, S., Valkonen, I., Karjalainen-Roikonen, P. & Suikkanen, P. 2015. Fracture properties of high-performance steels and their welds. *Engineering Fracture Mechanics,* 135**,** 219-231.

Wang, C. & Xu, X. W. 2016. An extended phantom node method study of crack propagation of composites under fatigue loading. *Composite Structures,* 154**,** 410-418.

Wang, F., Cui, W. C., Pan, B. B., Shen, Y. S. & Huang, X. P. 2014. Normalised fatigue and fracture properties of candidate titanium alloys used in the pressure hull of deep manned submersibles. *Ships and Offshore Structures,* 9**,** 297-310.

Wang, F., Cui, W. C., Wang, Y. Y. & Shen, Y. S. 2015a. Overload and dwell time effects on crack growth property of high strength titanium alloy TC4 ELI used in submersibles. *In:* Guedes Soares, C. & Shenoi, A. (eds.) *Analysis and Design of Marine Structures.* London, UK: Taylor & Francis Group.

Wang, F., Wang, K. & Cui, W. C. 2015b. A simplified life estimation method for the spherical hull of deep manned submersibles. *Marine Structures,* 44**,** 159-170.

Wang, J., Ma, Q. W. & Yan, S., 2016a, Numerical Investigation on Spectrum Evolution of Narrow-Banded Random Waves in Shallow Water Based on KdV and Fully Nonlinear Model Proceedings of the 35th International Conference on Ocean, Offshore and Arctic Engineering, Busan, Korea, Paper OMAE2016-54169.

Wang, Q., Liu, X. S., Yan, Z. J., Dong, Z. B. & Yan, D. J. 2017a. On the mechanism of residual stresses relaxation in welded joints under cyclic loading. *International Journal of Fatigue,* 105**,** 43-59.

Wang, R. Z., Zhang, X. C., Tu, S. T., Zhu, S. P. & Zhang, C. C. 2016b. A modified strain energy density exhaustion model for creep-fatigue life prediction. *International Journal of Fatigue,* 90**,** 12-22.

Wang, X. G., Feng, E. S. & Jiang, C. 2017b. A microplasticity evaluation method in very high cycle fatigue[J]. *International Journal of Fatigue,* 94**,** 6-15.

Wang, Y. & Susmel, L. 2016. he Modified Manson-Coffin Curve Method to estimate fatigue life under complex constant and variable amplitude multiaxial fatigue loading. *International Journal of Fatigue,* 83**,** 135 - 149.

Wang, Y. Y., Chen, H. B. & Zhou, H. W. 2016c. A fatigue life estimation algorithm based on Statistical Energy Analysis in high-frequency random processes. *International Journal of Fatigue,* 83**,** 221-229.

Wei, Z. G. & Dong, P. S. 2014. A generalized cycle counting criterion for arbitrary multi-axial fatigue loading conditions. *Journal of Strain Analysis for Engineering Design,* 49**,** 325-341.

Wu, H., Meggiolaro, M. A. & de Castro, J. T. P. 2016. Computational implementation of a non-linear kinematic hardening formulation for tension-torsion multiaxial fatigue calculations. *International Journal of Fatigue,* 91**,** 304-312.

Wu, J., Lekkala, B. R., Ong, M. C., Passano, E. & Voie, P. E., 2017, Prediction of combined IL and CF VIV of deep-water risers, Proceedings of the 36th International Conference on Ocean, Offshore and Arctic Engineering, Trondheim, Norway, Paper OMAE2017-61766.

Xie, X. F., Jiang, W. C., Luo, Y., Xu, S. G., Gong, J. M. & Tu, S. T. 2017. A model to predict the relaxation of weld residual stress by cyclic load: Experimental and finite element modelling. *International Journal of Fatigue,* 95**,** 293-301.

Xing, S. Z. & Dong, P. S. 2016. An analytical SCF solution method for joint misalignments and application in fatigue test data interpretation. *Marine Structures,* 50**,** 143-161.

Xing, S. Z., Dong, P. S. & Threstha, A. 2016. Analysis of fatigue failure mode transition in load-carrying fillet-welded connections. *Marine Structures,* 46**,** 102-126.

Xing, S. Z., Dong, P. S. & Wang, P. 2017. A quantitative weld sizing criterion for fatigue design of load-carrying fillet-welded connections. *International Journal of Fatigue,* 101**,** 448-458.

Xu, S. H. & Wang, Y. D. 2015. Estimating the effects of corrosion pits on the fatigue life of steel plate based on the 3D profile. *International Journal of Fatigue,* 72**,** 27-41.

Yamamoto, M., Makino, K. & Ishiduka, H. 2017. Comparison of crack growth behaviour between full-scale railway axle and scaled specimen. *International Journal of Fatigue,* 92**,** 159-165.

Yan, X., Huang, X. & Liu, F., 2014, Research on the application of storm model in fatigue life prediction for offshore platform, *In:* Zheng, I., ed., Proceedings of the 2014 International

Conference on Industrial, Mechanical and Manufacturing Science, Taylor & Francis Group, 49-52.

Yan, X. S. & Huang, X. P. 2015. Prediction of fatigue life reliability for ship details based on crack growth. *Shanghai Jiaotong Daxue Xuebao/Journal of Shanghai Jiaotong University,* 49**,** 214-219.

Yan, X. S., Huang, X. P., Huang, Y. C. & Cui, W. C. 2016. Prediction of fatigue crack growth in a ship detail under wave-induced loading. *Ocean Engineering,* 113**,** 246-254.

Yang, S. O., Yang, H. Q., Liu, G., Huang, Y. & Wang, L. D. 2016. Approach for fatigue damage assessment of welded structure considering coupling effect between stress and corrosion. *International Journal of Fatigue,* 88**,** 88-95.

Yang, X. H., Zou, L. & Deng, W. 2015. Fatigue life prediction for welding components based on hybrid intelligent technique. *Materials Science and Engineering a-Structural Materials Properties Microstructure and Processing,* 642**,** 253-261.

Ye, W., Ran, A., Li, J., Li, G., Tang, X., Wang, Z. & Hongwu, W., 2016, Tapered Column Deep Draft Semi-submersible (TCDD-Semi) Platform for Dry-tree Application, Proceedings of the 26th International Ocean and Polar Engineering Conference Rhodes, Greece, Paper ISOPE-I-16-703.

Yeter, B., Garbatov, Y. & Guedes Soares, C. 2014a. Fatigue damage analysis of a fixed offshore wind turbine supporting structure. *In:* Guedes Soares, C. & Pena, F. (eds.) *Developments in Maritime Transportation and Exploitation of Sea Resources.* London, UK: Taylor & Francis Group, 415-424.

Yeter, B., Garbatov, Y. & Guedes Soares, C. 2014b. Spectral fatigue assessment of an offshore wind turbine structure under wave and wind loading. *In:* Guedes Soares, C. & Pena, F. (eds.) *Developments in Maritime Transportation and Exploitation of Sea Resources.* London, UK: Taylor & Francis Group, 425-433.

Yeter, B., Garbatov, Y. & Guedes Soares, C. 2015a. Assessment of the retardation of in-service cracks in offshore welded structures subjected to variable amplitude load. *In:* Guedes Soares, C. (ed.) *Renewable Energies Offshore.* London, UK: Taylor & Francis group, 855-863.

Yeter, B., Garbatov, Y. & Guedes Soares, C. 2015b. Fatigue crack growth analysis of a plate accounting for retardation effect. *In:* Guedes Soares, C. & Santos, T. A. (eds.) *Marine Technology and Engineering.* London, UK: Taylor & Francis Group, 585-595.

Yeter, B., Garbatov, Y. & Guedes Soares, C. 2015c. Fatigue reliability assessment of an offshore supporting structure. *In:* Guedes Soares, C. & Santos, T. A. (eds.) *Marine Technology and Engineering.* London, UK: Taylor & Francis Group, 671-681.

Yeter, B., Garbatov, Y. & Guedes Soares, C. 2015d. Fatigue reliability of an offshore wind turbine supporting structure accounting for inspection and repair. *In:* Guedes Soares, C. & Shenoi, A. (eds.) *Analysis and Design of Marine Structures.* London, UK: Taylor & Francis Group, 737-747.

Yeter, B., Garbatov, Y. & Guedes Soares, C. 2015e. Low cycle fatigue assessment of offshore wind turbine monopile supporting structure subjected to wave-induced loads. *In:* Guedes Soares, C., Dejhalla, R. & Pavletic, D. (eds.) *Towards Green Marine Technology and Transport.* London: Taylor & Francis Group, 287-294.

Yeter, B., Garbatov, Y. & Guedes Soares, C. 2016a. Evaluation of fatigue damage model predictions for fixed offshore wind turbine support structures. *International Journal of Fatigue,* 87**,** 71-80.

Yeter, B., Garbatov, Y. & Guedes Soares, C., 2016b, Reliability of offshore wind turbine support structures subjected to extreme wave-induced loads, Proceedings of the 35th International Conference on Ocean, Offshore and Arctic Engineering, Busan, South Korea, ASME, paper OMAE2016-54240.

Yeter, B., Garbatov, Y. & Guedes Soares, C. 2016c. Structural design of an adaptable jacket offshore wind turbine support structure for deeper waters. *In:* Guedes Soares, C. & Santos,

T. (eds.) *Maritime Technology and Engineering.* London: Taylor & Francis Group, 583-594.

Yeter, B., Garbatov, Y. & Guedes Soares, C. 2017a. Probabilistic life-cycle assessment for offshore wind turbines. *In:* Guedes Soares, C. & Teixeira, A. (eds.) *Maritime Transportation and Harvesting of Sea Resources.* 1229-1241.

Yeter, B., Garbatov, Y. & Guedes Soares, C. 2017b. Risk-based multi-objective optimisation of a monopile offshore wind turbine support structure. *Proceedings of the 36th International Conference on Ocean, Offshore and Arctic Engineering.* Trondheim, Norway, paper OMAE2017-61756.

Yeter, B., Garbatov, Y. & Guedes Soares, C. 2017c. System reliability of a jacket offshore wind turbine subjected to fatigue. *In:* Guedes Soares, C. & Garbatov, Y. (eds.) *Progress in the Analysis and Design of Marine Structures.* London: Taylor & Francis Group, 939-950.

Yıldırım, H. 2015. Review of fatigue data for welds improved by tungsten inert gas dressing. *International Journal of Fatigue,* 79**,** 36-45.

Yıldırım, H. 2016. Recent results on fatigue strength improvement of high-strength steel welded joints. *International Journal of Fatigue*.

Yildirim, H. & Marquis, G. 2015. Fatigue data of High-Frequency Mechanical Impact (HFMI) improved welded joints subjected to overloads. *In:* Guedes Soares, C. & Shenoi, A. (eds.) *Analysis and Design of Marine Structures.* London, UK: Taylor & Francis Group, 317-322.

Yin, D., Passano, E. & Larsen, C. M., 2017, Improved In-Line VIV prediction for combined In-Line and Cross-Flow VIV responses, Proceedings of the 36th International Conference on Ocean, Offshore and Arctic Engineering, Trondheim, Norway, Paper OMAE2017-61715.

Yin, D., Wu, J. & Lie, H., 2015, VIV Prediction of Steel Catenary Riser - A Reynolds Number Sensitivity Study, Proceedings of the 25th International Ocean and Polar Engineering Conference, Hawaii, USA, Paper ISOPE-I-15-125.

Yokozeki, K. & Miki, C. 2016. Fatigue evaluation for longitudinal-to-transverse rib connection of orthotropic steel deck by using structural hot spot stress. *Welding in the World,* 60**,** 83-92.

Yuan, K. L. & Sumi, Y. 2016. Simulation of residual stress and fatigue strength of welded joints under the effects of ultrasonic impact treatment (UIT). *International Journal of Fatigue,* 92**,** 321-332.

Yue, J., Dang, Z. & Guedes Soares, C. 2017. Prediction of fatigue crack propagation in bulb stiffeners by experimental and numerical methods. *International Journal of Fatigue* 99**,** 101-110.

Zappalorto 2015. Neubers rules and other solutions - theoretical differences and formal analogies and energy interpretations. *Theoretical and Applied Fracture Mechanics,* 79.

Zappalorto, M. & Lazzarin, P. 2014. Some remarks on the Neuber rule applied to a control volume surrounding sharp and blunt notch tips. *Fatigue & Fracture of Engineering Materials & Structures,* 37**,** 349-358.

Zerbst, U. & Madia, M. 2015. Fracture mechanics based assessment of the fatigue strength: approach for the determination of the initial crack size. *Fatigue & Fracture of Engineering Materials & Structures,* 38**,** 1066-1075.

Zhang, D., Huang, X. P. & Cui, W. C. 2015. A procedure to predict fatigue crack growth of ship structures under complex loading condition. *Chuan Bo LI Xue/Journal of Ship Mechanics,* 19**,** 541-552.

Zhang, J., Yang, S. & Lin, J. 2016a. A nonlinear continuous damage model based on short-crack concept under variable amplitude loading. *Fatigue & Fracture of Engineering Materials & Structures,* 39**,** 79-94.

Zhang, J. R., Fan, L. & Tang, X. S. 2016b. Energy density zone model and fatigue life prediction considering microscopic effects. *Fatigue & Fracture of Engineering Materials & Structures,* 39**,** 1542-1556.

Zhang, Y. H. & Maddox, S. J. 2009. Fatigue life prediction for toe ground welded joints. *International Journal of Fatigue,* 31**,** 1124-1136.

Zhang, Y. M., Fan, M., Xiao, Z. M. & Zhang, W. G. 2016c. Fatigue analysis on offshore pipelines with embedded cracks. *Ocean Engineering,* 117**,** 45-56.

Zhou, X. Y., Gosling, P. D., Ullah, Z., Kaczmarczyk, L. & Pearce, C. J. 2016. Exploiting the benefits of multi-scale analysis in reliability analysis for composite structures. *Composite Structures,* 155**,** 197-212.

Zhou, Z. G. & Jia, L. J. 2015. Damage index for crack initiation of structural steel under cyclic loading. *Journal of Constructional Steel Research,* 114**,** 1-7.

Zhu, L., Guo, K., Duan, L., Liu, J., Wang, H. & Wang, X., 2016, Wet-deck slamming pressure on SWATH-consideration for practical design, Proceedings of the 13th International Symposium on Practical design of ships and other floating structures, Copenhagen, Denmark.

Zhu, X.-K. 2017. Progress in development of fracture toughness test methods for SENT specimens. *International Journal of Pressure Vessels and Piping,* Article in press.

Zhu, X. K. 2015. Advances in Fracture Toughness Test Methods for Ductile Materials in Low-Constraint Conditions. *Pressure Vessel Technology: Preparing for the Future,* 130**,** 784-802.

Zhu, X. K. 2016. Review of fracture toughness test methods for ductile materials in low-constraint conditions. *International Journal of Pressure Vessels and Piping,* 139**,** 173-183.

Zhu, X. K. & Joyce, J. A. 2012. Review of fracture toughness (G, K, J, CTOD, CTOA) testing and standardization. *Engineering Fracture Mechanics,* 85**,** 1-46.

Zhu, X. K., Zelenak, P. & McGaughy, T. 2017. Comparative study of CTOD-resistance curve test methods for SENT specimens. *Engineering Fracture Mechanics,* 172**,** 17-38.

Zonfrillo, G. 2017. New Correlations Between Monotonic and Cyclic Properties of Metallic Materials. *Journal of Materials Engineering and Performance,* 26**,** 1569-1580.